

PHOTOCHEMICAL DEGRADATION OF AQUEOUS ARTIFICIAL SWEETENERS  
BY UV/H<sub>2</sub>O<sub>2</sub> AND THEIR BIODEGRADABILITY STUDIES

By

Ramtin Jahani

B.Eng. in Chemical Engineering

Ryerson University, Toronto, Ontario, 2016

A thesis

presented to Ryerson University

in partial fulfilment of the requirements for the degree of

Master of Applied Science

in the program of Chemical Engineering

Toronto, Ontario, Canada, 2019

© Ramtin Jahani, 2019

## **Author's Declaration for Electronic Submission of a Thesis**

I hereby declare that I am the sole author of this thesis. This is a true copy of the thesis, including any required final revisions, as accepted by my examiners.

I authorize Ryerson University to lend this thesis to other institutions or individuals for the purpose of scholarly research. I further authorize Ryerson University to reproduce this thesis by photocopying or by other means, in total or in part, at the request of other institutions or individuals for the purpose of scholarly research.

I understand that my thesis may be made electronically available to the public.

# **Photochemical Degradation of Aqueous Artificial Sweeteners by UV/H<sub>2</sub>O<sub>2</sub> and their Biodegradability Studies**

**Master of Applied Science**

**2019**

**Ramtin Jahani**

**Chemical Engineering**

**Ryerson University**

## **Abstract**

In this study, the photochemical degradations of three commonly used artificial sweeteners, namely *aspartame* (ASP), *acesulfame K* (ACE), and *sucralose* (SUC) were investigated in multicomponent aqueous systems through UV/H<sub>2</sub>O<sub>2</sub>. A recirculating batch photochemical reactor setup was utilized for experimental work. The treatability of the multicomponent system was monitored in the form of *total organic carbon* (TOC) reduction. A two-level fractional factorial *design of experiments* (DOE) was adopted. The individual and multifactor interaction effects of the concentration of the three sweeteners, the applied hydrogen peroxide dosage and the operating temperature on TOC reduction were investigated. The biodegradability characteristics of the sweeteners were investigated for both single and multicomponent systems through *respirometry*. Their degradations were compared to those of the UV/H<sub>2</sub>O<sub>2</sub> system. It was determined that the UV/H<sub>2</sub>O<sub>2</sub> process is suitable treatment technique, achieving TOC removal efficiencies over 90% with a UV exposure of 45 min. The operating temperature and the applied H<sub>2</sub>O<sub>2</sub> dosing on the final TOC removal were found to be significant. An interaction between ASP and SUC resulted in a temporary improvement in TOC removal midway through the treatment process. Respirometric studies confirmed that ACE and SUC are non-biodegradable. The biodegradation characteristics of ASP was found to be acceptable with a 6-day *biochemical to theoretical oxygen demand* (BOD<sub>6</sub>/ThOD) ratio of  $0.63 \pm 0.02$ .

## **Acknowledgements**

I would like to express my sincere acknowledgements to Dr. Mehrab Mehrvar, my supervisor, and Dr. Ramdhane Dhib, my co-supervisor, for offering me the opportunity to study and work with them and the rest of their research group members. Their guidance and financial support during my graduate studies are highly appreciated.

This journey was not possible without the continuous support of my beloved family. Thank you for your encouragement throughout my studies.

I would also like to thank engineering specialists Mr. Ali Hemmati and Mr. Daniel Boothe of Ryerson University's Department of Chemical Engineering for providing their support and assistance throughout my work.

I would also like to thank the members of my research team, Melody Johnson, Yi Ping Lin, Ciro Bustillo-Lecompte and Mohsen Nasirian for their help and guidance. I would also like to thank my dear friends Rana Rahmani, Filip Jelic, Ahmed Ali Manzoor, Mohammed Awad, Amir Kouhpour and Argang Kazemzadeh who supported me throughout my days of hard work.

Finally, the financial support of the Faculty of Engineering and Architectural Science (FEAS) of Ryerson University and the Natural Sciences and Engineering Council (NSERC) of Canada is highly appreciated.

# Table of Contents

Abstract .....	iii
List of Tables .....	ix
List of Figures .....	xi
List of Appendices .....	xiv
Nomenclature .....	xv
Chapter 1 – INTRODUCTION.....	1
1.1 Overview .....	1
1.2 Research Objectives .....	3
Chapter 2 – LITERATURE REVIEW .....	4
2.1 Introduction.....	4
2.2 Global Distribution of Artificial Sweeteners in Water Resources .....	5
2.3 Environmental Impact and Ecotoxicological Data .....	7
2.4 Health Impacts of Artificial Sweeteners in Humans.....	9
2.5 Fate of Artificial Sweeteners in Conventional Wastewater Treatment Processes .....	10
2.6 Advanced Oxidation Processes for the Removal of Artificial Sweeteners.....	13
2.6.1 Overview of Advanced Oxidation Processes (AOPs) .....	13
2.6.2 The Removal of Artificial Sweeteners through Advanced Oxidation Processes (AOPs) .....	17
2.7 Concluding Remarks.....	25
Chapter 3 – MATERIALS AND METHODS .....	27
3.1 Introduction.....	27
3.2 Materials .....	27

3.2.1 Artificial Sweeteners .....	28
3.2.2 Distilled Water.....	29
3.2.3 Artificial Sweetener Solutions.....	29
3.2.4 Hydrogen Peroxide .....	29
3.2.5 Potassium Hydrogen Phthalate and Phosphoric Acid Solutions .....	29
3.2.6 Potassium Hydroxide and Sulfuric Acid Solutions .....	30
3.2.7 Phosphate Buffer .....	30
3.2.8 Stock Nutrient Solution .....	30
3.2.9 Municipal Mixed Liquor Samples .....	31
3.3 Experimental Methods .....	31
3.3.1 Overview of the Recirculating Batch Reactor.....	32
3.3.2 Overview of Two-level Fractional Factorial Designs .....	33
3.3.3 Overview of Respirometry .....	36
3.3.4 Characteristics of the Photoreactors .....	38
3.3.5 Analytical Methods.....	41
3.4 Stage I – Preliminary Experiments .....	45
3.4.1 Experimental Setup for the treatment of Aspartame Solutions .....	45
3.4.2 Experimental Setup for the treatment of Acesulfame K and Sucralose Solutions .....	46
3.4.3 Experimental Procedure .....	48
3.5 Stage II – Statistical Design of Experiments .....	51
3.5.1 Experimental Setup.....	52
3.5.2 Experimental Procedure .....	54
3.6 Stage III – Respirometry .....	54
3.6.1 Experimental Setup.....	54
3.6.2 Experimental Procedure .....	55

Chapter 4 – RESULTS AND DISCUSSION .....	57
4.1 Introduction.....	57
4.2 Preliminary Experiments – Degradation of Artificial Sweeteners in Single-component Aqueous Solutions by UV/H <sub>2</sub> O <sub>2</sub> .....	57
4.2.1 Aspartame .....	57
4.2.2 Acesulfame K .....	64
4.2.3 Sucralose.....	68
4.2.4 Concluding Remarks .....	73
4.3 Statistical Design of Experiments – The Photochemical Degradation of Multicomponent Systems of Artificial Sweeteners by UV/H <sub>2</sub> O <sub>2</sub> .....	74
4.3.1 Identification of Significant Effects .....	75
4.3.2 The Effects of Factors and their interactions on TOC Removal .....	80
4.3.3 Regression Analysis .....	92
4.3.4 Concluding Remarks .....	96
4.4 Determination of the Biodegradation Characteristics of Aspartame, Acesulfame K and Sucralose through Respirometry in both Single and Multicomponent Systems.....	97
4.4.1 Acclimation of the Microbial Community .....	100
4.4.2 Biodegradation Characteristics of Aqueous Solutions of Aspartame .....	100
4.4.3 Biodegradation Characteristics of Aqueous Solutions of Acesulfame K.....	101
4.4.4 Biodegradation Characteristics of Aqueous Solutions Sucralose.....	102
4.4.5 Biodegradation Characteristics of Multicomponent Aqueous Systems of Aspartame, Acesulfame K, and Sucralose .....	102
4.4.6 Concluding Remarks .....	104
Chapter 5 – CONCLUSIONS AND RECOMMENDATIONS.....	106
5.1 Conclusions.....	106
5.2 Recommendations for Future Work.....	107

Appendices.....	109
Appendix A – Determination of MLSS and MLVSS .....	109
Appendix B – The Use of Center Point Replicates for Error Estimation and Curvature Tests .....	110
Appendix C – Determination of Theoretical H <sub>2</sub> O <sub>2</sub> Dosages (Mass Basis).....	112
Appendix D – Determination of ThOD and BOD/ThOD.....	113
Appendix E – Determination of Theoretical Total Organic Carbon (TOC) .....	114
Appendix F – Determination of UV Exposure Time and Conversion Per Pass .....	115
Appendix G – Calibration of the TOC Analyzer .....	116
Appendix H – Fit Statistics for Developed Models .....	117
Appendix I – Analysis of Residuals.....	118
References .....	124



## List of Tables

<b>Table 2-1:</b> Summary of global data for the concentrations (in <b>ng/L</b> ) of artificial sweeteners in WWTP influent and effluent streams. MQL = Method Quantification Limit. Adapted from (Tran et al., 2018) .....	12
<b>Table 2-2:</b> Comparison of the oxidizing potentials of various oxidants used in water and wastewater treatment processes. Adapted from (Metcalf and Eddy, 2014) .....	13
<b>Table 2-3:</b> Advantages and limitations of commercially available advanced oxidation processes. Adapted from (Crittenden et al., 2012).....	16
<b>Table 2-4:</b> Reaction mechanisms for the generation of hydroxyl radicals through the UV/H <sub>2</sub> O <sub>2</sub> process. Adapted from (Oppenländer, 2002).....	17
<b>Table 2-5:</b> Mechanisms for the reaction of hydroxyl radicals with organic compounds. “R” denotes unsaturated aliphatic or aromatic organic compound. Adapted from (Solarchem Environmental Services, 1994).....	17
<b>Table 2-6:</b> Summary of available data for the degradation of five commonly used artificial sweeteners through advanced oxidation processes (AOPs).....	22
<b>Table 3-1:</b> List of all the chemical reagents used in this study.....	28
<b>Table 3-2:</b> Physical and chemical properties of ASP, ACE and SUC.....	29
<b>Table 3-3:</b> Recipe for the stock nutrient solution (1 L) used as “control” in respirometry .....	31
<b>Table 3-4:</b> Common 2 <sup>k-p</sup> designs. Adapted from (Montgomery, 2005) .....	36
<b>Table 3-5:</b> The generalized biochemical breakdown of organic substrates by microorganisms. Adapted from (Grady et al., 2011).....	37
<b>Table 3-6:</b> Physical characteristics of the photoreactors used in this study .....	38
<b>Table 3-7:</b> Specifications of the UV lamps used in this study.....	39
<b>Table 3-8:</b> Specifications of the pump used in this study .....	39
<b>Table 3-9:</b> Apollo 9000 combustion-based TOC analyzer specifications .....	41
<b>Table 3-10:</b> General properties of the BI-2000 electrolytic respirometer .....	43
<b>Table 3-11:</b> Estimation of the required hydrogen peroxide doses based on the theoretical oxidation of ASP, ACE and SUC by hydrogen peroxide .....	45
<b>Table 3-12:</b> Experimental conditions used in the preliminary experiments involving aqueous ASP through UV/H <sub>2</sub> O <sub>2</sub> .....	49

<b>Table 3-13:</b> Experimental conditions used in the preliminary experiments involving aqueous ACE through UV/H <sub>2</sub> O <sub>2</sub> .....	50
<b>Table 3-14:</b> Experimental conditions used in the preliminary experiments involving aqueous SUC through UV/H <sub>2</sub> O <sub>2</sub> .....	51
<b>Table 3-15:</b> Actual and coded values of for the experimental conditions used in the statistical design of experiments .....	52
<b>Table 3-16:</b> Components of the respirometric reactors in each experiment .....	54
<b>Table 3-17:</b> Experimental conditions for respirometric investigations .....	56
<b>Table 4-1:</b> General relationship between absorption wavelengths and observed colour. Adapted from (Hornback, 2006). .....	63
<b>Table 4-2:</b> Overview of the experimental results for the treatment of multicomponent aqueous systems of ASP, ACE and SUC with UV/H <sub>2</sub> O <sub>2</sub> at a UV exposure of 45 min.....	75
<b>Table 4-3:</b> Experimental rate constant ( <i>k</i> ) values of the reaction of hydroxyl radicals with artificial sweeteners. Adapted from (Toth et al., 2012).....	85
<b>Table 4-4:</b> ANOVA performed on the experimental results and the regression models for TOC removal .....	95
<b>Table 4-5:</b> Summary of respirometric results of ASP, ACE and SUC in single and multicomponent systems.....	104

## List of Figures

<b>Figure 1-1:</b> Overview of the classification of artificial Sweeteners as contaminants of emerging concern .....	1
<b>Figure 2-1:</b> A generalized classification of various advanced oxidation processes. Adapted from (Biń and Sobera-Madej, 2012).....	14
<b>Figure 3-1:</b> Schematic diagram of a recirculating batch reactor for catalytic reactions. Adapted from (Levenspiel, 1972).....	32
<b>Figure 3-2:</b> Schematic diagram of the Siemens SL – LAB 2 photoreactor with UV lamp and quartz sleeve.....	40
<b>Figure 3-3:</b> Flow diagram of the operation of the Apollo 9000 TOC analyzer. Adapted from Teledyne Tekmar .....	42
<b>Figure 3-4:</b> Schematic diagram of an electrolytic respirometer with electrolysis cell and reaction vessel.....	44
<b>Figure 3-5:</b> Schematic diagram of the experimental setup used for preliminary experiments on ASP solutions.....	46
<b>Figure 3-6:</b> Schematic of experimental setup used for preliminary experiments on acesulfame K and sucralose .....	47
<b>Figure 3-7:</b> Schematic diagram of the experimental setup used for the treatment of multicomponent aqueous systems of ASP, ACE and SUC through UV/H <sub>2</sub> O <sub>2</sub> incorporating two photoreactors in series and a water bath for temperature control .....	53
<b>Figure 4-1:</b> The degradation trends of ASP (75 mg/L) under UV irradiation and various H <sub>2</sub> O <sub>2</sub> doses by UV/H <sub>2</sub> O <sub>2</sub> with a single photoreactor.....	58
<b>Figure 4-2:</b> The degradation trends of ASP (150 mg/L) under UV irradiation and various H <sub>2</sub> O <sub>2</sub> doses by UV/H <sub>2</sub> O <sub>2</sub> with a single photoreactor.....	59
<b>Figure 4-3:</b> The degradation trends of ASP (300 mg/L) under UV irradiation and various H <sub>2</sub> O <sub>2</sub> doses by UV/H <sub>2</sub> O <sub>2</sub> with a single photoreactor.....	60
<b>Figure 4-4:</b> Comparison of ASP Solution (300 mg/L) colour intensity in the presence pf various H <sub>2</sub> O <sub>2</sub> doses under UV exposure with increasing time .....	61
<b>Figure 4-5:</b> Comparison of initial and final solution colours for ASP (300 mg/L) under UV irradiation alone (no H <sub>2</sub> O <sub>2</sub> ) .....	61

<b>Figure 4-6:</b> The degradation of ACE (75 mg/L) under UV irradiation and various H <sub>2</sub> O <sub>2</sub> doses by UV/H <sub>2</sub> O <sub>2</sub> with two photoreactors in series .....	64
<b>Figure 4-7:</b> The degradation of ACE (150 mg/L) under UV irradiation and various H <sub>2</sub> O <sub>2</sub> doses by UV/H <sub>2</sub> O <sub>2</sub> with two photoreactors in series .....	65
<b>Figure 4-8:</b> The degradation of ACE (300 mg/L) under UV irradiation and various H <sub>2</sub> O <sub>2</sub> doses by UV/H <sub>2</sub> O <sub>2</sub> with two photoreactors in series .....	66
<b>Figure 4-9:</b> The degradation of SUC (75 mg/L) under UV irradiation and various H <sub>2</sub> O <sub>2</sub> doses by UV/H <sub>2</sub> O <sub>2</sub> with two photoreactors in series .....	69
<b>Figure 4-10:</b> The degradation of SUC (150 mg/L) under UV irradiation and various H <sub>2</sub> O <sub>2</sub> doses by UV/H <sub>2</sub> O <sub>2</sub> with two photoreactors in series .....	70
<b>Figure 4-11:</b> The degradation of SUC (300 mg/L) under UV irradiation and various H <sub>2</sub> O <sub>2</sub> doses by UV/H <sub>2</sub> O <sub>2</sub> with two photoreactors in series .....	71
<b>Figure 4-12:</b> Half-normal probability (%) plot of standardized effects investigated at a UV exposure of 45 min (experimental endpoint). Factors D (H <sub>2</sub> O <sub>2</sub> :TOC <sub>total,ini</sub> ) and E (operating temperature) were found to be the most significant effects .....	77
<b>Figure 4-13:</b> Pareto chart of standardized effects of decreasing rank order plotted against corresponding <i>t-values</i> at a UV exposure of 45 min (experimental endpoint). Factors D (H <sub>2</sub> O <sub>2</sub> :TOC <sub>total,ini</sub> ) and E (operating temperature) were found to be the most significant effects. ....	78
<b>Figure 4-14:</b> Half-normal probability (%) plot of standardized effects investigated at a UV exposure of 22.5 min (experimental midpoint). Factor E (operating temperature) was found to be the most significant effect. ....	79
<b>Figure 4-15:</b> Pareto chart of standardized effects of decreasing rank order plotted against the corresponding <i>t-values</i> at a UV exposure of 22.5 min (experimental midpoint). Factor E (operating temperature) was found to be the most significant effect, followed by the interaction effect of factors A and C .....	80
<b>Figure 4-16:</b> The influence of the independent factors on the mean TOC removal at their respective 2 levels in a UV/H <sub>2</sub> O <sub>2</sub> process with a UV exposure of 22.5 min. Red dots represent the fraction of TOC removed in each centre point replication. ....	82
<b>Figure 4-17:</b> The influence of independent factors on the mean TOC removal at their respective 2 levels in a UV/H <sub>2</sub> O <sub>2</sub> process with a UV exposure of 45 min. Red dots represent the fraction of TOC removed in each centre point replication. ....	83

<b>Figure 4-18:</b> The effect of temperature on the mean TOC removal response at two levels with a UV exposure of 22.5 min. Red dots represent the fraction of TOC removed in each centre point replication. ....	84
<b>Figure 4-19:</b> The effect of temperature on the mean TOC removal response at two levels with a UV exposure of 45 min. Red dots represent the fraction of TOC removed in each centre point replication. ....	85
<b>Figure 4-20:</b> The effect of $\text{H}_2\text{O}_2\text{:TOC}_{\text{ini}}$ ratio (mass basis) on the mean TOC removal response at two levels with a UV exposure time of 45 min. Red dots represent the fraction of TOC removed in each centre point replication. ....	86
<b>Figure 4-21:</b> The interaction of ASP and SUC on TOC removal at a UV exposure of 22.5 min. $\text{TOC}_{\text{SUC,ini}}$ held constant at 25 mg/L (black) and 50 mg/L (red) in (a). $\text{TOC}_{\text{ASP,ini}}$ held constant at 25 mg/L (black) and 50 mg/L (red) in (b). Red dots represent the fraction of TOC removed in each centre point replication. ....	88
<b>Figure 4-22:</b> The contour of TOC removal response as a function of ASP and SUC concentrations. The contour lines represent the magnitudes of fraction of TOC removed at a UV exposure of 22.5 min.....	89
<b>Figure 4-23:</b> Response surface plot for the interaction of ASP and SUC concentrations on TOC removal at a UV exposure of 22.5 min .....	90
<b>Figure 4-24:</b> The contour of TOC removal response as a function of operating temperature and applied $\text{H}_2\text{O}_2\text{:TOC}_{\text{ini}}$ ratio (mass basis) at a UV exposure of 45 min. The contour lines represent the magnitudes of the fraction of TOC removed after 45 min.....	94
<b>Figure 4-25:</b> The corresponding response surface of overall TOC removal as a function of operating temperature and applied $\text{H}_2\text{O}_2\text{:TOC}_{\text{ini}}$ ratio (mass basis) at a UV exposure of 45 min	94
<b>Figure 4-26:</b> Respirometric results for single component solutions of ASP, ACE and SUC (150 mg/L) in comparison to a control reference in the presence of activated sludge .....	98
<b>Figure 4-27:</b> Replicated respirometric results for single component solutions ASP, ACE and SUC (150 mg/L) in comparison to a control reference in the presence of activated sludge .....	99
<b>Figure 4-28:</b> The respirometric results of multicomponent aqueous systems containing ASP, ACE and SUC (150 mg/L) in comparison to a control reference in the presence of activated sludge .....	103

## List of Appendices

Appendix A – Determination of MLSS and MLVSS .....	109
Appendix B – The Use of Center Point Replicates for Error Estimation and Curvature Tests ..	110
Appendix C – Determination of Theoretical H <sub>2</sub> O <sub>2</sub> Dosages (Mass Basis).....	112
Appendix D – Determination of ThOD and BOD/ThOD.....	113
Appendix E – Determination of Theoretical Total Organic Carbon (TOC).....	114
Appendix F – Determination of UV Exposure Time and Conversion Per Pass .....	115
Appendix G – Calibration of the TOC Analyzer .....	116
Appendix H – Fit Statistics for Developed Models .....	117
Appendix I – Analysis of Residuals.....	118

# Nomenclature

## Abbreviations

A <sup>2</sup> /O	Anaerobic/Anoxic/Oxic Process
ACE	Acesulfame K
ADI	Acceptable Daily Intake
ANOVA	Analysis of Variance
AOP	Advanced Oxidation Processes
ASP	Aspartame
BDD	Boron Doped Diamond
BOD	Biochemical Oxygen Demand
CBOD	Carbonaceous Biochemical Oxygen Demand
CEC	Contaminant of Emerging Concern
CYC	Cyclamate
DO	Dissolved Oxygen
DOC	Dissolved Organic Carbon
DOE	Design of Experiments
DOM	Dissolved Organic Matter
$HO^{\bullet}$	Hydroxyl Radical
$I$	Light Intensity
$I_0$	Initial Light Intensity
IC	Inorganic Carbon
LOEC	Lowest Observed Effect Concentration
MLSS	Mixed Liquor Suspended Solids

MLVSS	Mixed Liquor Volatile Suspended Solids
MP	Micropollutant
NBOD	Nitrogenous Biochemical Oxygen Demand
NDIR	Non-Dispersive Infrared
NOM	Natural Organic Matter
OUR	Oxygen Uptake Rate
PPB	Parts Per Billion
PPCP	Pharmaceuticals and Personal Care Products
SAC	Saccharin
SBR	Sequencing Batch Reactors
SUC	Sucralose
TC	Total Carbon
ThOD	Theoretical Oxygen Demand
TOC <sub>total,ini</sub>	Initial Total Organic Carbon
TOC	Total Organic Carbon
TS	Total Solids
TSS	Total Suspended Solids
UV	Ultraviolet
VSS	Volatile Suspended Solids
WWTP	Wastewater Treatment Plant

### **Greek Letters**

$\lambda$	Wavelength of Electromagnetic Radiation
$\beta$	Regression Model Parameter Term
$\epsilon$	Regression Model Error Term



# Chapter 1 – INTRODUCTION

## 1.1 Overview

The purpose of wastewater treatment has always been to eliminate the discharge of harmful pollutants into the aquatic environment. By far, the biggest focus has been on the removal of compounds that would otherwise cause the depletion of dissolved oxygen in receiving waters due to their degradation by microbial activity. Hence, wastewater treatment processes have been designed so that the degradation of these biodegradable compounds are completed prior to discharge through biochemical processes (Grady et al., 2011; Metcalf and Eddy, 2014). Years of development have made these processes well developed. However, it is simply impossible to remove all contaminants through this approach. This is due to the inability of biochemical processes to eliminate non-biodegradable compounds. These compounds pass through wastewater treatment processes essentially unchanged and may be present in large or small concentrations. They come from a variety of sources such as *pharmaceuticals and personal care products* (PPCPs), oil and gas industries, pesticide usage, and even food additives. Collectively, these compounds are referred to as *contaminants of emerging concern* (CECs). In fact, CECs can be further classified as *micropollutants* (MPs), if they are proven to have significant adverse effects on organisms of any kind. One of the most recently identified classes of CECs are non-nutritive sweeteners, otherwise referred to as *artificial sweeteners*. A graphical overview of how artificial sweeteners fit within these definitions is shown in **Figure 1-1**.

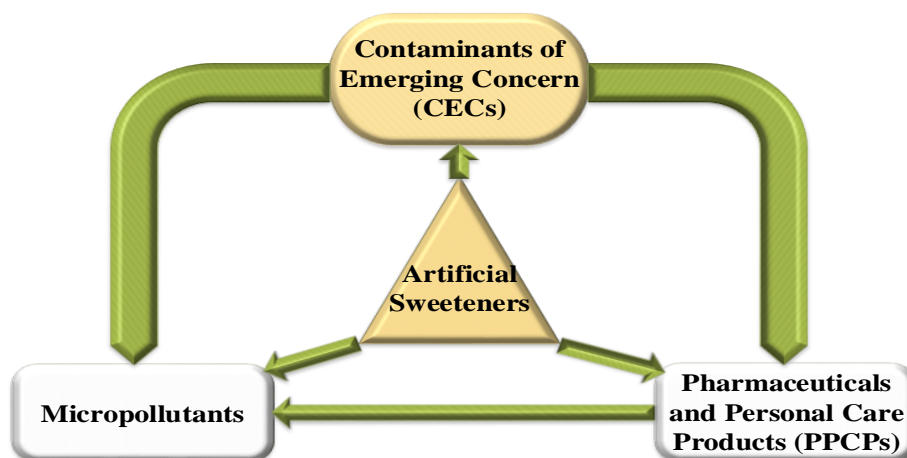


**Figure 1-1:** Overview of the classification of artificial Sweeteners as contaminants of emerging concern

The human body does not metabolize these compounds or may do so in very small amounts (Lange et al., 2012; Scheurer et al., 2011). These compounds are essentially unchanged when excreted. A surge in the development of more advanced analytical techniques for the detection of CECs has shed some light on the vast distribution of these compounds due to their persistence and the lack of relevant ecotoxicological data (Kokotou et al., 2012; Sang et al., 2014). Considering the already significant and ever-growing demand for low calorie confectionery products and beverages, the occurrence of these compounds in natural bodies of water have become of significant concern (Lange et al., 2012; Sang et al., 2014). *Advanced oxidation processes* (AOPs) are a class of technologies that have proven to be effective in dealing with compounds of poor biodegradation characteristics. Many studies have proven such technologies to be successful in eliminating target contaminants that fall under the classification of CECs (Ghafoori et al., 2015; Parsons, 2004; Suty et al., 2004). Therefore, it is not surprising that the focus of many studies for the removal of artificial sweeteners have been on a variety of AOPs.

With respect to the existing publications, the motivation for this study was to contribute to the understanding of the degradation of artificial sweeteners through AOPs. Therefore, the treatment of an aqueous system containing three artificial sweeteners (a multicomponent aqueous system of artificial sweeteners) was investigated in this study for the first time. The experiments in this study were carried out in multiple steps to investigate the effects of various parameters used in AOPs and to compare and justify their application with biochemical degradation through respirometry.

Chapter 2 covers a variety of topics involving artificial sweeteners, organized into two segments. The first highlights the concerns and the extent of the identified issues with artificial sweeteners in the environment such as their distribution, health impact and the ecotoxicological concerns. The focus is then shifted towards the current state of research involving application of AOPs in dealing with these MPs by surveying the existing reports.

Chapter 3 primarily focuses on the methodology and the justification behind the experimental approach. Details of chemicals, equipment and analytical instruments are presented along with the schematic diagrams of the various experimental setups. Detailed experimental procedures are also reported in this chapter.

In Chapter 4, all the experimental results are organized and discussed. The discussions begin with the results of single component degradation of artificial sweeteners in aqueous matrices with the purpose of understanding treatment response trends. The discussion is then extended to the degradation of the artificial sweeteners in a multicomponent aqueous system. The respirometric results are presented here as well, with discussions and justifications for the use of UV/H<sub>2</sub>O<sub>2</sub>.

Finally, all the concluding and closing remarks are presented in Chapter 6, with recommendations for future investigations.

## **1.2 Research Objectives**

The primary objective of this study was to extend the application of a UV/H<sub>2</sub>O<sub>2</sub> process to remove three artificial sweeteners, namely *aspartame* (ASP), *acesulfame potassium* or *acesulfame K* (ACE) and *sucralose* (SUC) in multicomponent aqueous matrices. The screening for significant effects and interactions of experimental factors such as sweetener concentration, operating temperature and applied H<sub>2</sub>O<sub>2</sub> dosages were screened through a statistical *design of experiments* (DOE). The biodegradation characteristics of the three sweeteners in the presence of activated sludge through respirometry were also investigated. Finally, the suitability of AOPs for targeting these MPs were assessed by a comparing the experimental results of the UV/H<sub>2</sub>O<sub>2</sub> process to the ones obtained from respirometry to assess whether the use of AOPs are justified.

## Chapter 2 – LITERATURE REVIEW

### 2.1 Introduction

In 2009, the occurrence of the artificial sweetener ACE in the aquatic environment was highlighted for the first time (Buerge et al., 2009). Due to its persistence, it was proposed that ACE could be used as an ideal marker for domestic wastewater in groundwater sources. In the same year, the presence of seven artificial sweeteners in German water, wastewater and soil samples were reported (Buerge et al., 2009; Scheurer et al., 2009). Newer and superior methods of detection with increased sensitivity and lower limits of detection were eventually employed to screen for another commonly used artificial sweeteners namely, SUC (Ferrer and Thurman, 2010). SUC and ACE were soon recognized as compounds that were so persistent that they were considered as potential tracers for rivers and soil sample contamination with wastewater (Scheurer et al., 2011; van Stempvoort et al., 2011). However, the first expression of concern was in the form of a review study in 2012 where authors recognized artificial sweeteners as a new class of emerging contaminants due to their persistence. It was determined that ACE, *sodium cyclamate* (CYC), *saccharin* (SAC) and SUC were all present in a variety of aquatic environment. Following the discovery of the extent of their distributions, they were flagged as micropollutants specific (but not limited) to the effluents of wastewater treatment plants (Lange et al., 2012).

The reported concentrations of artificial sweeteners found in the aquatic environment are typically in the *parts per billion* (PPB) range, several orders of magnitude lower than the *acceptable daily intake* (ADI) of 2-40 mg/kg (for various sweeteners) of body weight in humans (Kokotou et al., 2012; Lange et al., 2012). However, the ecotoxicological effects of these compounds are not very well understood. Furthermore, there is little information on the environmental persistence of these compounds, their transformation products, and their environmental impacts in the literature. Out of these four compounds, ACE and SUC have been found in much higher concentrations than any other PPCPs. Both compounds are easily soluble in water but are persistent with low adsorptivities (Spoelstra et al., 2013).

Since the publication of these studies, there has been a large flux of investigations in an attempt to understand the ecotoxicological effects of artificial sweeteners in natural bodies of water. New

data has emerged regarding their degradation in conventional wastewater treatment processes and various advanced techniques, including AOPs. Throughout the rest of this chapter, a survey of current available data is presented regarding the environmental occurrence of various artificial sweeteners. Furthermore, a comprehensive discussion of the available technologies to remove artificial sweeteners from aqueous matrices, especially AOPs, is provided.

## **2.2 Global Distribution of Artificial Sweeteners in Water Resources**

Artificial sweeteners have been detected globally in tap water, lakes, rivers, groundwater and even soil samples. Data is available for a total of 38 countries worldwide with the majority of studies being from European countries, with some data for North America and parts of Asia (Mangala, 2019). ACE and SUC have been reported in every study and consistently appear in the largest concentrations not only among artificial sweeteners, but also many other CECs (Lange et al., 2012; Lee et al., 2019).

In the United States, SUC has been detected in concentrations of 0.8 – 1.8 µg/L and SAC with a concentration of up to 5 µg/L downstream of a wastewater treatment plant effluent discharge point (Ferrer and Thurman, 2010). Available data for residential septic systems in the United States show that SUC cannot be degraded in such systems (Lange et al., 2012). SUC was detected in 15 out of 19 samples taken from source water used for drinking water treatment plants in a range of 47-2900 ng/L and in 13 out of 17 samples taken from drinking water treatment plants in a range of 49-2400 ng/L. The average SUC concentration in the source water for some drinking water plants was found to be 240 ng/L (Mawhinney et al., 2011). It should be noted that in these studies, SUC was present in source water only when *wastewater treatment plant* (WWTP) effluents were discharged into the same body of water. In Canada, data is more readily available for environmental samples involving SUC with reported concentrations ranging from 21 µg/L up to 40 µg/L. A study over six years during 2008-2014 showed that SUC concentrations were found to be decreasing from a concentration of 40 µg/L to approximately 1 µg/L. It has been concluded that SUC may be degrading naturally but at a slow rate (Robertson et al., 2016).

European publications have also highlighted the concern of drinking water contamination with artificial sweeteners. SUC has been in use in Europe only since 2004, yet by 2009 a comprehensive

study done across 27 European countries reported surface water samples from UK, Belgium, Netherlands, France, Switzerland, Spain, Italy, Norway and Sweden to contain SUC up to 1 µg/L (Loos et al., 2009). The issue is that more often than not, WWTP effluents are discharged into bodies of water where drinking water is eventually drawn from. In Switzerland, ACE concentrations ranged between 12-46 µg/L in various treated and untreated wastewater samples. Concentrations of up to 4.7 µg/L has been reported in groundwater where there has been a potential for infiltration from rivers receiving WWTP effluents. In some cases, where these surface waters are used as a withdrawal source for drinking water plants, ACE has been detected in concentrations of up to 7 µg/L in treated water while SUC has been detected in concentrations of up to 2.4 µg/L (Lange et al., 2012). In Finland, four artificial sweeteners including ACE, SUC, SAC and CYC were screened for and detected in environmental samples (rivers and lakes) collected. ACE and SAC were detected in all samples with maximum concentrations of 9600 ng/L and 490 ng/L respectively. CYC and SUC were detected in most samples with concentrations of up to 210 ng/L and 1000 ng/L respectively (Perkola and Sainio, 2014). In Sweden, SUC has been identified as one of the dominating MPs found in surface waters that are affected by WWTPs, comprising of 27% of the total concentration of the detected MPs (Gago-Ferrero et al., 2017). Five artificial sweeteners including ACE, SUC, SAC, CYC and ASP were screened for and detected in the bay of Cadiz in Spain, which is a body of water receiving WWTP effluents. Among them, SUC was found to have the highest concentrations in the range of 0.43 µg/L to 1.44 µg/L across four sampling points. All other sweeteners were detected in concentrations of one order of magnitude lower (Baena-Nogueras et al., 2018). It should be noted that in some reports, ACE has been found in much larger concentrations than SUC (Robertson et al., 2016; Spoelstra et al., 2013). Surface water samples from four sampling points in Barbados were screened for artificial sweeteners including ACE and SUC. ACE was detected in all samples ranging between 19 ng/L to 571 ng/L. SUC was detected in three out of four, however in much smaller concentrations in the range of 3 ng/L to 19 ng/L (Edwards et al., 2017).

SUC has been also been detected in surface water samples taken from the Dongjiang River basin in China, with an average concentration of 3640 ng/L. Groundwater samples showed an average concentration of 2440 ng/L for this compound (Yang et al., 2018). There are also reports of four sweeteners in tap water samples taken in Tianjin, China, with two compounds being ACE and

SUC. The concentrations of the sweeteners are as follows: 0.12 µg/L for SUC, 0.68 µg/L for ACE, 0.10 µg/L for SAC and 36.0 µg/L for CYC (Berset and Ochsenbein, 2012). The same compounds have been detected in surface water samples in Singapore. Interestingly, their occurrence was attributed to surface water runoff as opposed to WWTP effluent discharge. Nevertheless, ACE was the most frequently detected artificial sweetener, with a median concentration of 47 ng/L in surface water, with reports of its concentration being as high as 780 ng/L. The frequency of the occurrence of SUC was not nearly the same; nevertheless, there are reports of SUC contaminations of up to 530 ng/L (Tran et al., 2014). Groundwater sources in Korea have been found to contain artificial sweeteners as well. Once again, ACE was found with the largest concentrations at a range of 90 ng/L to 1330 ng/L. SAC was detected with a range of 5 ng/L to 36 ng/L while the concentration of CYC was detected up to 155 ng/L. ASP was tested for and detected for the first time with concentrations of up to 9 ng/L (Lee et al., 2019). It is worth mentioning that some sweeteners such as SAC are registered as an additive in piglet feed. It has been observed that SAC fed to piglets was largely unchanged and found in manure in concentrations of up to 12 mg/L (Buerge et al., 2011). Hence, contamination due to surface runoff in water sources adjacent to farms is very possible.

## 2.3 Environmental Impact and Ecotoxicological Data

Studies of various bodies of water have shown that artificial sweeteners are found at levels that are much higher than that of many other CECs (Lange et al., 2012; Lee et al., 2019; Nguyen et al., 2018). Considering the widespread distribution of artificial sweeteners in the aquatic environment, the biggest concern regarding these compounds is the long-term environmental impact due to chronic exposure. Unfortunately, data is very scarce as these compounds are relatively new and have not been fully studied. Nevertheless, the existing data are concerning. These concerns will be discussed next.

Some common short-term ecotoxicological tests include the OECD 209 activated sludge respiration inhibition test (10-min test), acute immobilization test with *Daphnia magna* (48 h) and the reproduction inhibition assay with limnic green algae *Scenedesmus vacuolatus* (24 h). Long-term exposure can be studied with the growth inhibition assay with duckweed *Lemna minor*. The response parameter in these tests is the *lowest observed effect concentration* (LOEC). The LOEC

of SUC, ACE, SAC and CYC were found to be 1000 mg/L in all the tests (Stolte et al., 2013). These findings suggest that these sweeteners did not have adverse effects on activated sludge and *D. magna*, *L. minor* could not use any of the compounds as a carbon source. Surprisingly, SUC was also found to significantly increase photosynthesis in *L. minor* in a 21 day exposure test as opposed to previous reports (Amy-Sagers et al., 2017).

Other studies have shown that SUC has no significant acute and long-term effects on mobility, survival and reproduction of *D. magna* (Sladkova et al., 2016). It was however observed that the organisms' swimming speed and height were noticeably altered under environmentally relevant concentrations (Wiklund et al., 2012). Based on the alarming observations, the authors pursued experiments beyond common standard ecotoxicological tests to find out SUC is capable of inducing significant feeding and behavioural abnormalities in crustaceans. These results suggest concerning neurological and other physiological changes in these organisms (Wiklund et al., 2014). As for other artificial sweeteners, CYC and SAC have been found to possess cytotoxic and mutagenic effects on *Allium cepa* and *Mus musculus* with environmentally relevant concentrations (Victor et al., 2017).

The ecotoxicity of many heavy metals depends on their speciation and can be influenced by the presence of other compounds. This effect has been studied on *Scenedesmus obliquus* for  $\text{Cd}^{2+}$  and  $\text{Cu}^{2+}$  in the presence of ACE and SUC. It has been observed that the toxicities of the two heavy metals on the algae species can decrease in the presence of SUC and ACE, more so with the latter. Hence, an increased concentration of ACE in the environment correlates to increased bio-concentration of  $\text{Cd}^{2+}$  in micro algae and consequently, bio-magnification in the same food chain (Hu et al., 2016). Chronic exposure of higher order organisms such as the *Cyprinus carpio* (common carp) to SUC has shown to induce oxidative damage in lipids and proteins of the fish, especially in the gills. Modified antioxidant enzyme levels were also observed. The potential for bioaccumulation of SUC in the common carp was however deemed to be insignificant (Saucedo-Vence et al., 2017).

A significant concern with various CECs is their transformation products due to photodegradation (e.g. due to UV exposure in the environment). This is already shown for certain PPCPs (Dantas et al., 2010; Jung et al., 2008). The same concern exists for artificial sweeteners. For example, the



intermediates of the photocatalytic degradation in the presence of  $\text{TiO}_2$  for SUC have shown toxicity levels significantly higher than the parent compound. Similar results have been obtained for ACE (Sang et al., 2014). Other PPCPs that were found to have such toxic intermediates have received a lot of attention. More studies on toxicity screening are presented later in Section 2.6.2.

## **2.4 Health Impacts of Artificial Sweeteners in Humans**

Artificial sweeteners have been subjected to some controversy primarily due to a few early reports of carcinogenic effects seen in laboratory mice. These compounds have since been studied in depth to establish links to cancer and other problems caused by them. Overall, the effect of artificial sweetener consumption on cancer has been the subject of debate for decades. There have been a growing number of publications in the past decade focusing on this subject. It should be noted that the studies have focused on the direct consumption of artificial sweeteners by humans. Studies on the consumption of chronic consumption of these compounds in environmentally relevant concentrations do not exist as of yet.

The largest review publication on the subject has compiled data from various publications with a total sample population of nearly 600,000 participants. A large variety of cancers has been the primary focus of the studies reviewed. The data has been inconclusive in linking cancers to the consumption of artificial sweeteners (Mishra et al., 2015).

There are a few publications that have linked the consumption of artificial sweeteners to some health impacts in both humans and animals (Bian et al., 2017; Ali and Devrukhkar, 2016). In biochemistry, glycation is defined as the bonding of the carbonyl groups of a sugar molecule to the amino groups of a protein, nucleic acid and a lipid molecule. Glycation has been linked to a number of diseases such as Alzheimer's, Parkinson's, diabetes mellitus, etc. and has been associated with sugar consumption. ASP and SUC are artificial sweeteners used as a sugar substitute in foods and beverages. Both of these compounds (and commercial products containing them) have been found to go through glycation reactions much like natural sugars (Ali and Devrukhkar, 2016). Furthermore, chronic SUC exposure in mice was found to be influential in altering gut microbiota and was associated with inflammation in the hosts. Based on the observations, it has been concluded that long term SUC exposure in humans in the suggested ADI

levels may increase the risk of tissue inflammation by disrupting the gut microbiota (Bian et al., 2017).

## **2.5 Fate of Artificial Sweeteners in Conventional Wastewater Treatment Processes**

Back in 2012, a review study summarized the concentrations of ACE, SUC, SAC and CYC in various WWTPS in Switzerland, Germany, United States and Israel (Lange et al., 2012). It was highlighted that both ACE and SUC did not undergo any noticeable degradation in Switzerland and Germany. In addition, no degradation was observed for SUC in Sweden. Only septic system effluent data was reported in the United States and Israel. Nevertheless, the presence of both sweeteners in high concentrations suggest the same trend.

Data from two WWTPs in the United States show that some sorption to suspended particulate matters is possible for ACE (~10%) (Subedi and Kannan, 2014). In comparison, all of the influent SUC was essentially discharged with the effluent without any sorption (<1%) as reported in the same study. The only American study on ASP suggest that up to 50% sorption to suspended particulate matter is possible (Subedi and Kannan, 2014). Data for SUC is available for treated wastewater discharged to wetlands in Florida. SUC was detected in the inflow to the wetlands at a concentration of 0.024 mg/L and a concentration of 0.021 mg/L in the outflow. Although data from the WWTP influent was not reported, it is evident that biological treatment was not effective in the removal of SUC (Heider et al., 2018). Furthermore, data obtained from a Canadian aerated lagoon study of various PPCPs also show that SUC is very persistent, with no degradation and even accumulation in biochemical treatment systems (Hoque et al., 2014). Hence, all North American studies on SUC agreed with each other (see Section 2.2).

Although the persistence of ACE has been agreed upon in the scientific community, newer studies done on full scale WWTPs in China have shown other trends. A comprehensive study done on various WWTPs in China has shown an average removal efficiency of 85% for this compound (Yang et al., 2017). Yet in another study, it was found that the removal of ACE is up to 50% in multiple WWTPs. It was also concluded that biological processes that involve denitrification were better in removing ACE, with the A<sup>2</sup>/O being the most efficient process (Li et al., 2018). Similar

trends were obtained from 13 WWTPs in Germany, where a removal range of 6% - 88% has been reported for ACE (Castronovo et al., 2017). Additionally, ACE was found to have the highest influent concentration among several MPs screened for in two WWTPs in Vietnam. A removal of approximately 50% for ACE was observed based on the comparison of influent and effluent concentrations (Nguyen et al., 2018). Data from four WWTPs in Spain show the presence of both SUC and ACE along with SAC, CYC and ASP. Interestingly, a negative average removal efficiency of -200% was observed for SUC, while ACE was found to have an average removal of 76%. The other three sweeteners were degraded quite well with efficiencies approaching 90% (Baena-Nogueras et al., 2018).

Overall, the most recent review of global data have been essentially show that SUC remains as the most persistent artificial sweetener globally, with virtually no degradation in conventional wastewater treatment processes (Tran et al., 2018). The majority of available data for ACE suggest poor removal by biological means. This is especially true for older studies (prior to 2014). However, removal of various degrees has been reported in parts of Asia and Europe. A possible explanation is the evolution of a catabolic pathway in microorganisms resulting in better potential for the removal of this compound (Kahl et al., 2018). A summary of the global distribution of artificial sweeteners is shown in ***Table 2-1***.

**Table 2-1:** Summary of global data for the concentrations (in **ng/L**) of artificial sweeteners in WWTP influent and effluent streams. MQL = Method Quantification Limit. Adapted from (Tran et al., 2018)

Compound	Asia		North America		Europe	
	<i>Influent</i>	<i>Effluent</i>	<i>Influent</i>	<i>Effluent</i>	<i>Influent</i>	<i>Effluent</i>
<b>ACE</b>	560 – 13400	5840 – 9147	90 – 2270	600 – 4330	12000 – 43000	15000 – 46000
<b>SUC</b>	1100 – 6520	1300 – 5490	17500 – 46100	18700 – 48900	2000 – 9100	2000 – 8800
<b>CYC</b>	< <i>MQL</i> – 66400	< <i>MQL</i> – 160	-	-	10000 – 65000	< <i>MQL</i> – 450
<b>SAC</b>	9310 – 389000	< <i>MQL</i> – 2370	1860 – 2500	220 – 700	7100 – 18000	< <i>MQL</i> – 1800

## 2.6 Advanced Oxidation Processes for the Removal of Artificial Sweeteners

### 2.6.1 Overview of Advanced Oxidation Processes (AOPs)

AOPs are a class of treatment processes used in both water and wastewater treatment. They are typically used to destroy trace constituents in water matrices after other treatment methods have been applied. They can also be used to partially degrade compounds to improve biodegradability prior to conventional treatment processes (Metcalf and Eddy, 2014). The principle by which AOPs operate are primarily through the generation of *hydroxyl radicals* ( $HO^\bullet$ ), which are very strong oxidizing agents. In sufficient amounts,  $HO^\bullet$  are capable of completely oxidizing (ultimate degradation or mineralization) of most organic compounds. Other degrees of degradation are reported in the literature. Primary degradation is simply a structural change in the parent compound. Acceptable degradation (defusing) is a structural change where the toxicity of a compound is reduced. Unacceptable degradation (fusing) is a structural change in the parent compound in which the toxicity is increased (Rice, 1994). The products of mineralization include carbon dioxide, water and mineral acids. **Table 2-2** summarizes the relative strength of  $HO^\bullet$  in comparison to that of other commonly used oxidizing agents in water and wastewater treatment.

**Table 2-2:** Comparison of the oxidizing potentials of various oxidants used in water and wastewater treatment processes. Adapted from (Metcalf and Eddy, 2014)

Oxidant	Electrical Potential (V)
Fluorine (not used, comparison purposes only)	2.87
<b><i>Hydroxyl Radical</i></b>	<b>2.80</b>
Ozone	2.08
Hydrogen Peroxide	1.78
Permanganate	1.67
Free Chlorine	1.36
Chlorine dioxide	1.27
Oxygen	1.23

It should be noted that AOPs are different from other advanced treatment processes (e.g. adsorption/absorption, ion exchange, stripping and other processes) as the target compounds are actually destroyed rather than transferred. This property of AOPs renders them very attractive in

dealing with the current issues imposed by artificial sweeteners (see Section 2.3 ). Several processes exist to achieve the generation of  $HO^\bullet$ . Overall, the processes can be grouped under two classifications. Photochemical AOPs are a class of AOPs in which the generation of hydroxyl radicals is achieved through ultraviolet (UV) illumination. If  $HO^\bullet$  are generated through reactions other than UV illumination, they are classified simply as chemical AOPs. The classification of common AOPs as reported is shown in **Figure 2-1**.

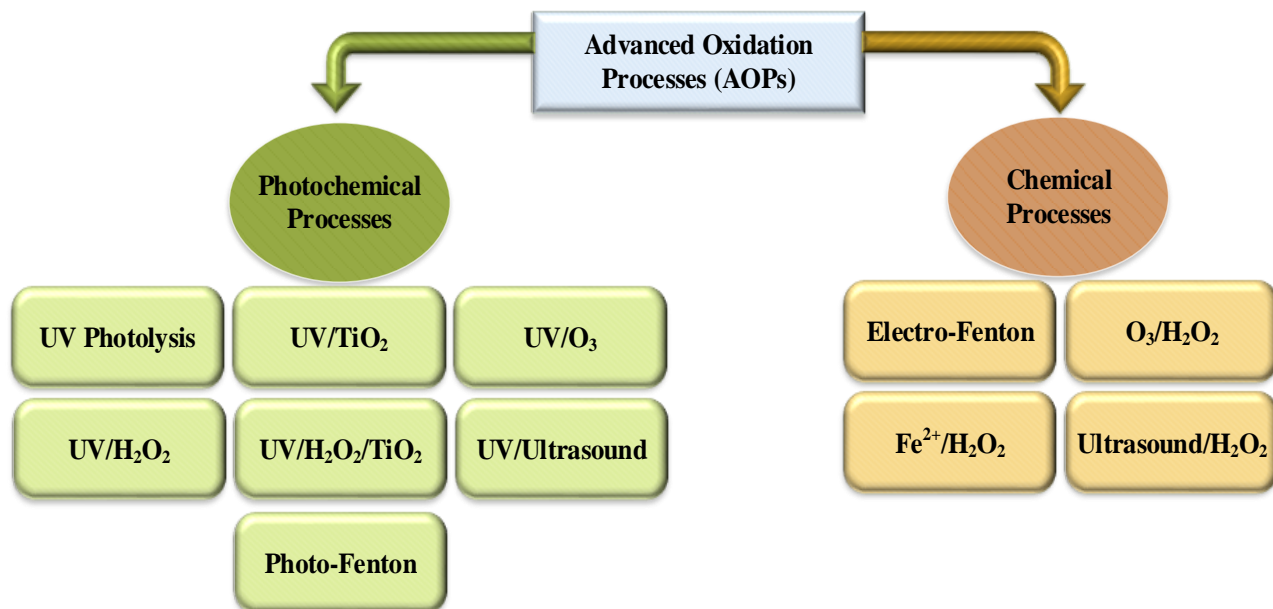


**Figure 2-1:** A generalized classification of various advanced oxidation processes. Adapted from (Biń and Sobera-Madej, 2012)

Photochemical processes occur due to a phenomenon known as photolysis. Photolysis refers to processes in which the constituents of a water matrix are broken down through exposure to photonic energy from a light source. Traditionally, two types of mercury-based UV lamps have been utilized in photolysis processes. These include low-pressure mercury lamps, and medium-pressure mercury lamps. Low-pressure lamps emit most of their energy in the UV-C ( $\lambda \cong 254$  nm) region, while medium pressure lamps emit their energy in a variety of wavelengths ( $\lambda \cong 200$ -320 nm). The absorption of photons by compounds in water cause the electrons in the outer orbitals of compounds to become unstable, resulting in increased reactivity or even splitting (Metcalf and Eddy, 2014). In general, the absorption of light by any compound dissolved in water can be described by the Beer-Lambert Law as follows:

$$A_{\lambda} = -\log\left(\frac{I}{I_0}\right) = \varepsilon_{\lambda} C x = k_{\lambda} x$$

Where:

$A_{\lambda}$  = absorbance, dimensionless

$I$  = light intensity after passing through a solution at wavelength ( $\lambda$ ),  $\left(\frac{\text{einsteins}}{\text{cm}^2 \text{ s}}\right)$

$I_0$  = light intensity after passing through a blank solution at wavelength ( $\lambda$ ),  $\left(\frac{\text{einsteins}}{\text{cm}^2 \text{ s}}\right)$

$\varepsilon_{\lambda}$  = base 10 extinction coefficient of light absorbing solute at wavelength ( $\lambda$ ),  $\left(\frac{\text{L}}{\text{mol cm}}\right)$

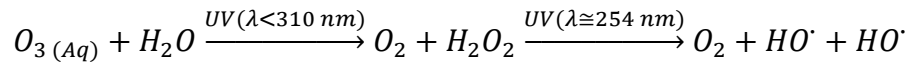
$\lambda$  = wavelength, (cm)

$C$  = concentration of light absorbing solute,  $\left(\frac{\text{mol}}{\text{L}}\right)$

$x$  = length of light path (cm)

$k_{\lambda}$  = absorptivity (base 10),  $\left(\frac{1}{\text{cm}}\right)$

Photolysis by itself is not very efficient in degradation of organic constituents in water. However, it can be engineered so that  $HO^{\cdot}$  can be produced. Under UV illumination,  $O_3$  lead to the production of  $HO^{\cdot}$ . This occurs according to the following chemical reaction:



An example of an AOP in which  $HO^{\cdot}$  is generated in absence of UV illumination is Fenton's reaction. The primary reaction of interest is the reaction of  $H_2O_2$  with Iron (II) to generate  $HO^{\cdot}$  (Rachmilovich-Calis et al., 2005). This process will not be discussed in detail.

Major factors to consider when choosing a treatment process such as AOPs, include the capability of continuous operation and the commercial availability of the process. Commercially available AOPs include UV/ $O_3$ , UV/ $H_2O_2$  and a variety of Fenton's reactions. The advantages and limitations of common AOPs are summarized in **Table 2-3** (Crittenden et al., 2012).

**Table 2-3:** Advantages and limitations of commercially available advanced oxidation processes. Adapted from (Crittenden et al., 2012)

Process	Advantages	Limitations
UV/H <sub>2</sub> O <sub>2</sub>	H <sub>2</sub> O <sub>2</sub> is fairly inexpensive and stable for on-site storage	Residual H <sub>2</sub> O <sub>2</sub> removal is required, not feasible if water matrix absorbs more UV light energy than H <sub>2</sub> O <sub>2</sub>
O <sub>3</sub> /H <sub>2</sub> O <sub>2</sub>	Waters with poor UV transmittance can be treated	Can be expensive and inefficient
UV/O <sub>3</sub>	Residual removal of O <sub>3</sub> is not necessary	H <sub>2</sub> O <sub>2</sub> needs to be produced first from UV and O <sub>3</sub> , very inefficient process
Fenton's Reactions	Effluents may already contain Fe required to drive the Fenton's process	Only possible in low pH limits
UV/TiO <sub>2</sub>	Activated in near UV light, greater light transmission is achievable	Fouling of the catalyst, fouling of the UV lamp, lack of commercial availability

Of course, the wastewater characteristics ultimately dictate the choice of AOP. However, the applicability of the UV/H<sub>2</sub>O<sub>2</sub> has been proven for real wastewater matrices and is operable in continuous mode (Bustillo-Lecompte et al., 2015; Bustillo-Lecompte and Mehrvar, 2017; Crittenden et al., 2012). Furthermore, the UV/H<sub>2</sub>O<sub>2</sub> process is commercially available with its applications demonstrated in the treatment of wastewater in textile industries and pulp and paper industries (Parsons, 2004). It should be noted that the reaction pathways for the generation of HO· under UV illumination are complicated and very difficult to predict. Exposure of H<sub>2</sub>O<sub>2</sub> to UV irradiation initiates a chain of reactions starting with the cleavage of the molecule and the production of HO·. Reactions can be classified as initiation, propagation, and recombination/termination (Oppenländer, 2002). With that said, the generation of HO· through UV illumination through the UV/H<sub>2</sub>O<sub>2</sub> process is carried out by mechanisms shown in **Table 2-4**. The mechanism by which HO· can destroy trace organic compounds such as artificial sweeteners are shown in **Table 2-5** as suggested in the literature (Solarchem Environmental Systems, 1994).



**Table 2-4:** Reaction mechanisms for the generation of hydroxyl radicals through the UV/H<sub>2</sub>O<sub>2</sub> process. Adapted from (Oppenländer, 2002).

Reaction	Mechanism
Initiation	$H_2O_2 \xrightarrow{UV (\lambda \cong 254 \text{ nm})} 2 HO^\cdot$
Propagation	$H_2O_2 + HO^\cdot \rightarrow HO^\cdot_2 + H_2O$ $HO^\cdot_2 + H_2O_2 \rightarrow HO^\cdot + H_2O + O_2$
Recombination	$HO^\cdot + HO^\cdot \rightarrow H_2O_2$ $HO^\cdot + HO^\cdot_2 \rightarrow H_2O + O_2$ $HO^\cdot_2 + HO^\cdot_2 \rightarrow H_2O_2 + O_2$
Net Reaction	$2H_2O_2 \rightarrow 2H_2O + O_2$

**Table 2-5:** Mechanisms for the reaction of hydroxyl radicals with organic compounds. “R” denotes unsaturated aliphatic or aromatic organic compound. Adapted from (Solarchem Environmental Services, 1994)

Reaction Mechanism	Chemical Equation
Radical Initiation	$R + HO^\cdot \rightarrow ROH^\cdot$
Hydrogen Abstraction	$R + HO^\cdot \rightarrow R^\cdot + H_2O$
Electron Transfer	$R_n + HO^\cdot \rightarrow R_n^\cdot + OH^-$
Radical Combination	$HO^\cdot + HO^\cdot \rightarrow H_2O_2$

## 2.6.2 The Removal of Artificial Sweeteners through Advanced Oxidation Processes (AOPs)

### 2.6.2.1 Overview

Currently, the control and partial removal of artificial sweeteners are carried out through technologies such as activated carbon filtration and reverse osmosis. However, their complete removal is not attainable through these techniques. This is especially true for SUC and ACE (Salimi et al., 2017). AOPs have been proposed as suitable alternatives. The generation of  $HO^\cdot$  in such processes facilitate the removal of trace organic compounds such as artificial sweeteners.

The removal of artificial sweeteners through the application of AOPs have been studied to some extent in recent years. Due to their popularities, ACE and SUC have been the primary focus of these studies, with various attempts to understand their oxidation kinetics and transformation products. For these sweeteners, UV based AOPs have been investigated the most (Chen et al.,

2014; Hollender et al., 2009; Kattel et al., 2017; Li et al., 2016; Scheurer et al., 2014; Sharma et al., 2014; Xu et al., 2018). In general, treatment through  $HO^\bullet$  has been very promising in the degradation of SUC (up to 100%) and ACE (approximately 70%). Meanwhile, the degradation of ASP through the same approach has not been very good, with a degradation of up approximately 50% (Toth et al., 2012).

#### **2.6.2.2 Laboratory Studies on Sucralose**

A variety of AOPs have been studied for the removal of SUC from aqueous matrices. Considering its commercial availability, ozonation has been one of the most applied techniques for this purpose. It has been reported that in the presence of excess  $O_3$ , SUC undergoes primary degradation in ultrapure water, especially under neutral to basic conditions. The *total organic carbon* (TOC) removal in such systems has been found to vary between 20-30%. The rate of the degradation has been found to decrease significantly under acidic conditions and in the presence of carbonate and bicarbonate. This is not surprising as carbonate and bicarbonate species are well known  $HO^\bullet$  scavengers, resulting in significant reduction in the efficiencies of AOPs. SUC transformation products after ozonation processes include carbonyl compounds, carboxylic acids, aldehydes and probable chlorine containing compounds (Hu et al., 2017).

The degradation of SUC has also been investigated in other AOPs utilizing UV irradiation. Ozonation has proven to be effective in degrading SUC when accompanied by UV irradiation. Under neutral pH conditions, UV/ $O_3$  has been shown to result in a mineralization efficiency of up to 90% after a 120 min of treatment. Furthermore, the use of UV is proven to significantly improve the detoxification of SUC degradation intermediates in presence of *D. magna* in comparison to  $O_3$  alone (Xu et al., 2018). Removals of 2% for UV treatment alone, 70% for UV/ $H_2O_2$  and 93% for UV/peroxydisulfate have been reported all at a treatment time of 60 min. The highest removal was observed under slightly acidic to neutral conditions. Toxicity screening tests on *Vibrio fischeri* have shown that toxic intermediates do form initially, but disappear as the reaction approaches completion (Xu et al., 2016).

Photo-Fenton and  $TiO_2$  photocatalytic processes have also been investigated for the degradation of SUC. Through statistical analysis by means of response surface methodology, optimal conditions have been identified and resulted in a maximal degradation efficiency of 96% for the

Photo-Fenton process (pH~3) and 89% for the TiO<sub>2</sub> photocatalytic process. Toxicity tests revealed that inhibition increased significantly until the halfway point of treatment, and reduced to levels below that of the initial solution for *V. fischeri* (Calza et al., 2013).

Other Fenton-based AOPs have also been studied for the degradation of SUC. Electro-Fenton oxidation is another proven method of mineralizing SUC effectively at room temperature. Parameters studied included catalyst concentration, applied current, and anode type. A removal of 94% was achieved in one study. Of the various transformation products, only oxalic acid was identified to remain in the solution in small amounts. A sharp inhibition increase was observed initially in all cases with *V. fischeri*, and dropped to below zero after a treatment time of 350 min. The presence of chloride ions has been reported in the final solution with the Pt anode. A *boron doped diamond* (BDD) anode was also tested by in the same study. Some degradation was observed but complete removal was not achieved (Lin et al., 2017).

#### **2.6.2.3 Laboratory Studies on Acesulfame K**

Photocatalytic degradation of ACE has been investigated quite thoroughly. Three Ti-O<sub>2</sub> based photocatalysts, namely TiO<sub>2</sub>-P25, TiO<sub>2</sub>-SG1 and TiO<sub>2</sub>-SG2, have been used to investigate the degradation of ACE under UV irradiation ( $\lambda$ ~315-400 nm). The concentration of ACE and the photocatalysts were 10 mg/L and 1 g/L respectively. In all cases, ACE was completely eliminated after 30 min of UV irradiation (López-Muñoz et al., 2018). The efficiency of photocatalytic degradation of ACE through immobilized nano-TiO<sub>2</sub>/UV has also been studied in the presence of persulfate. Under optimal conditions, complete removal of ACE has been achieved after 180 min, with 80% removal after 30 min and 88% removal after 60 min (Nam et al., 2018). Using non-modified TiO<sub>2</sub>, degradation ranges between 70% - 90% have been reported with UV-LED illumination at 120 min (Srivastava et al., 2019). Other studies suggest complete mineralization of ACE in the presence of non-modified TiO<sub>2</sub>. Treatment time was however much longer, with 19 h of irradiation and a TiO<sub>2</sub>:ACE mass ratio of 20:1. Embryotoxicity tests on zebra fish *Danio rerio* revealed that toxicity of transformation products was insignificant at lower ACE concentrations (up to 1000 ppm). Significant toxicity was reported at higher ACE concentrations (>5000 ppm) (Li et al., 2016). Another photocatalyst that has been studied is ZnO. However, with maximal

degradation of below 65%,  $\text{TiO}_2$  and its derivatives are better choices of photocatalysts (Srivastava et al., 2019).

Although not an AOP, chlorination can also degrade ACE, especially under acidic conditions. However, this was linked to the greater oxidizing strength of  $\text{HOCl}$  as compared to that of dissociated  $\text{OCl}^-$ . Furthermore, very high removal of ACE was observed in ultrapure water and tap water (>93%) after 6 h, while a removal of only 68% was observed in wastewater samples. Toxicity tests revealed that the intermediates were considerably more toxic than ACE parent compound. The intermediates were very toxic from the beginning of the treatment process to the midpoint and gradually decreased in toxicity towards completion. The final chlorination products of ACE were slightly more toxic than the compound itself. Due to this fact, the use of chlorination is not recommended for the removal of ACE from aqueous matrices (Li et al., 2017).

At a concentration of 200  $\mu\text{g/L}$ , ACE has been known to undergo complete transformation in ultrapure water with an applied ozone dosage of 1  $\text{mg/L}$ . However, less than 10% mineralization was observed for this compound (Wick et al., 2011). UV irradiation ( $\lambda \cong 254 \text{ nm}$ ) has been shown to be effective in degrading ACE in low concentrations. Removals of up to 90% were observed in ultrapure water for concentrations of 0.001 -100  $\text{mg/L}$ . Interestingly, no degradation was observed with UV irradiation ( $\lambda \cong 254 \text{ nm}$ ) alone when the initial concentration of ACE was increased to 1000  $\text{mg/L}$ . The effect of pH was proven negligible in this study. The photodegradation of ACE was found to be different in environmental water matrices, with removal levels of 19-37%. This is of course expected, and likely due to the presence of *natural organic matter* (NOM) (Scheurer et al., 2014). A removal of 64% after 19 h of UV irradiation ( $\lambda \cong 254 \text{ nm}$ ) has been reported with an initial ACE concentration of 400  $\text{mg/L}$  (Li et al., 2016).

The complete degradation of ACE has been achieved through  $\text{UVA}/\text{H}_2\text{O}_2/\text{Fe}^{2+}$  and  $\text{UVA}/\text{S}_2\text{O}_8^{2-}/\text{Fe}^{2+}$  ( $\lambda \cong 315 - 400 \text{ nm}$ ) processes in ultrapure water. The same trend has been observed in ground water and WWTP effluent, although at a slower rate.  $\text{UVA}/\text{H}_2\text{O}_2/\text{Fe}^{2+}$  resulted in faster degradation due to  $\text{HO}^\cdot$  species being more effective than  $\text{SO}_4^\cdot$  species in oxidation of ACE. It has been shown that the  $\text{HO}^\cdot$  performs better in such systems in comparison to  $\text{SO}_4^\cdot$ , likely due to its superior oxidizing potential (Toth et al., 2012). In some cases, acidic conditions ( $\text{pH} \sim 3$ ), resulted in better TOC removal (up to 82%) (Kattel et al., 2017). In contrast, the effects of pH were found to be

negligible in the treatment of ACE with permanganate under environmentally relevant conditions. Oxidation of ACE in WWTP influent and effluent water samples showed similar trends to tests in deionized water initially and decreased over time, likely due to high concentrations of *dissolved organic matter* (DOM). Interestingly, ACE was more effectively oxidized in river and lake water samples than in ultrapure water. Finally, it was determined that the intermediates and final transformation products of the oxidation of ACE with permanganate were much higher in toxicity than the initial compound when tested with *V. fischeri* (Yin et al., 2017).

#### **2.6.2.4 Laboratory Studies on Aspartame**

The removal of ASP through the generation of  $HO^\bullet$  through *low linear energy transfer* hydrolysis of water has been studied. The authors defined the concept of radical degradation efficiency as the percentage of contaminants destroyed per 100 hydroxyl radical reactions in the solution. By this definition,  $HO^\bullet$  were found to have an efficiency of 59% in degrading ASP (Toth et al., 2012). The removal of ASP from aqueous media has also been studied by means of electrochemical advanced oxidation. Electrogenenerated Fenton's reagent was employed to form  $HO^\bullet$ . The use of a Pt anode resulted in complete mineralization of ASP in a 20 min treatment time. The use of a BDD anode resulted in complete mineralization of ASP in 15 min. A  $Fe^{2+}$  concentration of up to 0.2 mM was found to be the most effective, while higher concentrations resulted in lower removal, likely due to the role of  $Fe^{2+}$  as a scavenger of  $HO^\bullet$ . Interestingly, intermediates of significantly higher toxicities were formed with maximal concentrations after 15 min treatment. Toxicity was minimal after 120 min of treatment for *V. fischeri* (Lin et al., 2017). No other data is available for this compound.

#### **2.6.2.5 Other Artificial Sweeteners**

Although scarce, some studies have been carried out for CYC and SAC. Complete mineralization of SAC has been achieved through  $HO^\bullet$  by electrochemical AOPs. It was shown that a BDD anode was resulted in faster degradation of SAC than a Pt anode. An increase in the toxicity of the solution was observed in the first 30 min of the treatment and complete detoxification was observed after a 60 min treatment time (Lin et al., 2016). The photocatalytic and Photo-Fenton oxidation of SAC have also been studied. It has been shown that the Photo-Fenton process can effectively remove saccharin within 10 min of treatment time. Maximum TOC removal of 93%

was reported. The TiO<sub>2</sub> photocatalytic process achieved complete mineralization after an irradiation time of 3 h (Chen et al., 2014). As for CYC, its degradation pathways and transformation products under Ozonation have been identified to be amidosulfonic acid and cyclohexanone. Some mineralization was observed after Ozonation (Wick et al., 2011). The results of the literature survey on the application of AOPs for the degradation of artificial sweeteners are shown in *Table 2-6*.

**Table 2-6:** Summary of available data for the degradation of five commonly used artificial sweeteners through advanced oxidation processes (AOPs)

Process		SUC	ACE	ASP	CYC	SAC
<b>Chlorination</b>	Achievable Degradation	-	68%-93%	-	-	-
	Choice of Parameters	-	Treatment time, water sample type (natural vs. ultrapure), ozone dosage	-	-	-
	References	-	(Li et al., 2017)	-	-	-
<b>Ozonation</b>	Achievable Degradation	20% -90% TOC Removal	10% mineralization, (full transformation)	-	Some mineralization (elucidation study only)	-
	Choice of Parameters	pH, O <sub>3</sub> dosage, Treatment time	ACE concentration, Ozone dosage,	-	Ozone dosage, treatment time,	-
	References	(Hu et al., 2017; Yin Xu et al., 2018)	(Wick et al., 2011)	-	(Wick et al., 2011)	-
<b>Photo-Fenton</b>	Achievable Degradation	93% Removal	-	-	-	93% (TOC removal)
	Choice of Parameters	pH, treatment time, pollutant concentration	-	-	-	Treatment time, catalyst dosage
	References	(Calza et al., 2013)	-	-	-	(Chen et al., 2014)
<b>Electrochemical (including electro-Fenton)</b>	Achievable Degradation	94%	-	100%	-	100%
	Choice of Parameters	Catalyst dosage, applied current, anode type	-	Catalyst dosage, applied current,	-	Catalyst dosage, applied current, anode

				anode type		type, treatment time
	References	(Lin et al., 2018)	-	(Lin et al., 2017)	-	(Lin et al., 2016)
<b>UV Irradiation</b>	Achievable Degradation	2%	19%-100%	-	-	-
	Choice of Parameters	Irradiation time, pH	Irradiation time, various water matrices, ACE concentration,	-	-	-
	References	(Xu et al., 2016)	(Li et al., 2016; Scheurer et al., 2014)	-	-	-
<b>UVC/H<sub>2</sub>O<sub>2</sub></b>	Achievable Degradation	60%	-	-	-	-
	Choice of Parameters	Irradiation time, pH, H <sub>2</sub> O <sub>2</sub> dosage,	-	-	-	-
	References	(Xu et al., 2016)	-	-	-	-
<b>UVC/PDS</b>	Achievable Degradation	93%	-	-	-	-
	Choice of Parameters	Irradiation time, pH, PDS dosage	-	-	-	-
	References	(Xu et al., 2016)	-	-	-	-
<b>UVA/H<sub>2</sub>O<sub>2</sub>/Fe<sup>2+</sup></b>	Results Summary	-	100% transformation of parent compound, 75% TOC removal	-	-	-
	Choice of Parameters	-	Irradiation time, various water matrices, ACE concentration, pH	-	-	-
	References	-	(Kattel et al., 2017)	-	-	-
<b>UVA/S<sub>2</sub>O<sub>8</sub><sup>2-</sup> /Fe<sup>2+</sup></b>	Results Summary	-	100% transformation of parent compound, 75% TOC removal	-	-	-

<b>Photocatalytic (TiO<sub>2</sub> based)</b>	Choice of Parameters	-	Irradiation time, various water matrices, ACE concentration, pH	-	-	
	References	-	(Kattel et al., 2017)	-	-	
	Results Summary	89%	70%-100%	-	-	100%
	Choice of Parameters	pH, TiO <sub>2</sub> dosage, treatment time, pollutant concentration	TiO <sub>2</sub> dosage, treatment time	-	-	Treatment time, TiO <sub>2</sub> dosage
<b>Photocatalytic (ZnO based)</b>	References	(Calza et al., 2013)	(Li et al., 2016; López-Muñoz et al., 2018; Nam et al., 2018; Srivastava et al., 2019)	-	-	(Chen et al., 2014)
	Results Summary	-	65%	-	-	-
	Choice of Parameters	-	ZnO dosage	-	-	-
	References	-	(Srivastava et al., 2019)	-	-	-
<b>Permanganate</b>	Results Summary	-	40%-80%	-	-	-
	Choice of Parameters	-	Treatment time, various water matrices, pH	-	-	-
	References	-	(Yin et al., 2017)	-	-	-

#### 2.6.2.6 Studies on Full-Scale Water and Wastewater Treatment Plants

Switzerland has been one of the pioneering countries in protecting the ecosystem and drinking water resources. Some WWTPs in Switzerland are among the first ones in the world to employ full-scale ozonation to target a wide spectrum of MPs. Artificial sweeteners have also been removed to some extent, but not all results have been satisfactory. For example, SUC was detected at concentrations of 3000-4700 ng/L in a secondary clarifier effluent in a particular case. With an applied O<sub>3</sub> concentration of 0.6 g O<sub>3</sub>/g DOC, SUC concentration was found to decrease to



2200 ng/L at its lowest (Hollender et al., 2009). In drinking water treatment plants, an  $O_3$  dosing of 5 mg/L has shown to effectively remove 30% of the SUC in concentrations of 0.14  $\mu\text{g/L}$ . However, lower  $O_3$  dosages were found to be very ineffective with no observable degradation at applied concentrations of 1 mg/L and 0.5 mg/L (Scheurer et al., 2010).

The project was expanded in 2016, with many more Swiss WWTPs being equipped with ozonation. A particular study involved varying ozone doses in the range of 0.35-0.97 g  $O_3$ /g DOC in multiple plants across the country. In one of the plants, 51 MPs were selected for screening, including ACE and SUC. Interestingly, 88-95% of ACE was removed successfully by biological system in various tests and 96-99% removal was observed by both biological and ozone treatment combined. On the other hand, SUC was found to be persistent through biological treatment (0-9% removal) and the combined biological and ozone treatment processes (28-44% removal). The study concluded that an  $O_3$  dosage of 0.4 g  $O_3$ /g DOC was optimal to ensure a recommended average removal of 80% for all the screened MPs. The recommended dosage corresponds to 90% biological removal, 59% for ozonation removal and 96% total removal for ACE and 13% to biological removal, 27% ozonation removal, and a 36% total removal for SUC (Bourgin et al., 2018). As for other technologies and sweeteners such as ASP, no data is currently available.

## 2.7 Concluding Remarks

Based on the studies reviewed thus far, it is now evident as to why artificial sweeteners have been classified as CECs. The reported concentrations of artificial sweeteners in WWTP influent and effluent streams vary significantly by geographical locations, being typically in the PPB range. Various studies suggest that while some degradation was observed for ACE, the compound was still persistent in most WWTPs. SUC was found to be very persistent in all studies. Even though chronic human exposure to environmentally relevant concentrations of these compounds seem to be negligible, recent ecotoxicological data show concerning adverse effects on some species.

Based on recent advances in AOPs for water and wastewater treatment and their proven effectiveness in targeting trace organic compounds, efforts have been made to investigate such technologies for the treatment of these contaminants. Although promising, further research is required in understanding the removal of artificial sweeteners through AOPs, especially for a compound like ASP. Furthermore, a key area that requires further investigation is treatment of a

matrix containing multiple sweeteners as no such studies have been carried out. In this context, the  $HO^\bullet$  has been found to yield satisfactory results in degradation of various artificial sweeteners in comparison to other radical molecules in AOP. The commercial availability of the UV/H<sub>2</sub>O<sub>2</sub> process, its proven application in treating real wastewater matrices and the possibility for it to be operated in continuous mode, makes this process an attractive option in dealing with the concerns caused by artificial sweeteners. It was also demonstrated that the application of the UV/H<sub>2</sub>O<sub>2</sub> process has not been thoroughly investigated for the removal of artificial sweeteners from aqueous matrices. Therefore, the UV/H<sub>2</sub>O<sub>2</sub> process was selected in this study to investigate the photochemical degradation of multicomponent systems of aqueous artificial sweeteners.

## Chapter 3 – MATERIALS AND METHODS

### 3.1 Introduction

Several experiments were carried out to meet the objectives of this study. A set of preliminary experiments were performed to assess the general behaviour and degradation response of each of the artificial sweeteners independently in a UV/H<sub>2</sub>O<sub>2</sub> process. The results were then used to design experiments (by statistical means) to investigate the behaviour of a multicomponent aqueous system containing ASP, ACE and SUC in the same matrix. Finally, respirometric studies were carried out to screen for the degradation of each sweetener in the presence of activated sludge both in individual and multicomponent systems. The purpose of this chapter is therefore to discuss all the materials and methods used in this study.

### 3.2 Materials

In this study, several chemicals and reagents were used to carry out the experiments and the analytical techniques. All chemicals were purchased from either VWR or Sigma Aldrich as required. Detailed description of all purchased and/or prepared reagents are presented in this section. A complete list of the chemicals used in this study can be found in *Table 3-1*.

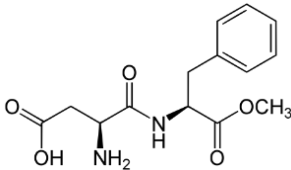
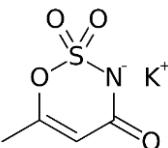
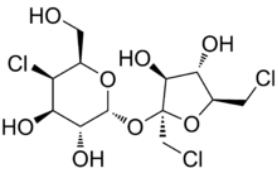
**Table 3-1:** List of all the chemical reagents used in this study

Test/Experiment	Chemical	Chemical Formula	Molecular Weight (g/mol)
UV/H <sub>2</sub> O <sub>2</sub>	Distilled Water	H <sub>2</sub> O	18.02
	Aspartame	C <sub>14</sub> H <sub>18</sub> N <sub>2</sub> O <sub>5</sub>	294.30
	Acesulfame K	C <sub>4</sub> H <sub>4</sub> KNO <sub>4</sub> S	201.24
	Sucralose	C <sub>12</sub> H <sub>19</sub> Cl <sub>3</sub> O <sub>8</sub>	397.64
	Hydrogen Peroxide	H <sub>2</sub> O <sub>2</sub>	34.05
Respirometry	Sulfuric Acid	H <sub>2</sub> SO <sub>4</sub>	98.08
	Potassium Hydroxide	KOH	56.11
	Sodium Hydroxide	NaOH	39.99
	Dextrose	C <sub>6</sub> H <sub>12</sub> O <sub>6</sub>	180.16
	Peptone	-	-
	Yeast Extract	-	-
	Butyric Acid	C <sub>4</sub> H <sub>8</sub> O <sub>2</sub>	88.11
	Magnesium Sulfate	MgSO <sub>4</sub>	120.34
	Ammonium Chloride	NH <sub>4</sub> Cl	53.49
	Ferric Chloride	FeCl <sub>3</sub>	162.20
	Sodium Dihydrogen Phosphate	NaH <sub>2</sub> PO <sub>4</sub>	119.98
TOC Analysis	Potassium Hydrogen Phthalate	C <sub>8</sub> H <sub>5</sub> KO <sub>4</sub>	204.22
	Phthalate		
	Phosphoric Acid	H <sub>3</sub> PO <sub>4</sub>	97.994

### 3.2.1 Artificial Sweeteners

Analytical grade ASP, ACE and SUC were purchased from VWR and used in desired amounts as received. The sweeteners were stored in original packaging in a cool dry place. The physical and chemical properties of these compounds can be found in **Table 3-2**.

**Table 3-2:** Physical and chemical properties of ASP, ACE and SUC

Compound	Aspartame	Acesulfame K	Sucralose
Structure			
Molecular Formula	C <sub>14</sub> H <sub>18</sub> N <sub>2</sub> O <sub>5</sub>	C <sub>4</sub> H <sub>4</sub> KNO <sub>4</sub> S	C <sub>12</sub> H <sub>19</sub> Cl <sub>3</sub> O <sub>8</sub>
Molecular Weight (g/mol)	294.31	201.242	397.64
Solubility in water (g/L)	10 (25 °C)	270 (20°C)	283 (20°C)
Organic Carbon Fraction	0.57	0.24	0.36

### 3.2.2 Distilled Water

Distilled water was prepared in the laboratory with a sterilized distillation unit. The water was withdrawn directly from the distillation unit whenever required. Distilled water was used for the preparation of samples in all experiments and the preparation of calibration standards. The use of the same water source for standards and experimental samples was preferred in order to eliminate background noise in sample analysis.

### 3.2.3 Artificial Sweetener Solutions

Synthetic wastewater samples were prepared by dissolving the desired amounts of the sweeteners in distilled water. The volume for all synthetic samples was 3 L. The solutions were used immediately after preparation.

### 3.2.4 Hydrogen Peroxide

Analytical grade aqueous H<sub>2</sub>O<sub>2</sub> was purchased from VWR at a concentration of 30% (by weight) and used as received. The solution was stored in a cool dry place away from light.

### 3.2.5 Potassium Hydrogen Phthalate and Phosphoric Acid Solutions

Analytical grade granular *potassium hydrogen phthalate* (KHP) and concentrated phosphoric acid (H<sub>3</sub>PO<sub>4</sub>) were purchased from Sigma Aldrich for use in TOC analysis. KHP served as an organic

carbon source for the preparation of calibration standards. When required, a batch was obtained and dried in an oven at 105°C for at least 2 h prior to usage. The powder was stored in its original packaging in a cool dry place, away from light. The solution was stored in a refrigerator for up to a week.

Phosphoric acid served as the acid source for *inorganic carbon* (IC) sparging in TOC analysis. A diluted solution of 20% (by volume) aqueous  $\text{H}_3\text{PO}_4$  was prepared by adding 50mL of 85% phosphoric acid to 150 mL of distilled water. The solution was stored in a cool dry place for no more than a month.

### **3.2.6 Potassium Hydroxide and Sulfuric Acid Solutions**

Potassium hydroxide (KOH) pellets and 1.0 *N* sulfuric acid ( $\text{H}_2\text{SO}_4$ ) were purchased from Sigma Aldrich for use in respirometry. The  $\text{H}_2\text{SO}_4$  solution was used as received. A 45% (by weight) solution of KOH was prepared by slowly dissolving 45.0 g of KOH pellets in distilled water and making up the volume to 100 mL. Both solutions were stored in a cool dry place.

### **3.2.7 Phosphate Buffer**

A phosphate buffer solution was used in Respirometry to control the solution pH. The buffer solution was prepared by dissolving 204 g of potassium phosphate monobasic ( $\text{KH}_2\text{PO}_4$ ) in 800 mL of distilled water. The pH was then adjusted to 7.1 (required pH~7.0-7.2) and diluted to 1 L with distilled water. This is equivalent to 48 g P/mL, which is recommended for aerobic respirometry applications (Young and Cowan, 2004).

### **3.2.8 Stock Nutrient Solution**

A stock solution was prepared to provide nutrients and minerals for aerobic biomass growth for use in respirometry. This solution was also used as a control reference in respirometric analysis. The solution was prepared according to the recipe shown in **Table 3-3**.

**Table 3-3:** Recipe for the stock nutrient solution (1 L) used as “control” in respirometry

Compound	Amount Used (mg)
Dextrose	7000
Peptone	8000
Yeast Extract	300
Butyric Acid	1000
Magnesium Sulfate	170
Ammonium Chloride	260
Ferric Chloride	60
Sodium Dihydrogen Phosphate	800

The compounds listed in **Table 3-3** were dissolved in distilled water. The pH of the solution was adjusted to 7.5 and the solution was diluted to 1 L with distilled water. The solution was stored in a refrigerator at 4°C for future use (no more than two weeks).

### 3.2.9 Municipal Mixed Liquor Samples

When needed, municipal sludge mixed liquor was collected from Toronto’s Ashbridge’s Bay WWTP. The samples were collected at a point immediately after aeration basin prior to secondary clarification. The mixed liquor was then transported and aerated for at least 2 days prior to usage. The delay in the usage was done as precautionary step to ensure the depletion of any remaining organics and nutrients from the WWTP process to minimize interference with the experiments. The *mixed liquor suspended solids* (MLSS) and *mixed liquor volatile suspended solids* (MLVSS) were measured on the day the respirometric tests were initiated. The complete procedure for MLVSS determination is described in Appendix A – Determination of MLSS and MLVSS.

## 3.3 Experimental Methods

The experimental investigation in this study was carried out in three stages. The first stage was performed for a preliminary screening of the general behaviour for each species under UV exposure ( $\lambda \cong 254$  nm) alone and various H<sub>2</sub>O<sub>2</sub> doses. The second stage involved a statistical DOE with all the components combined to screen for significant effects and interactions. Experiments in the first two stages were carried out in a recirculating batch reactor setup. Respirometry was

performed in the final stage of the experimental investigations to screen for biodegradation characteristics (or lack thereof) and inhibition effects on municipal mixed liquor. An electrolytic respirometer was used in this stage. The details of the methodology used in all experiments will be discussed next.

### 3.3.1 Overview of the Recirculating Batch Reactor

The experimental investigations in this study were carried out in what is referred to as a recirculating batch reactor. This system is essentially a recycle reactor with no outflow. In theory, such systems employ a batch of catalyst and a fixed volume of fluid. The change in the composition of the holding tank is followed over time (Levenspiel, 1972). For the purpose of this study, the recirculating batch of fluid was a solution containing any of the artificial sweeteners and photoreactors as the catalyst batch. **Figure 3-1** illustrates the general schematic of a recirculating batch reactor.

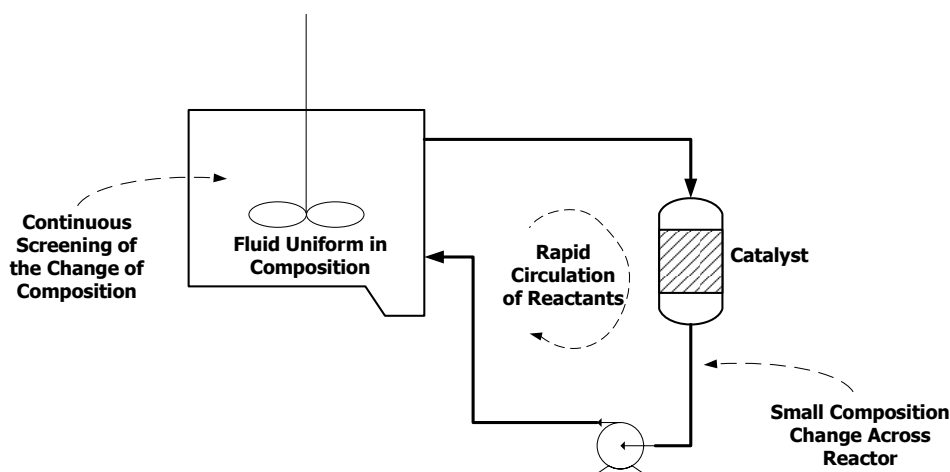


**Figure 3-1:** Schematic diagram of a recirculating batch reactor for catalytic reactions. Adapted from (Levenspiel, 1972).

For valid and meaningful results, Levenspiel recommends that the following conditions should be met:

- The composition of the fluid must be uniform throughout the system at any instance. This is achieved by rapid mixing of the fluid in the holding tank and a flowrate high enough to achieve turbulent flow.
- The circulation of the fluid through the reactor must be very rapid



- The conversion per pass (through the reactor) must be small, typically less than 5% (*less than 1% in this study*, see Appendix F – Determination of UV Exposure Time and Conversion Per Pass)

Experimental data is required for the calculation of conversion per pass. Furthermore, only a fraction of the sample is in the reactor at any point in time. Hence, the changes in the composition of species in such systems are expressed per units of *catalyst exposure time*. In this study, this is the equivalent of UV exposure time. The calculation can be performed according to the following equation:

$$t_{exposure} = \left( \frac{V_{reactor}}{V_{sample}} \right) \times t_{reaction}$$

Where:

$V_{reactor}$  = *effective reactor volume*

$V_{sample}$  = *Total Sample Volume*

$t_{reaction}$  = *total reaction run time*

### 3.3.2 Overview of Two-level Fractional Factorial Designs

The ultimate objective in any experimental work is to obtain some knowledge about the behaviour of a particular system. This is typically achieved by purposefully changing an input variable and monitoring the change in the output variable. It is of utmost importance to carefully design experiments to collect appropriate data for sound and unbiased conclusions. Statistical DOE is a technique used to collect appropriate data which can be analyzed by formal statistical methods resulting in meaningful and unbiased conclusions (Montgomery, 2005).

Factorial designs are the most efficient designs for experimental investigations. In such designs, the effect of all possible combinations of two or more *factors*<sup>1</sup> and their discrete possible levels (typically categorized two levels of high and low) on a response variable are investigated. The term *main effect* is used to refer to the effect of a change in one factor level on the response output.

---

<sup>1</sup> The term “factor(s)” is used to refer to any experimental parameter (e.g. temperature, concentration, etc.) in the context of statistical design of experiments.

Factorial experiments are very useful in determining the interaction between two or more factors (Montgomery, 2005). However, a large number of experimental runs will be required if many factors are to be investigated. This can be overcome by performing a fraction (e.g. half or quarter, etc.) of the required runs in the expense of confounding multilevel effects. However, it is still possible to obtain good information about the main effects and some information about the interactions of factors. Such designs are referred to as *fractional factorial designs*. The number of runs for such designs can be calculated as follows:

$$\# \text{ runs} = 2^{k-p}$$

Where:

$k = \text{number factors to be studied}$

$p = \text{power of fraction } \left(\frac{1}{2^p}\right) \text{ to be applied to the number of runs (see footnote)}^2$

A fractional factorial design containing  $2^{k-p}$  runs is called a  $1/2^p$  fraction of the  $2^k$  design.

The  $2^k$  system is suitable for systems whose models are *linear in parameters*. However, perfect linearity is not required as such designs work quite well even with the linearity assumption holding only very approximately. Based on this knowledge, the following general model is used for regression in such systems (Montgomery, 2005):

$$y = \beta_0 + \sum_{j=1}^k \beta_j x_j + \sum_{i < j} \sum \beta_{ij} x_i x_j + \epsilon$$

Where:

$\beta_0 \equiv \text{model intercept parameter}$

$\beta_j \equiv \text{model parameter of the effect of component (j)}$

---

<sup>2</sup> A full factorial design with 3 factors has  $2^{k-p} = 2^{3-0} = 8 \text{ runs}$ . A fractional factorial design with 3 factors and only half of the runs has  $2^{k-p} = 2^{3-1} = 4 \text{ runs}$ .

$x_j \equiv \text{effect of component } (j)$

$\beta_{ij} \equiv \text{model parameter of the interaction effect of components } (i) \text{ and } (j)$

$x_i x_j \equiv \text{effect of the interaction of components } (i) \text{ and } (j)$

$\epsilon \equiv \text{error term}$

For the above model to hold, it should be able to explain all observations within an experimental set. Furthermore, the values of the independent variable must be known for each trial. Finally, the errors must be additive to the true values of the quantity being measured. The error should not covary with each other and must be of constant variance (Montgomery, 2005).

The design *Resolution* (denoted as  $R$ ) is a measure of the amount of information obtained about multi-factor interactions. A design of resolution  $R$  (ranges between  $III - VI$ , in Roman Numerals), confounds effects of order ( $p$ ) with other effects containing no less than  $R - p$  factors. As an example, in a design of resolution  $III$  (denoted as  $R = III$ ), the main effects (*denoted as*  $p = 1$ ) are confounded with the 2-factor interaction ( $R - p = 3 - 1 = 2$ ), whereas in a design of  $R = V$ , the main effects are confounded with 4-factor interactions ( $R - p = 5 - 1 = 4$ ) and 2-factor ( $p = 2$ ) with 3-factor interactions ( $R - p = 5 - 2 = 3$ ). Since the objective is often to investigate main effects and potential 2-factor interactions, it is always desirable to have a higher resolution design. **Table 3-4** outlines some of the possible designs for the  $2^{k-p}$  systems.

**Table 3-4:** Common  $2^{k-p}$  designs. Adapted from (Montgomery, 2005)

		Number of Runs		
Number of Factors		4	8	16
	3	$2_{III}^{3-1}$	$2^3$	$2^3$ (2 times)
	4		$2_{IV}^{4-1}$	$2^4$
	5		$2_{III}^{5-2}$	$2_V^{5-1}$
	6		$2_{III}^{6-3}$	$2_{IV}^{6-2}$

*Note: the highlighted entry is in reference with the selected design in Phase II of experimental Studies. A more in-depth discussion is presented in Section 4.3 .*

As a final note, statistical designs typically employ coded factors instead of the raw magnitudes of each factor level (e.g. +1 and -1 for temperature levels of 35°C and 20 °C, respectively). Although not a requirement, this aids in interpretation of the experimental data. By coding the factors, the estimated model intercept (denoted as  $\beta_0$ ) will be placed at the center of the design space.

### 3.3.3 Overview of Respirometry

Respirometry is a characterization technique for aggregate organic constituents in wastewater samples. Respirometers are devices that are able to effectively measure the rate of respiration of living microorganisms. These devices record respiration data in a continuous manner over time. Hence, detailed plots of *oxygen uptake rate* (OUR) and BOD curves can be obtained through respirometry. Depending on the device type, tests can be performed in aerobic, anoxic or anaerobic environments (Metcalf and Eddy, 2014).

Heterotrophic oxidation reactions of organic constituent are the primary focus of respirometric applications. In such reactions, organic substrate is broken down through enzymatic oxidation by microorganisms for energy and synthesis of new cells. These reactions are summarized in **Table 3-5** (Grady et al., 2011).

**Table 3-5:** The generalized biochemical breakdown of organic substrates by microorganisms. Adapted from (Grady et al., 2011)

Energy Reaction
$COHNS + O_2 + bacteria \rightarrow CO_2 + H_2O + NH_3 + energy + byproducts$
Synthesis Reaction
$COHNS + O_2 + bacteria + energy \rightarrow C_5H_7NO_2$
Endogenous Respiration
$C_5H_7NO_2 + 5O_2 \rightarrow 5CO_2 + NH_3 + 2H_2O$
$COHNS = Organic\ substrate\ (Carbon, Oxygen, Hydrogen, Nitrogen, Sulfur)$
$C_5H_7NO_2 = New\ Cell\ Tissue$

Respirometers are built upon the simplified reactions shown in **Table 3-5**. Commercially available respirometers are categorized into two groups, namely the headspace gas respirometers and the *dissolved oxygen* (DO) depletion respirometers. Headspace gas respirometers are further categorized into oxygen input respirometers and headspace oxygen depletion respirometers. Oxygen input respirometers are designed to replace the oxygen consumed by microorganisms by adding oxygen in small amounts (Young and Cowan, 2004).

Respirometers are very useful in assessing the biodegradation characteristics and the toxicity of specific organic compounds. These studies are typically done in batch respirometers. Batch respirometry is classified as either a low-rate or a high-rate test. For biodegradation studies, a low rate respirometry test is commonly used. In low-rate batch tests, the compounds of interest are added to a growth medium containing a small amount of active biomass (typically  $\leq 30\text{ mg VSS/L}$ )<sup>3</sup>. The *oxygen uptake rate* (OUR) is then monitored over several days (Cooper et al., 1990). It should be noted that a low-rate test might not represent the biomass response seen in treatment processes. Nevertheless, low-rate tests are able to produce meaningful data for

<sup>3</sup> VSS = Volatile Suspended Solids. See Nomenclature (page xiv)

biodegradation trends of organic compounds in the environment. A number of standard protocols are available for such tests (Young and Cowan, 2004). The operating mechanism of the respirometer used in this study will be discussed in Section 3.3.5.2.

### 3.3.4 Characteristics of the Photoreactors

Two identical steel photoreactors (annular) were used for experimental investigations in this study. The photoreactors are of cylindrical shape and were manufactured by Siemens Inc. (model: SL-LAB 2). The use of specialized photoreactors are critical in UV based AOPs. Such reactors are designed to be maximally reflective (internally) of emitted photons from a light source for increased efficiency. A 45 W Iwaki centrifugal pump (model: MD – 30RZ – 115NL, max head: 11) was used to pump samples from a holding tank into the photoreactors. The photoreactors were connected in series for all experimental investigations (except for ASP, this is discussed in Section 3.4.1 ). Low-pressure mercury lamps (14 W) were used as UV irradiation source. The lamps were housed in a quartz sleeve within the reactors to prevent lamp fouling. Physical characteristics of the reactors and UV lamps are listed in *Table 3-6* and *Table 3-7* respectively. The pump characteristics are listed in *Table 3-8*. The schematic diagram of the photoreactors are shown in *Figure 3-2*.

**Table 3-6:** Physical characteristics of the photoreactors used in this study

<b>Manufacturer</b>	Siemens Inc.
<b>Model</b>	SL-LAB 2
<b>Geometry</b>	Annular Cylindrical
<b>Orientation</b>	Horizontal
<b>Material</b>	304 SST
<b>Chamber Length</b>	30.5 cm
<b>Inner Diameter</b>	5.11 cm
<b>Wall Thickness</b>	3.18 mm
<b>Effective Reactor Volume</b>	0.46 L

**Table 3-7:** Specifications of the UV lamps used in this study

<b>Type</b>	Low Pressure Mercury Lamp - Germicidal
<b>Model</b>	Siemens LP 4130
<b>Input Power</b>	14 W
<b>Output Power</b>	3.6 W
<b>Wavelength</b>	254 nm
<b>Length</b>	28.5 cm
<b>Diameter</b>	2 cm

**Table 3-8:** Specifications of the pump used in this study

<b>Manufacturer</b>	Iwaki Co, LTD
<b>Model</b>	MD – 30RZ – 115NL
<b>Max Capacity</b>	17
<b>Max Head</b>	11
<b>Output</b>	45 W
<b>Power Consumption</b>	95 W
<b>Speed</b>	2950 rpm

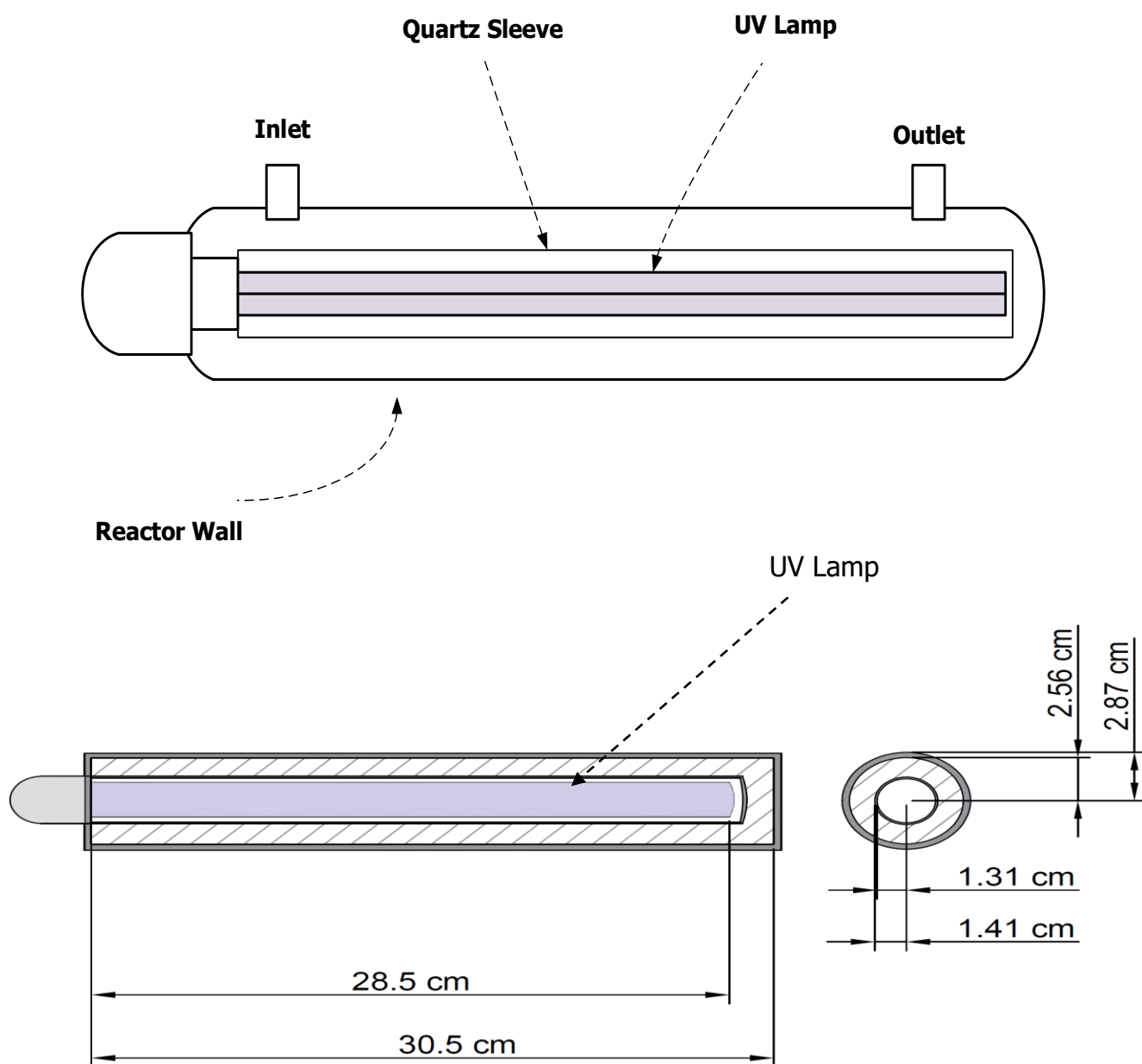


**Figure 3-2:** Schematic diagram of the Siemens SL – LAB 2 photoreactor with UV lamp and quartz sleeve



### 3.3.5 Analytical Methods

TOC analysis was the primary method of sample analysis in the UV/H<sub>2</sub>O<sub>2</sub> experiments. The Apollo 9000 Combustion Based TOC Analyzer was used for this method. Respirometric tests were performed with the BI-2000 Electrolytic Respirometer. The operation of these instruments will be discussed next.

#### 3.3.5.1 TOC Analysis

The degradation of ASP, ACE and SUC was monitored in terms of TOC reduction. The Apollo 9000 Combustion based TOC analyzer was used for all TOC analyses. The instrument operation involves stripping the collected sample off of inorganic carbon by sparging it with 20% (by volume) H<sub>3</sub>PO<sub>4</sub>. The oxidation of the organic carbon is then performed in a combustion chamber with a 50  $\mu$ L aliquot of the sparged sample. A carrier gas (O<sub>2</sub>, grade 4.5) transports the CO<sub>2</sub> through a *nondispersive infrared* (NDIR) detector for analysis. This instrument operates by oxidizing organic carbon in a sample and converting it to CO<sub>2</sub>. It then detects and quantifies the oxidized product. Sampling is done by an auto-sampler. The instrument specifications are shown in **Table 3-9**. A flow diagram of the instrument operation is shown in **Figure 3-3**.

**Table 3-9:** Apollo 9000 combustion-based TOC analyzer specifications

<b>Manufacturer</b>	Teledyne Tekmar
<b>Model</b>	Apollo 9000
<b>Operational Basis</b>	Combustion Based
<b>Oxidizing Gas</b>	High Grade O <sub>2</sub>
<b>IC Sparging Solution</b>	Phosphoric Acid

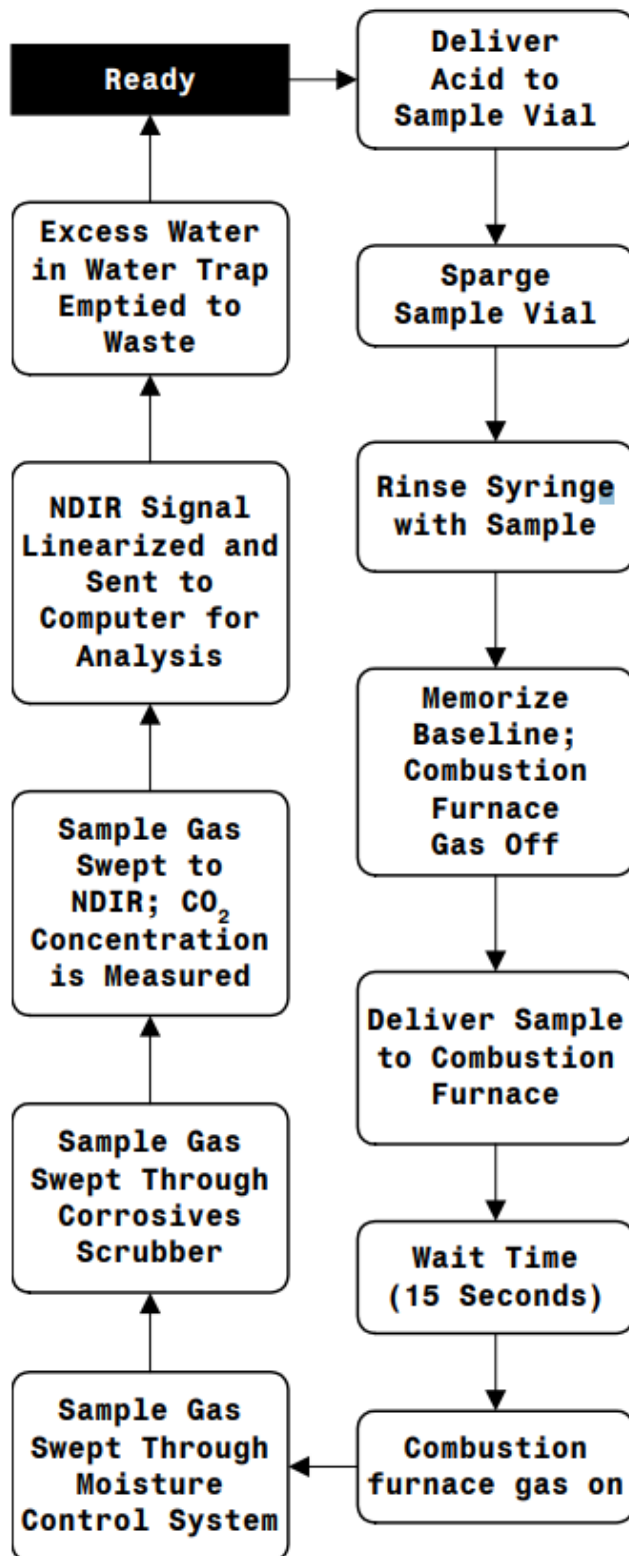


**Figure 3-3:** Flow diagram of the operation of the Apollo 9000 TOC analyzer. Adapted from Teledyne Tekmar

### 3.3.5.2 *Respirometry*

In this study, a headspace gas respirometer was used. Headspace gas respirometers are sealed bioreactors that contain a known volume of liquid and headspace gas (usually air) and are operated isothermally. The respirometer has a built-in temperature control unit. The operation of this respirometer is based on the general equations shown in **Table 3-5**. The one used in this study is referred to as an *electrolytic manometric respirometer*. The electrolytic cell contains a dilute solution of sulfuric acid and is located at the opening of the reaction vessel. Three electrodes are in contact with the electrolyte solution. One is a switch electrode, the second is a hydrogen-producing electrode and the third is an oxygen electrode. As the organic substrate is broken down by microorganisms, the concentration of DO is reduced in the vessel. The reduction of DO results in the formation of an oxygen concentration gradient across the interphase of the aqueous medium and the headspace gas. This results in the diffusion of oxygen into the aqueous phase. The resultant CO<sub>2</sub> due to the microbial activity escapes the aqueous phase and is scrubbed by a strong solution of potassium hydroxide. This leads to a slight vacuum within the system. The vacuum results in the suction of the electrolyte liquid towards the reaction vessel contents (never entering the vessel). This shift results in a drop in the liquid level of the electrolyte solution, breaking contact with the switch electrode. The hydrogen-producing electrode is then activated to hydrolyse the electrolyte solution, resulting in the production of oxygen gas to replenish the headspace volume. As the pressure is equalized, the electrolyte liquid level increases and contact is made with the switch electrode once again. The oxygen generation process is then paused until further changes in the headspace gas pressure. The general information about the respirometer is outlined in **Table 3-10**. A schematic of a typical electrolytic respirometer (such as the one used in this study) is shown in **Figure 3-4**.

**Table 3-10:** General properties of the BI-2000 electrolytic respirometer

<b>Manufacturer</b>	<b>Bioscience, Inc.</b>
<b>Model</b>	BI-2000 Electrolytic Respirometer
<b>Reaction Vessel Volume</b>	1000 mL
<b>Temperature Control Unit</b>	Recirculating Heating/Colling Water Bath
<b>Reactor Module Capacity</b>	Up to 8 Reactor Vessels

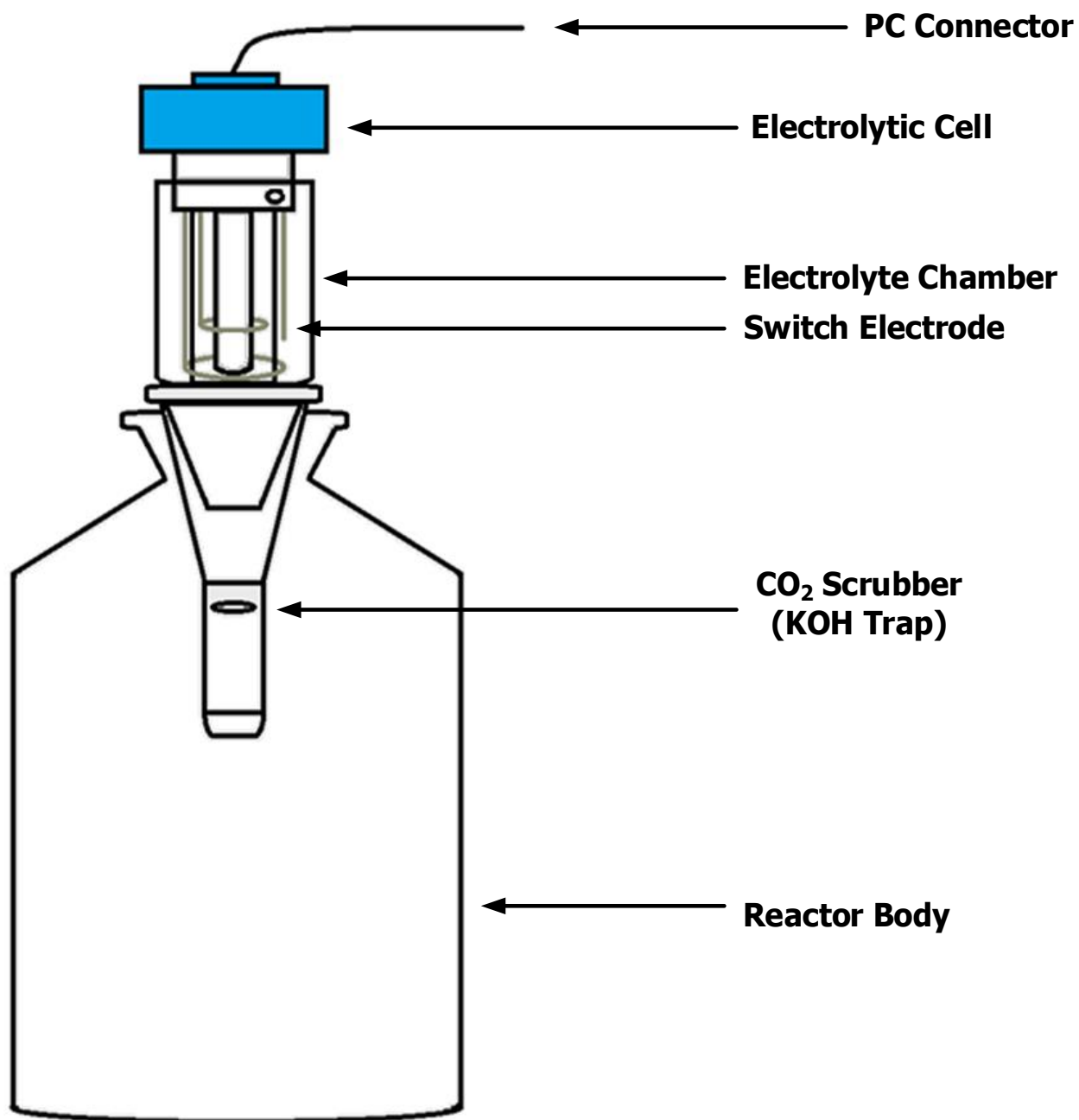


**Figure 3-4:** Schematic diagram of an electrolytic respirometer with electrolysis cell and reaction vessel

### 3.4 Stage I – Preliminary Experiments

A series of preliminary experiments were performed to have a better understanding of the effects of UV exposure ( $\lambda \cong 254$  nm),  $H_2O_2$ , treatment time and the overall system behaviour on the degradation of each of the sweeteners. The  $H_2O_2$  dosage was initially estimated according to the theoretical chemical reactions described in **Table 3-11**.

**Table 3-11:** Estimation of the required hydrogen peroxide doses based on the theoretical oxidation of ASP, ACE and SUC by hydrogen peroxide

<b>Aspartame</b>	<b><math>H_2O_2</math>:ASP (Mass basis)</b>
$C_{14}H_{18}N_2O_5 + 38H_2O_2 \rightarrow 14CO_2 + 47H_2O + 3NO_3$	4.39
<b>Acesulfame K</b>	<b><math>H_2O_2</math>:ACE (Mass basis)</b>
$C_4H_4KNO_4S + 13H_2O_2 \rightarrow 4CO_2 + 15H_2O + NO_3 + SO_4 + K$	2.20
<b>Sucralose</b>	<b><math>H_2O_2</math>:ACE (Mass Basis)</b>
$C_{12}H_{19}Cl_3O_8 + 75H_2O_2 \rightarrow 24CO_2 + 94H_2O + 6ClO_4$	3.21

In these reactions, it was assumed that each compound theoretically undergoes complete oxidation by  $H_2O_2$ . Using the stoichiometric coefficients of the chemical equations described in **Table 3-11**, mass ratios of  $H_2O_2$ :ASP,  $H_2O_2$ :ACE and  $H_2O_2$ :SUC were obtained. Sample calculations can be found in Appendix C – Determination of Theoretical  $H_2O_2$  Dosages (Mass Basis). For these experiments, the solutions of each sweetener were prepared in various concentrations (75 – 300 mg/L) with  $H_2O_2$  to sweetener mass ratios of 2:1, 6:1 and 10:1. Large ranges of concentrations and applied  $H_2O_2$  doses were selected simply to obtain a general idea of the system behaviour. More specifically, these preliminary experiments carried out to investigate how the experimental setup performed in terms of overall TOC loading and to define a range for  $H_2O_2$  dosing to be studied in experiments of stage II. Such an approach was necessary due to the lack of information regarding applicable doses in the literature.

#### 3.4.1 Experimental Setup for the treatment of Aspartame Solutions

ASP was the first compound to be investigated. As a starting point, solutions of ASP were prepared at three concentrations of 75, 150 and 300 mg/L. For each concentration, the effects of the UV irradiation ( $\lambda \cong 254$  nm) alone and the UV irradiation in the presence of varying doses of  $H_2O_2$  were investigated. Three  $H_2O_2$  dosages were selected for every concentration of ASP based on the

calculated mass ratio of 4.39, as seen in **Table 3-11**. One  $\text{H}_2\text{O}_2$ :ASP (mass basis) dose was selected to be lower than the calculated ratio (2:1, mass basis). Two larger doses were also selected for further investigation (namely 6:1 and 10:1, mass basis). The solution was passed through a cooling coil after each pass to prevent a rise in temperature due to pump and UV lamp operation. With this setup, the samples were exposed to UV irradiation for 22.5 min as a starting point. The schematic of the experimental setup is shown in **Figure 3-5**.

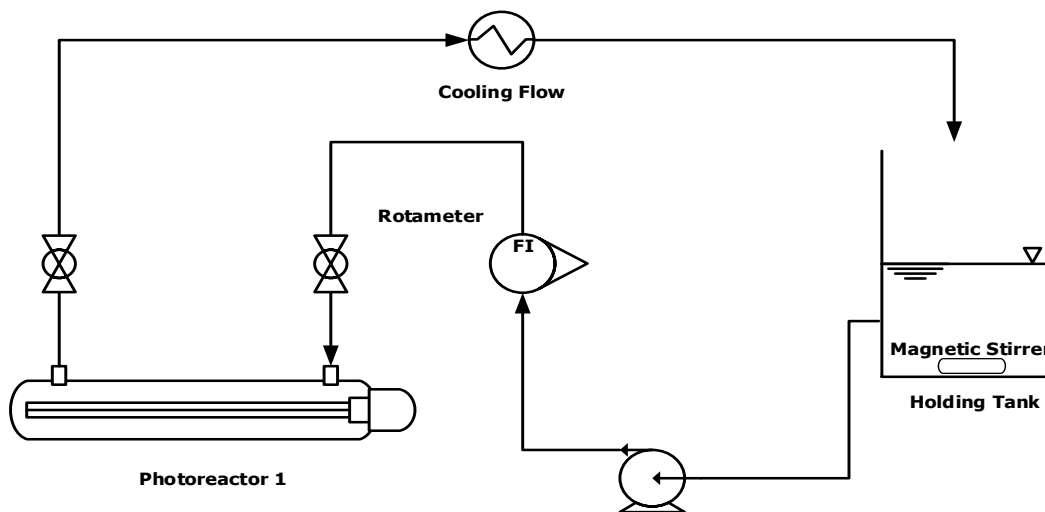


**Figure 3-5:** Schematic diagram of the experimental setup used for preliminary experiments on ASP solutions

### 3.4.2 Experimental Setup for the treatment of Acesulfame K and Sucralose Solutions

Based on the system behaviour observed for the degradation of ASP, modifications were made to the experimental setup to accommodate for a longer UV exposure of 70 min for the experiments that followed. This was achieved by the addition of a second photoreactor of identical physical characteristics (volume, material and lamp) and increasing the overall experimental runs. These modifications were used for experimental investigations involving ACE and SUC.

Solutions of 75, 150 and 300 mg/L were prepared with ACE and SUC. The effect of the UV irradiation ( $\lambda \cong 254$  nm) alone and the UV irradiation in the presence of varying doses of  $\text{H}_2\text{O}_2$  were investigated. A total of three  $\text{H}_2\text{O}_2$  dosages were applied three concentrations of ACE and SUC based on the calculated mass ratios of 2.20 and 3.21 respectively, as previously shown in **Table 3-11**. The schematic of the experimental setup used for ACE and SUC is shown in **Figure 3-6**.

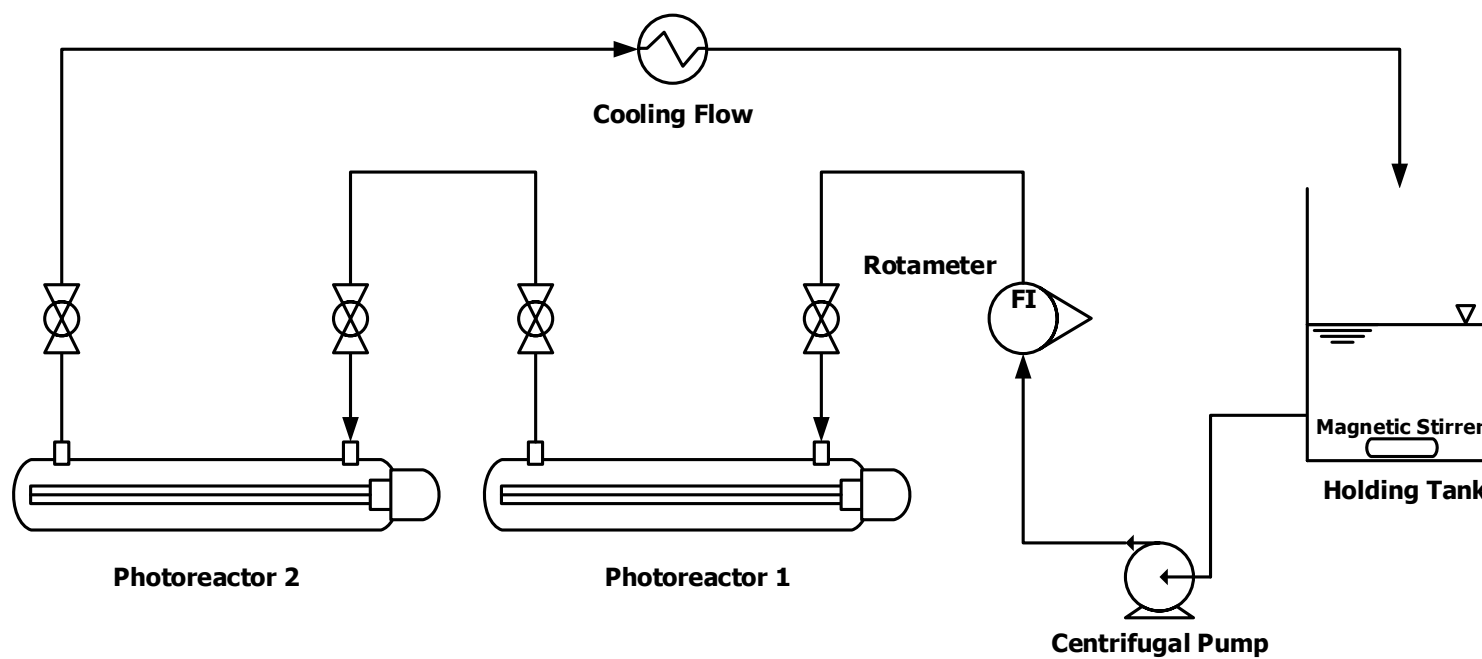


**Figure 3-6:** Schematic of experimental setup used for preliminary experiments on acesulfame K and sucralose

### 3.4.3 Experimental Procedure

Prior to each experiment, distilled water was pumped through the system for at least 30 min to rinse off any residues from previous experimental runs. The UV lamps were also operated for a minimum of 30 min during this run. This was done to warm the lamps to achieve uniform radiation of UV light in the desired wavelength of 254 nm. Three litre solutions of the desired artificial sweetener and H<sub>2</sub>O<sub>2</sub> (when applicable) were also prepared and transferred into the holding tank. The system was then fed with sufficient sample volume to ensure all the residual distilled water was flushed out of the system. The UV lamps were powered off for this step to prevent any reactions prior to the initiation of the experiment. The experiments were then started by simultaneously starting the pump and the UV lamps. Samples were taken immediately at time zero ( $t_0$ ). A flowrate of 8.5 L/min was used to meet the condition of rapid fluid recirculation (see Section 3.3.1).

Samples were periodically collected directly from the holding tank until the experimental run was completed. The first three samples (including initial samples at  $t_0$ ) were collected in 15 min intervals until the 30 min mark, and every 30 min afterwards. The samples were analyzed for TOC content. TOC analysis was performed with the Apollo 9000 TOC Analyzer (see Section 3.3.5). The experimental conditions for varying ASP, ACE and SUC and the corresponding H<sub>2</sub>O<sub>2</sub> doses are summarized in *Table 3-12*, *Table 3-13* and *Table 3-14* respectively.



**Table 3-12:** Experimental conditions used in the preliminary experiments involving aqueous ASP through UV/H<sub>2</sub>O<sub>2</sub>

Compound	Concentration (mg/L)	H <sub>2</sub> O <sub>2</sub> :ASP (mass basis)
Aspartame	75	0 (UV Only)
		2
		6
		10
	150	0 (UV Only)
		2
		6
		10
	300	0 (UV Only)
		2
		6
		10
<b>Theoretical H<sub>2</sub>O<sub>2</sub>:ASP Ratio</b>	4.39	

**Table 3-13:** Experimental conditions used in the preliminary experiments involving aqueous ACE through UV/H<sub>2</sub>O<sub>2</sub>

Compound	Concentration (mg/L)	H <sub>2</sub> O <sub>2</sub> :ACE (mass basis)
Acesulfame K	75	0 (UV Only)
		2
		6
		10
	150	0 (UV Only)
		2
		6
		10
	300	0 (UV Only)
		2
		6
		10
Theoretical H <sub>2</sub> O <sub>2</sub> :ASP Ratio	2.20	

**Table 3-14:** Experimental conditions used in the preliminary experiments involving aqueous SUC through UV/H<sub>2</sub>O<sub>2</sub>

Compound	Concentration (mg/L)	H <sub>2</sub> O <sub>2</sub> :ASP (mass basis)
Aspartame	75	0 (UV Only)
		2
		6
		10
	150	0 (UV Only)
		2
		6
		10
	300	0 (UV Only)
		2
		6
		10
Theoretical H <sub>2</sub> O <sub>2</sub> :ASP Ratio	3.21	

### 3.5 Stage II – Statistical Design of Experiments

In Stage II of the experimental investigations, experimental work was expanded to study the degradation of artificial sweeteners in a multicomponent aqueous system, which was the first primary objective of this study. A two-level fractional factorial DOE was used for experimental investigations. Five factors were selected to study. The first three factors were the concentrations (TOC basis) of ASP (factor A), ACE (factor B) and SUC (factor C). The remaining two factors were the H<sub>2</sub>O<sub>2</sub>:TOC<sub>total,ini</sub> mass ratio (factor D) and the operating temperature (factor E) respectively. The ( $2^{5-1}$ ) design was selected from **Table 3-4**. This design accommodates the investigation of five factors in 16 experimental runs. Being a resolution V design (see Section 3.3.2), the concentration levels of the artificial sweeteners were selected (in terms of TOC) so that the TOC in the system (at  $t = t_o$ ) was within the TOC range in the preliminary experiments in all runs. The H<sub>2</sub>O<sub>2</sub> doses were also selected according to the observations from Stage I. Multicomponent solutions of ASP, ACE and SUC were prepared ahead of each run with the

appropriate amounts of  $\text{H}_2\text{O}_2$ . Based on the trends observed in the preliminary studies, no TOC removal was observed beyond a UV exposure of 45 min. Therefore, the total time of UV exposure was held constant at 45 min throughout all runs in stage II. A total of six center-point replications (level 0) were added to the design for estimation of experimental error. This number of replications results in sufficient degrees of freedom (a total of 5 in this case) to perform an F-test with a large detection limit (lower  $F_{\text{critical}}$  value) within a reasonable confidence interval (95% in this case). The theory of the determination of experimental error from centre-point replicates is discussed in Appendix B – A randomized experimental design was generated using the Design Expert 11 software by Stat-Ease, Inc. **Table 3-15** outlines the experimental design used in this study, including all factor levels in both actual and coded levels.

**Table 3-15:** Actual and coded values of for the experimental conditions used in the statistical design of experiments

Independent Variable	Unit	Factor (X)	Coded Levels	
			-1	+1
$\text{TOC}_{\text{ASP}, \text{ini}}$	mg/L	A	25	50
$\text{TOC}_{\text{ACE}, \text{ini}}$	mg/L	B	25	50
$\text{TOC}_{\text{SUC}, \text{ini}}$	mg/L	C	25	50
$\text{H}_2\text{O}_2\text{:TOC}_{\text{total}, \text{ini}}$	(mass basis)	D	5	10
Operating Temperature	°C	E	20	35

### 3.5.1 Experimental Setup

The introduction of temperature as a factor required the addition of a water bath for the holding tank for temperature adjustment and control. Using the UV/ $\text{H}_2\text{O}_2$  setup shown in **Figure 3-6**, a water bath was introduced to the setup (around the holding tank) to enable temperature control. A recirculating temperature control unit was used to pump water into and out of the water bath. The flowrate was maintained at 8.5 L/min. The schematic diagram of the setup used in Stage II of the experimental investigations is shown in **Figure 3-7**.

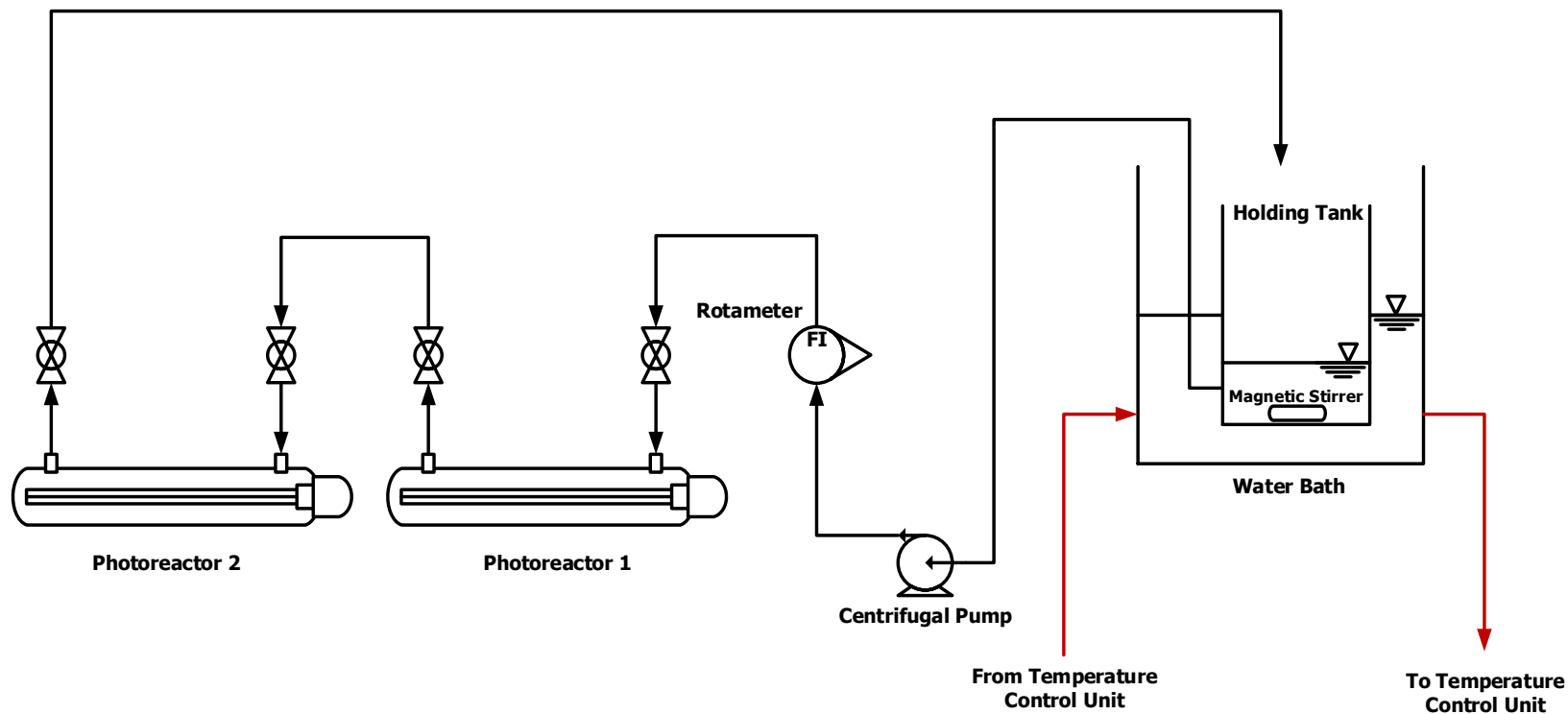


**Figure 3-7:** Schematic diagram of the experimental setup used for the treatment of multicomponent aqueous systems of ASP, ACE and SUC through UV/H<sub>2</sub>O<sub>2</sub> incorporating two photoreactors in series and a water bath for temperature control

### 3.5.2 Experimental Procedure

Prior to each run, multicomponent samples of ASP, ACE and SUC were prepared with the desired H<sub>2</sub>O<sub>2</sub> amounts and transferred to the holding tank. The water bath temperature was adjusted so that the sample temperature was at the desired level prior to starting the experiments. The remainder of the steps were identical to that of the ones in Stage I. Samples were collected directly from the holding tank until the end of the experimental runs. TOC analysis was performed with the Apollo 9000 TOC Analyzer (see Section 3.3.5).

## 3.6 Stage III – Respirometry

The second primary objective of this study was to investigate the biodegradation characteristics of ASP, ACE and SUC in both single and multicomponent systems. Experiments were carried out to see if the presence of each sweetener would alter the degradation of a readily biodegradable substrate of known composition. The details of the relevant experimental setup and procedure are discussed next.

### 3.6.1 Experimental Setup

A BI-2000 Electrolytic Respirometer was used in aerobic mode for these investigations (see Section 3.3.5.2). Six reactor vessels were prepared for each experiment according to *Table 3-16*.

**Table 3-16:** Components of the respirometric reactors in each experiment

Reactor #	Municipal Sludge	Control Substrate	Aspartame	Acesulfame K	Sucralose	Phosphate Buffer	Nitrification Inhibitor
1	✓	-	-	-	-	-	✓
2	✓	✓	-	-	-	✓	✓
3	✓	✓	✓	-	-	✓	✓
4	✓	✓	-	✓	-	✓	✓
5	✓	✓	-	-	✓	✓	✓
6	✓	✓	✓	✓	✓	✓	✓

Each reactor vessel was seeded with municipal sludge as the source of microorganisms in the form of MLVSS (see Section 3.2.9 ). One of the reactors was operated only with the seed culture as a

blank for each experiment. A stock nutrient solution was prepared and added to the remaining five reactors for each experiment to provide the required nutrients for microbial growth. The nutrient solution was also used as a reference cell for each experiment. The preparation of the stock nutrient solution was carried out according to the recipe provided in **Table 3-3** (see Section 3.2.8). A phosphate buffer was used for pH control in each reactor (except for the seed culture reactor). A pH buffer was used to maintain the pH of the test solution in the neutral range. This is required as the breakdown of the substrate results in the formation of organic acids in the form of by-products (Young and Cowan, 2004). Buffer doses were calculated according to the estimated *theoretical oxygen demand* (ThOD) (see Appendix D – Determination of ThOD and BOD/ThOD). Due to the presence of nitrifying bacteria in seed culture, a nitrification inhibitor was used to inhibit oxygen uptake due to nitrification. The oxygen demand due to nitrification can be quite significant and can mask the true trends when analyzing the biodegradation characteristics of an organic compound (see Section 4.4.2).

### 3.6.2 Experimental Procedure

The experimental setup and procedures were adapted from standard biodegradation protocols such as ISO 9408 and OECD 301. The concentration of each artificial sweetener was selected based on its ThOD to be *no less than* the recommended concentration of 100 mg/L. Municipal sludge and nitrification inhibitor were added to reactor vessels 1 through 6. Control substrate was added to reactor vessels 2 through 6. The required doses of phosphate buffer were added to reactors 2 through 6. The desired amounts of ASP, ACE and SUC were added to reactors 3 through 6. Solutions of 45% KOH (~5 mL) and 1.0 N H<sub>2</sub>SO<sub>4</sub> were used in each reactor vessel for CO<sub>2</sub> absorption and as electrolyte respectively. All glass joints were sealed using vacuum grease. The experiments were carried out at 20 °C simultaneously for 6 days (144 h). Data was recorded every 15 min. **Table 3-17** outlines the experimental conditions used for the respirometric investigations.

**Table 3-17:** Experimental conditions for respirometric investigations

	<b>Artificial Sweetener Concentration (150 mg/L)</b>					
<b>Reactor # and Description</b>	1 (Seed Culture)	2 (Seed + Control)	3 (Seed + Control + ASP)	4 (Seed + Control + ACE)	5 (Seed + Control + SUC)	6 (Seed + Control + ACE + ASP + SUC)
<b>Estimated ThOD (mg/L)</b>	n/a	~200	~437	~301	~427	~765
<b>Buffer (mL)</b>	n/a	4	9	6	8.5	27.5
<b>MLVSS (mg)</b>	30 mg	30 mg	30 mg	30 mg	30 mg	30 mg
<b>Nitrification Inhibitor (g)</b>	0.53	0.53	0.53	0.53	0.53	0.53
<b>Control Substrate (mL)</b>	10	10	10	10	10	10



## Chapter 4 – RESULTS AND DISCUSSION

### 4.1 Introduction

In this chapter, the experimental results of the treatment of artificial sweeteners through UV/H<sub>2</sub>O<sub>2</sub> in both individual and multicomponent systems are discussed. All the results are reported in terms of TOC removal and normalized to the initial TOC concentrations in each run for comparison. The respirometric results are also presented. The primary focus of the preliminary experiments was to investigate how well ASP, ACE and SUC respond to treatment under UV irradiation alone and UV irradiation in the presence of varying doses of H<sub>2</sub>O<sub>2</sub>. The rationale behind the choices of experimental conditions was discussed in Section 3.4.

### 4.2 Preliminary Experiments – Degradation of Artificial Sweeteners in Single-component Aqueous Solutions by UV/H<sub>2</sub>O<sub>2</sub>

#### 4.2.1 Aspartame

Prior to the addition of H<sub>2</sub>O<sub>2</sub>, the degradation of ASP in various concentrations was studied under UV irradiation ( $\lambda \cong 254$  nm) alone. H<sub>2</sub>O<sub>2</sub> was then added to the solutions in subsequent experiments. H<sub>2</sub>O<sub>2</sub> doses (mass basis) are reported in *Table 3-12*. The TOC removal trends (in terms of [TOC]/[TOC]<sub>0</sub>) with all H<sub>2</sub>O<sub>2</sub> doses are shown in *Figure 4-1*, *Figure 4-2*, and *Figure 4-3* for ASP concentrations of 75, 150 and 300 mg/L respectively.

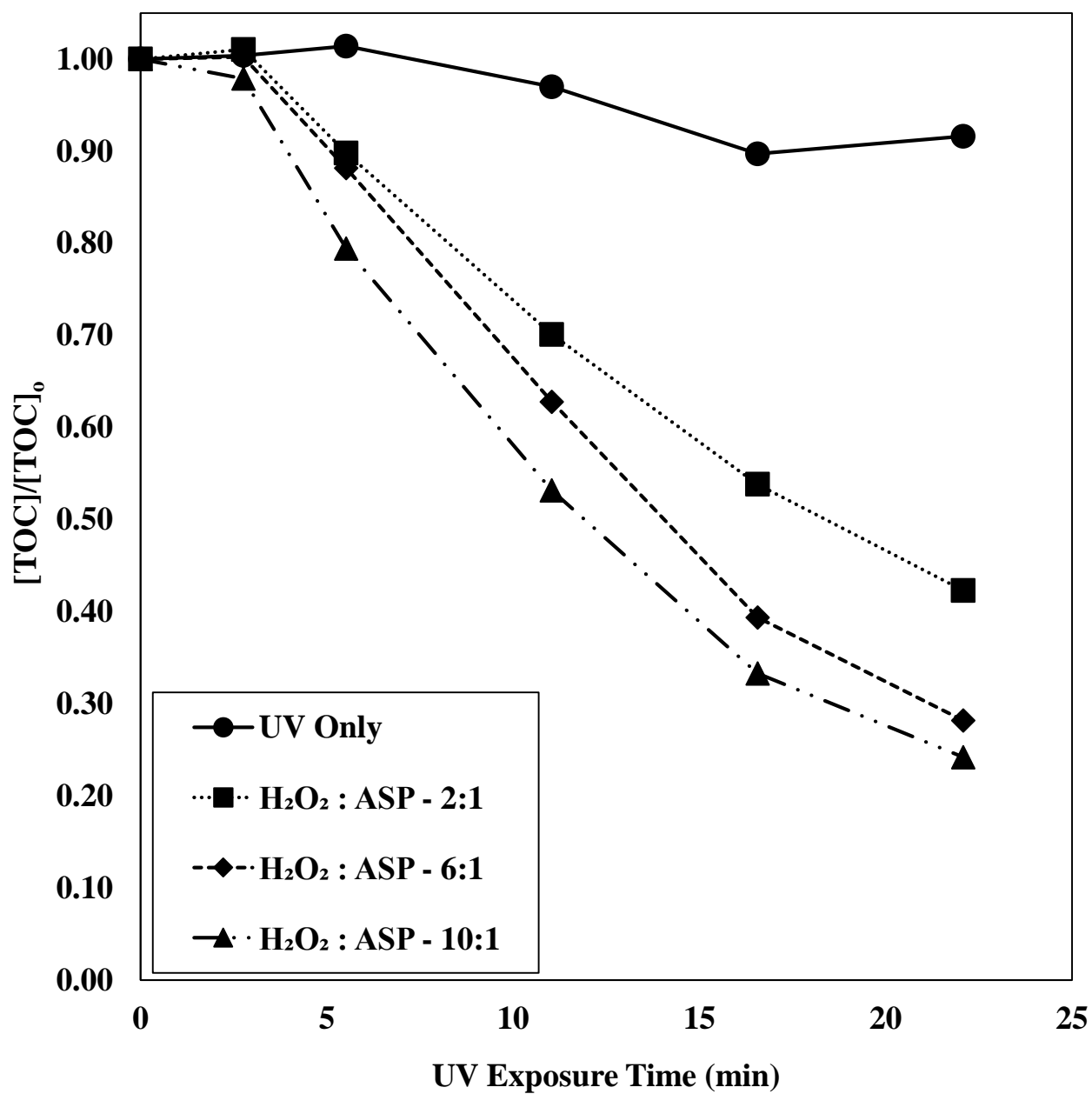


**Figure 4-1:** The degradation trends of ASP (75 mg/L) under UV irradiation and various H<sub>2</sub>O<sub>2</sub> doses by UV/H<sub>2</sub>O<sub>2</sub> with a single photoreactor

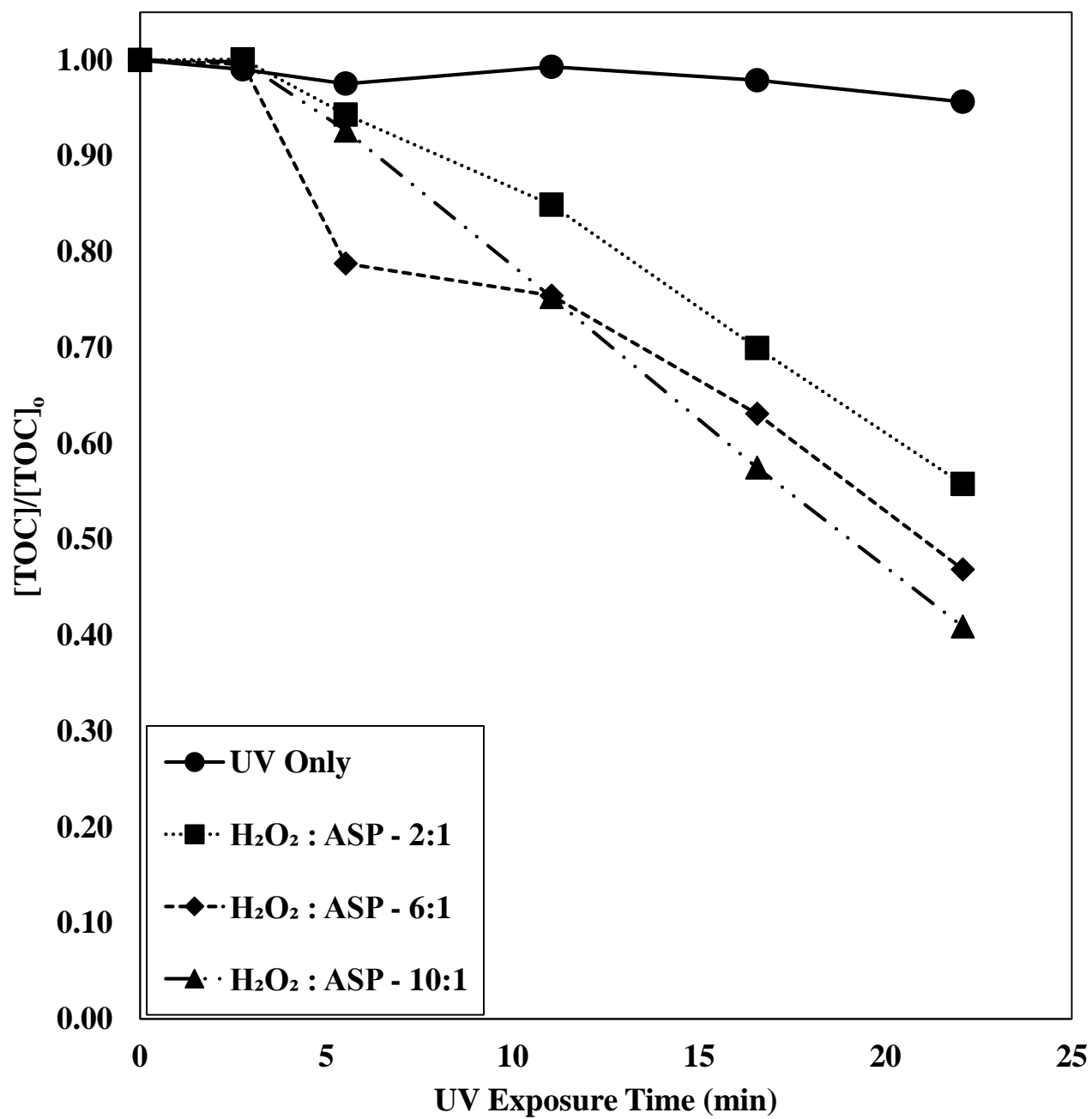


**Figure 4-2:** The degradation trends of ASP (150 mg/L) under UV irradiation and various H<sub>2</sub>O<sub>2</sub> doses by UV/H<sub>2</sub>O<sub>2</sub> with a single photoreactor

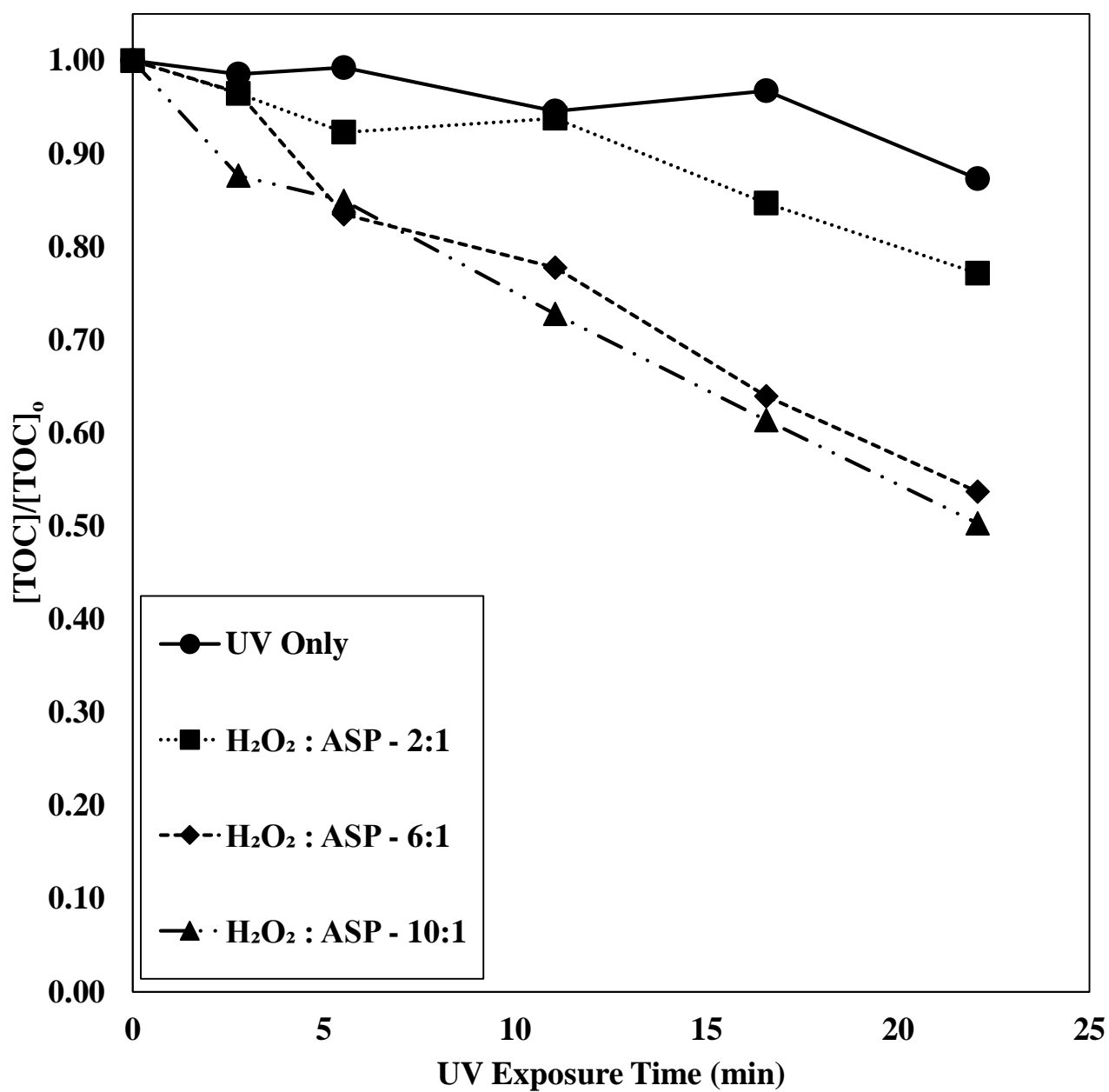


**Figure 4-3:** The degradation trends of ASP (300 mg/L) under UV irradiation and various H<sub>2</sub>O<sub>2</sub> doses by UV/H<sub>2</sub>O<sub>2</sub> with a single photoreactor

#### 4.2.1.1 Effect of UV Irradiation on TOC Removal

Based on TOC removal trends seen in **Figure 4-1**, **Figure 4-2**, and **Figure 4-3**, it is evident that UV irradiation ( $\lambda \cong 254$  nm) alone does not have any significant effect on TOC removal after 22.5 min. The mean  $[\text{TOC}]/[\text{TOC}]_0$  reading was found to be  $0.91 \pm 0.04$  under UV irradiation alone after 22.5 min for all concentrations of ASP. Although the observed TOC removal was unsatisfactory, physical observations strongly suggest that the parent undergoes transformation under UV irradiation. This is evident by a change of solution colour as seen in **Figure 4-4** and **Figure 4-5**.

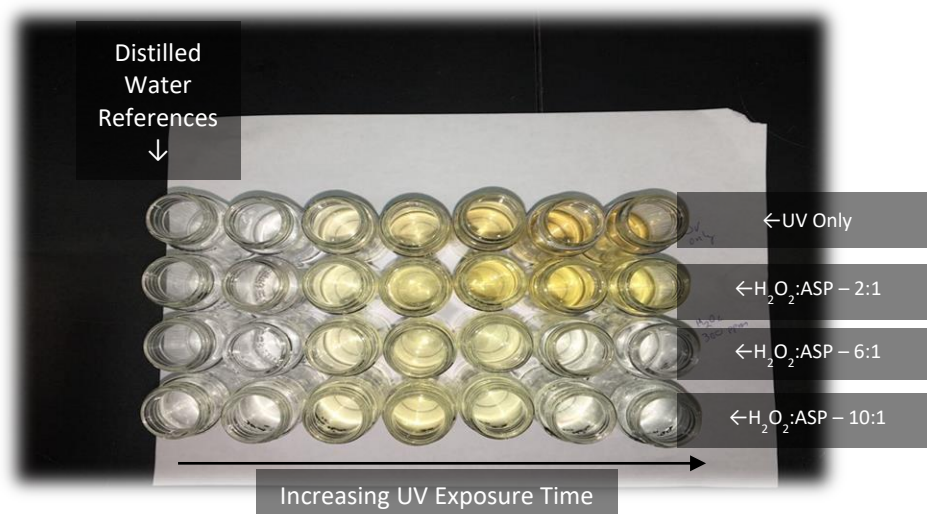


**Figure 4-4:** Comparison of ASP Solution (300 mg/L) colour intensity in the presence of various  $\text{H}_2\text{O}_2$  doses under UV exposure with increasing time

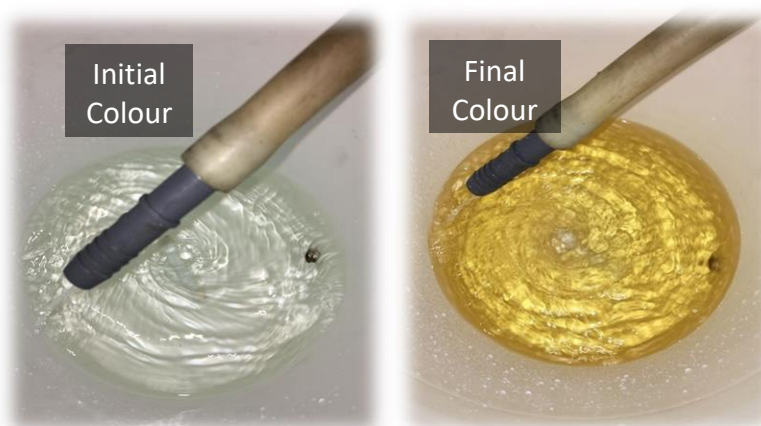


**Figure 4-5:** Comparison of initial and final solution colours for ASP (300 mg/L) under UV irradiation alone (no  $\text{H}_2\text{O}_2$ )

Although unexpected, this observation is not surprising as ASP is known to absorb electromagnetic radiation quite well in the UV range used in this study, with maximal absorbance at wavelengths of ~225 nm and ~260 nm (Dattatreya et al., 2003; Llamas et al., 2008). The observed colour change is discussed in more detail in Section 4.2.1.3.

#### ***4.2.1.2 Effect of H<sub>2</sub>O<sub>2</sub> Dosing on TOC Removal***

The addition of H<sub>2</sub>O<sub>2</sub> resulted in a rapid reduction of TOC in ASP solutions in all experiments, as shown in **Figure 4-1**, **Figure 4-2**, and **Figure 4-3**. Interestingly, an H<sub>2</sub>O<sub>2</sub>:ASP ratio of 2:1 (mass basis) resulted in a significant drop in TOC in comparison to that of UV irradiation alone after 22.5 min of UV exposure. TOC removal was improved with H<sub>2</sub>O<sub>2</sub>:ASP ratios (mass basis) of 6:1 and 10:1. However, the mean TOC removal was improved only by approximately 5% when the H<sub>2</sub>O<sub>2</sub>:ASP ratio (mass basis) was increased from 6:1 to 10:1. This is most likely attributed to the scavenging effect of H<sub>2</sub>O<sub>2</sub> molecules. The scavenging effect occurs when a very large quantity of H<sub>2</sub>O<sub>2</sub> is present. This increases the likelihood of the reaction of HO· with H<sub>2</sub>O<sub>2</sub>, leading to the formation of HO<sub>2</sub>· radicals. These radicals are much weaker in their relative oxidizing potentials in comparison to HO·. When the applied H<sub>2</sub>O<sub>2</sub> doses are larger than the optimal ratio, this phenomenon results in a lower reduction in TOC (Rao et al., 2013). In this case, a reduction in TOC removal was not observed in any of the runs. Hence, it can be concluded that the H<sub>2</sub>O<sub>2</sub>:ASP ratios (mass basis) studied here are close to an optimal point. In other words, an eventual drop in the ultimate TOC removal is expected if H<sub>2</sub>O<sub>2</sub> doses beyond the applied dosages in this study.

#### ***4.2.1.3 Discussion of UV Induced Colourization***

Under UV irradiation alone, a change in solution colour from clear to yellow-orange was observed within approximately 10 min of UV exposure. The intensity of the colour was found to be a function of the concentration of ASP, as the intensity of the colour was observed to be at its peak when the ASP concentration was at its highest level of 300 mg/L. These observations are highlighted in **Figure 4-4** and **Figure 4-5**. In absence of H<sub>2</sub>O<sub>2</sub>, the colour simply continued to intensify until the end of the experimental run. The appearance of colour was also observed in the presence of H<sub>2</sub>O<sub>2</sub>. However, the colour intensity rapidly diminished over time when H<sub>2</sub>O<sub>2</sub> was present in the system. Initially, at an H<sub>2</sub>O<sub>2</sub>:ASP ratio (mass basis) of 2:1, the colour formation and intensity were found to be essentially identical to the one observed under UV irradiation alone.

The colour then disappeared over time. Similar trends were observed for H<sub>2</sub>O<sub>2</sub>:ASP ratios (mass basis) of 6:1 and 10:1 until the midpoint of the treatment. No colour was present at the endpoint of the reaction. This is likely due to the rapid degradation of the intermediates that caused the colour in the first place. Since some TOC is still present at the endpoint, the intermediates responsible for colour are most likely complex organic compounds that are broken down throughout the course of treatment.

Only one study exists in the literature on the degradation of ASP through the generation of HO<sup>•</sup> (Lin et al., 2017). An appearance of colour was not reported. However, the generation of HO<sup>•</sup> was not done through UV irradiation. Therefore, the appearance of colour is likely attributed to by products formed through UV irradiation alone. The suggested intermediates of the reaction of ASP with HO<sup>•</sup> are carboxylic acids, namely, oxalic and oxamic acids (Lin et al., 2017). Both of these compounds are known to form colourless solutions when dissolved in water (CRC Press, 2018). The presence of two amine groups (one primary and one secondary amine) and a benzene group in ASP may have a role in this phenomenon. If polycyclic aromatic compounds are formed, they may be responsible for the colour formation. However, this cannot be confirmed without a thorough investigation of the reaction mechanisms involved. This was beyond the scope of this study. However, it can be concluded that the absorbed wavelength of the compound responsible for colour is likely between 400-490 nm ranges. The general relationship between wavelength absorbed and colour observed can be found in *Table 4-1*.

**Table 4-1:** General relationship between absorption wavelengths and observed colour. Adapted from (Hornback, 2006).

Wavelength Absorbed (nm)	Colour Absorbed	Colour Observed
<b>400</b>	Violet	Yellow – green
<b>425</b>	<i>Blue – violet</i>	<i>Yellow</i>
<b>450</b>	<i>Blue</i>	<i>Orange</i>
<b>490</b>	<i>Blue-green</i>	<i>Red</i>
<b>510</b>	Green	Purple
<b>530</b>	Yellow – green	Violet

*Note: highlighted entries are probable absorption properties of the compound responsible for the coloured appearance of the solution.*

#### 4.2.2 Acesulfame K

The degradation of ACE under UV irradiation ( $\lambda \cong 254 \text{ nm}$ ) alone was examined prior to the addition of  $\text{H}_2\text{O}_2$ . More experiments were carried out under the same exposure time with the addition of  $\text{H}_2\text{O}_2$ . The doses of  $\text{H}_2\text{O}_2$  (mass basis) for various concentrations of ACE are reported in *Table 3-13*. The TOC removal trends with all  $\text{H}_2\text{O}_2$  doses are illustrated in *Figure 4-6*, *Figure 4-7*, and *Figure 4-8* for ACE concentrations of 75, 150 and 300 mg/L respectively.

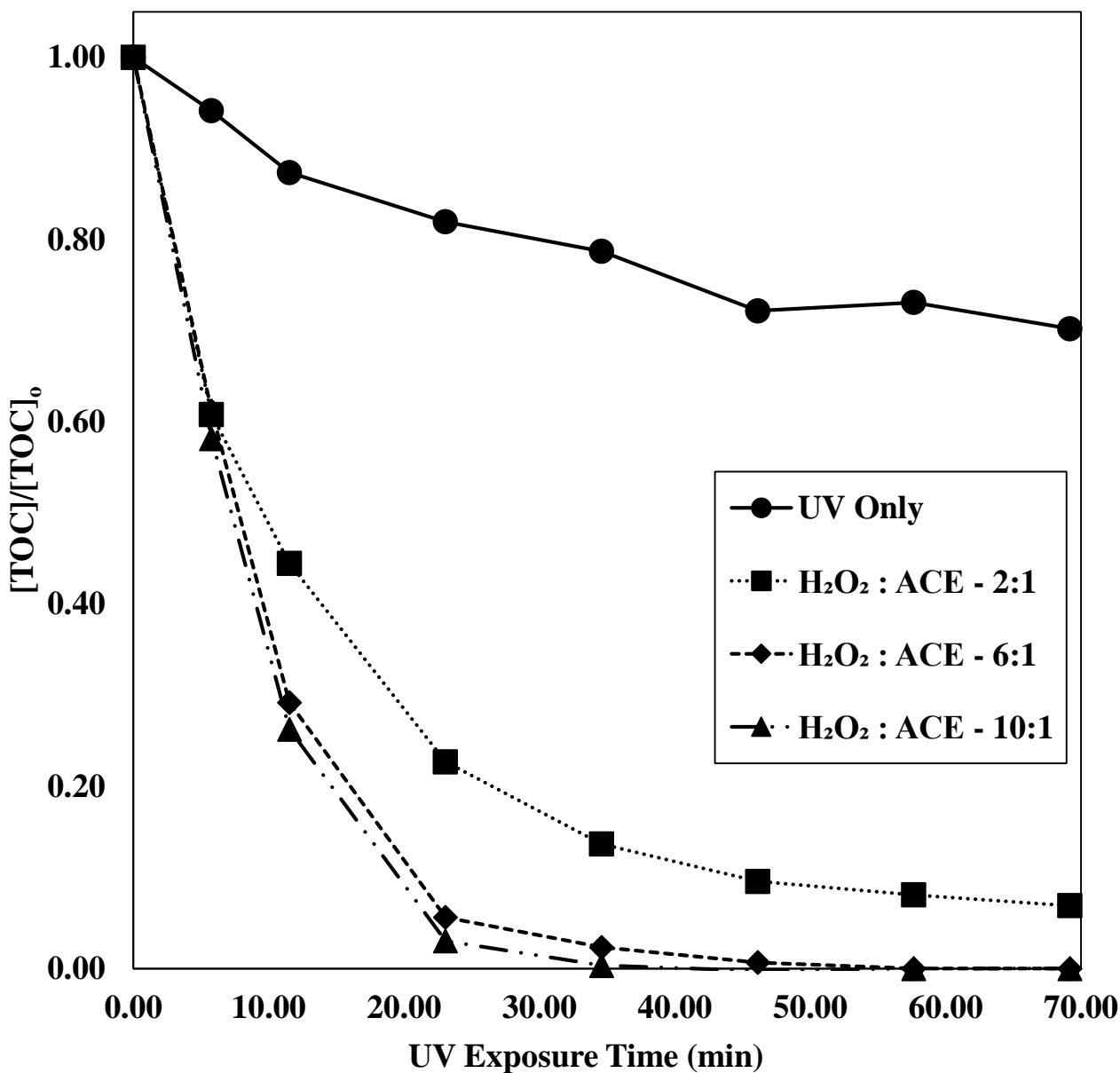


*Figure 4-6:* The degradation of ACE (75 mg/L) under UV irradiation and various  $\text{H}_2\text{O}_2$  doses by UV/ $\text{H}_2\text{O}_2$  with two photoreactors in series



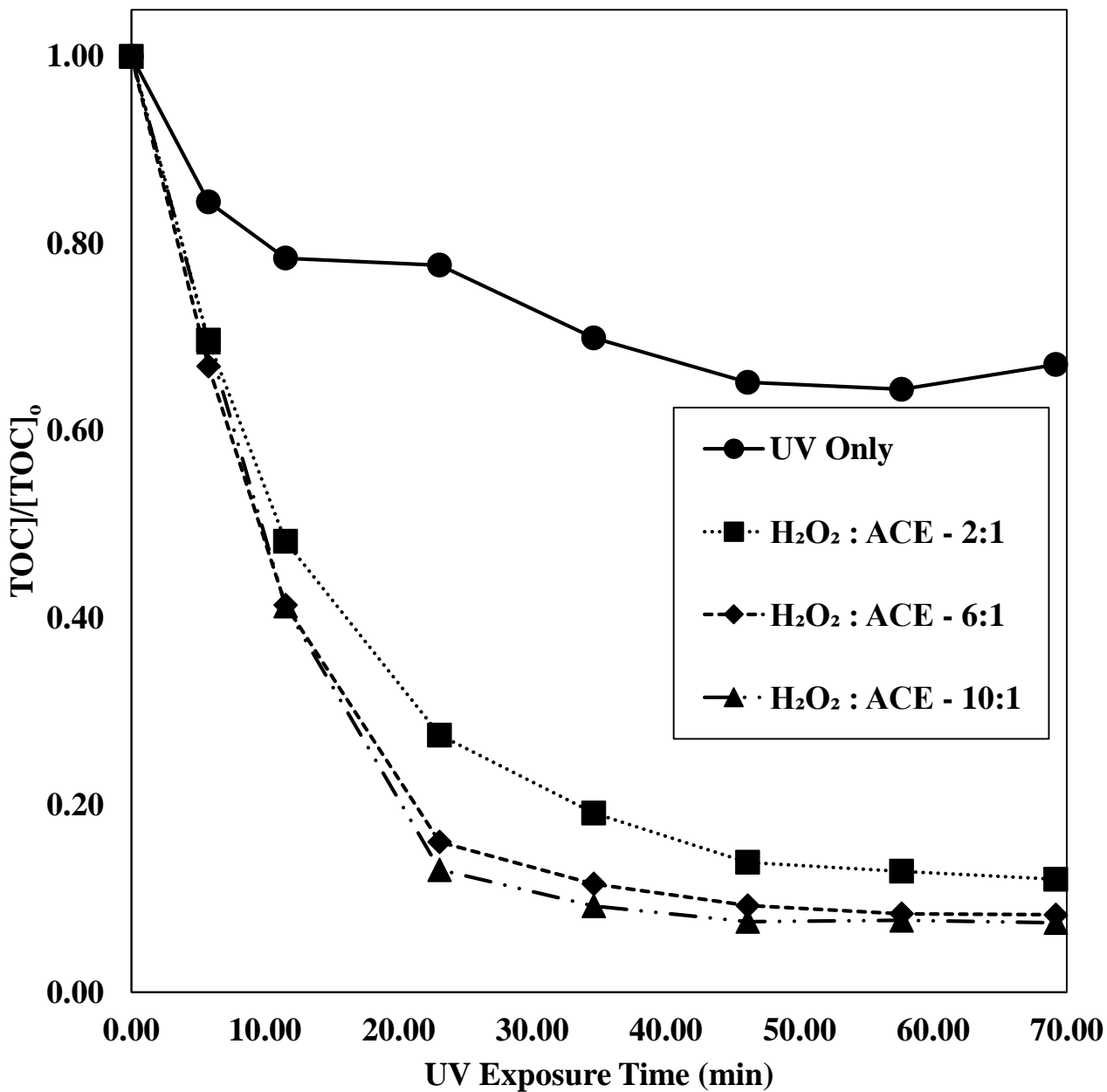


**Figure 4-7:** The degradation of ACE (150 mg/L) under UV irradiation and various  $H_2O_2$  doses by UV/ $H_2O_2$  with two photoreactors in series

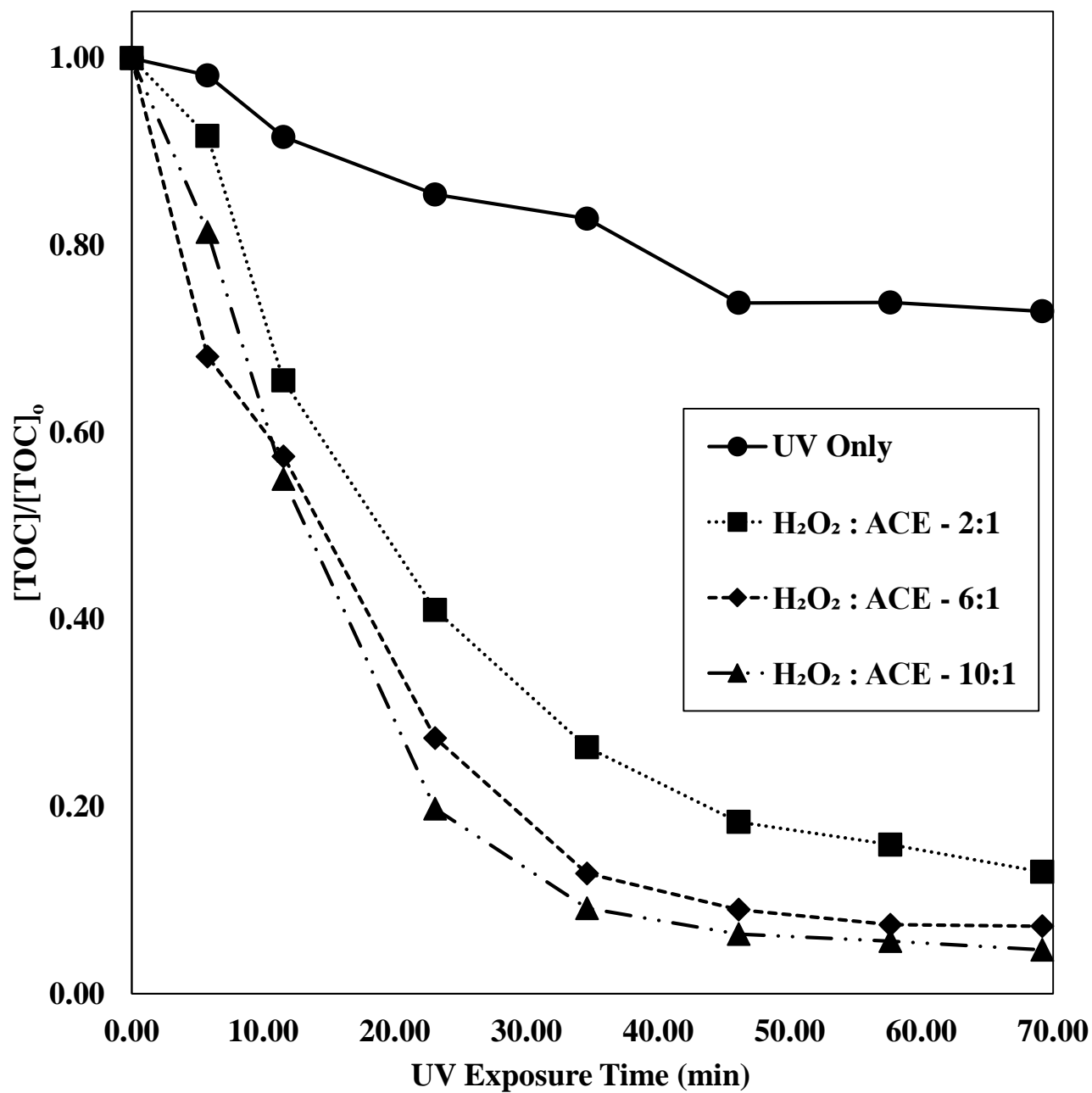


**Figure 4-8:** The degradation of ACE (300 mg/L) under UV irradiation and various H<sub>2</sub>O<sub>2</sub> doses by UV/H<sub>2</sub>O<sub>2</sub> with two photoreactors in series

#### ***4.2.2.1 Effect of UV Irradiation on TOC Removal***

UV irradiation ( $\lambda \cong 254$  nm) alone was found to be somewhat effective in TOC removal for the ACE solution. After 70 min of UV exposure, the mean  $[\text{TOC}]/[\text{TOC}]_0$  was found to be  $0.71 \pm 0.03$  throughout all experimental runs. ACE is known to absorb UV irradiation in the of 220-250 nm range, with a maximal peak at  $\sim 225$  nm (Llamas et al., 2008). Hence, the results obtained for the degradation of ACE under UV irradiation are in agreement with the reports in the literature (Li et al., 2016; Scheurer et al., 2014). The transformation of ACE under UV irradiation ( $\lambda \cong 254$  nm) has also been reported in other studies to various extents. A total of ten transformation products have been identified with UV irradiation ( $\lambda \geq 290$  nm) alone and sixteen with UV irradiation ( $\lambda \cong 254$  nm) in the presence of  $\text{TiO}_2$ . Nine of the transformation products of ACE under UV irradiation alone were also identified in the presence of  $\text{TiO}_2$ . All the transformation products were found to be fragments of the parent ACE compound (Li et al., 2016; Scheurer et al., 2014). This indicates a strong absorbance of a broad range of UV irradiation by the parent compound. Fragmentation of a molecule such as ACE may result in small organic chains which may ultimately be destroyed under high-energy irradiation such as UV ( $\lambda \cong 254$  nm), which explains the overall reduction in TOC. However, a transformation does not necessarily mean complete mineralization. This is why only partial amounts of TOC was removed in this study.

#### ***4.2.2.2 Effect of $\text{H}_2\text{O}_2$ Dosing on TOC Removal***

As expected, the addition of  $\text{H}_2\text{O}_2$  resulted in a rapid reduction of TOC in the ACE solutions in all experimental runs. At lower concentrations (75 mg/L) after 70 min of UV exposure, the mean  $[\text{TOC}]/[\text{TOC}]_0$  was  $0.12 \pm 0.02$  with a 2:1 ratio of  $\text{H}_2\text{O}_2$ :ACE (mass basis). For higher concentrations of ACE (150 and 300 mg/L) with a 2:1 mass ratio of  $\text{H}_2\text{O}_2$ :ACE, the mean  $[\text{TOC}]/[\text{TOC}]_0$  were measured to be  $0.05 \pm 0.04$  and  $0.04 \pm 0.04$ , respectively. Increasing the  $\text{H}_2\text{O}_2$ :ACE ratio from 2:1 to 6:1 and 10:1 resulted in the complete mineralization of ACE (75 mg/L) with essentially overlapping TOC reduction curves, within only 45 min of UV exposure. Complete mineralization was not achieved with higher concentrations of ACE, most likely due to the scavenging effect caused by a larger concentration of  $\text{H}_2\text{O}_2$ . The mean TOC removal was over 88% in all cases (below a  $[\text{TOC}]/[\text{TOC}]_0$  reading of 0.12). Such an observation is also reported in the literature where the parent compound of ACE was completely transformed after 20 min of

treatment in a UVA/H<sub>2</sub>O<sub>2</sub>/Fe<sup>2+</sup> system, while TOC was still detectable (20% of the initial TOC concentration) after 120 min of treatment (Kattel et al., 2017). The relatively poor TOC reduction was likely due to the usage of UV ( $\lambda \cong 315\text{-}400$  nm), which carries considerably less energy and therefore less effective for the generation of *HO*<sup>•</sup> radicals. Near identical TOC removal, results were obtained for H<sub>2</sub>O<sub>2</sub>:ACE ratios (mass basis) of 6:1 and 10:1. This can be attributed to the scavenging effect of H<sub>2</sub>O<sub>2</sub> when present in high concentrations. This was also observed with the degradation of ASP. Hence, it can be concluded that implementing an H<sub>2</sub>O<sub>2</sub>:ACE ratio larger than 6:1 is not necessary.

#### 4.2.3 Sucralose

SUC was the last of the three artificial sweeteners to be studied individually under UV/H<sub>2</sub>O<sub>2</sub>. Aqueous solutions of SUC were first treated with UV irradiation alone. More experiments were then carried out under the same exposure time with the addition of H<sub>2</sub>O<sub>2</sub>. The doses of H<sub>2</sub>O<sub>2</sub> (mass basis) for various concentrations of SUC are reported in **Table 3-14**. The TOC removal trends with all H<sub>2</sub>O<sub>2</sub> doses are illustrated in **Figure 4-9**, **Figure 4-10** and **Figure 4-11** for SUC concentrations of 75, 150 and 300 mg/L respectively.

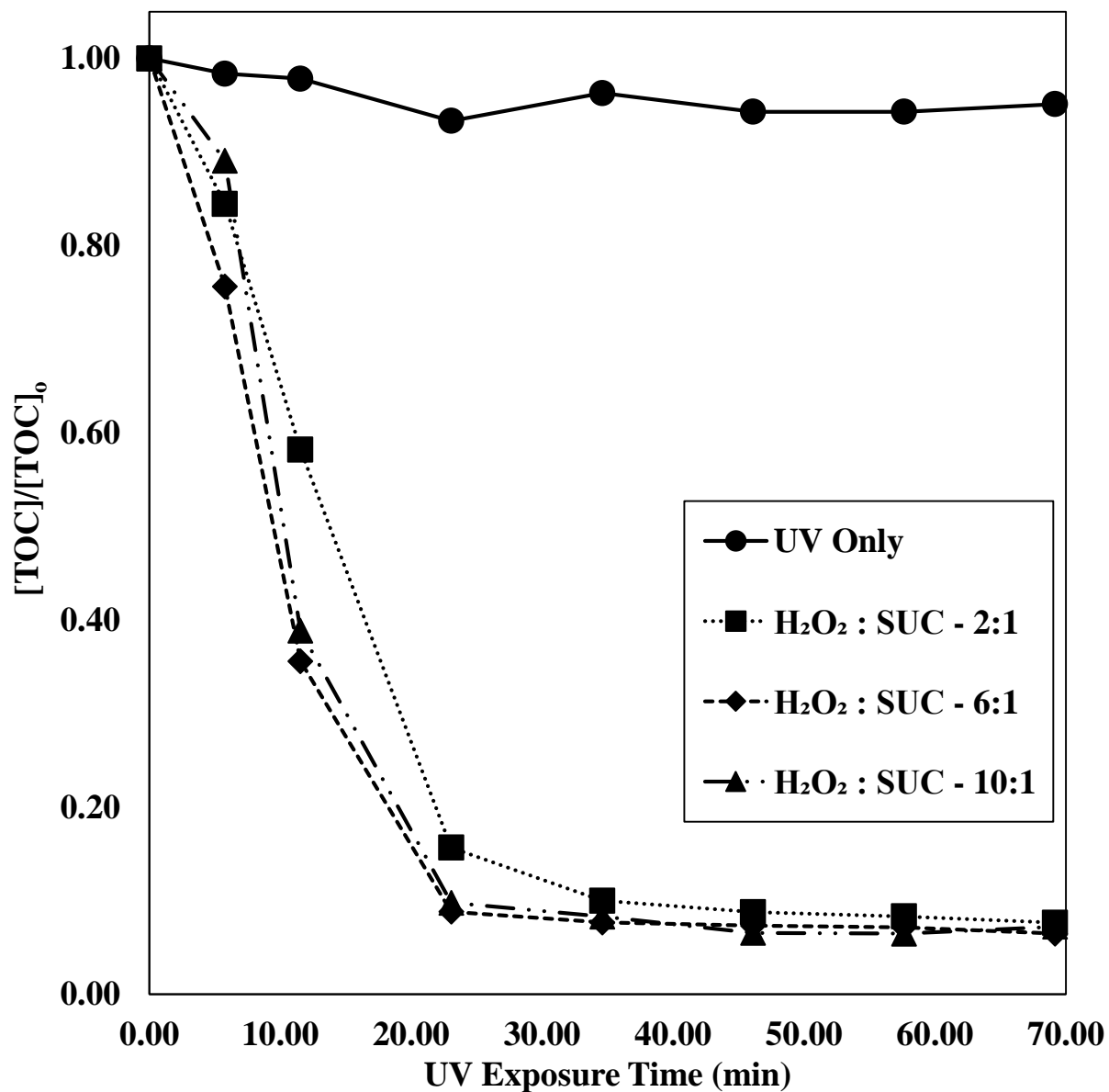


**Figure 4-9:** The degradation of SUC (75 mg/L) under UV irradiation and various H<sub>2</sub>O<sub>2</sub> doses by UV/H<sub>2</sub>O<sub>2</sub> with two photoreactors in series

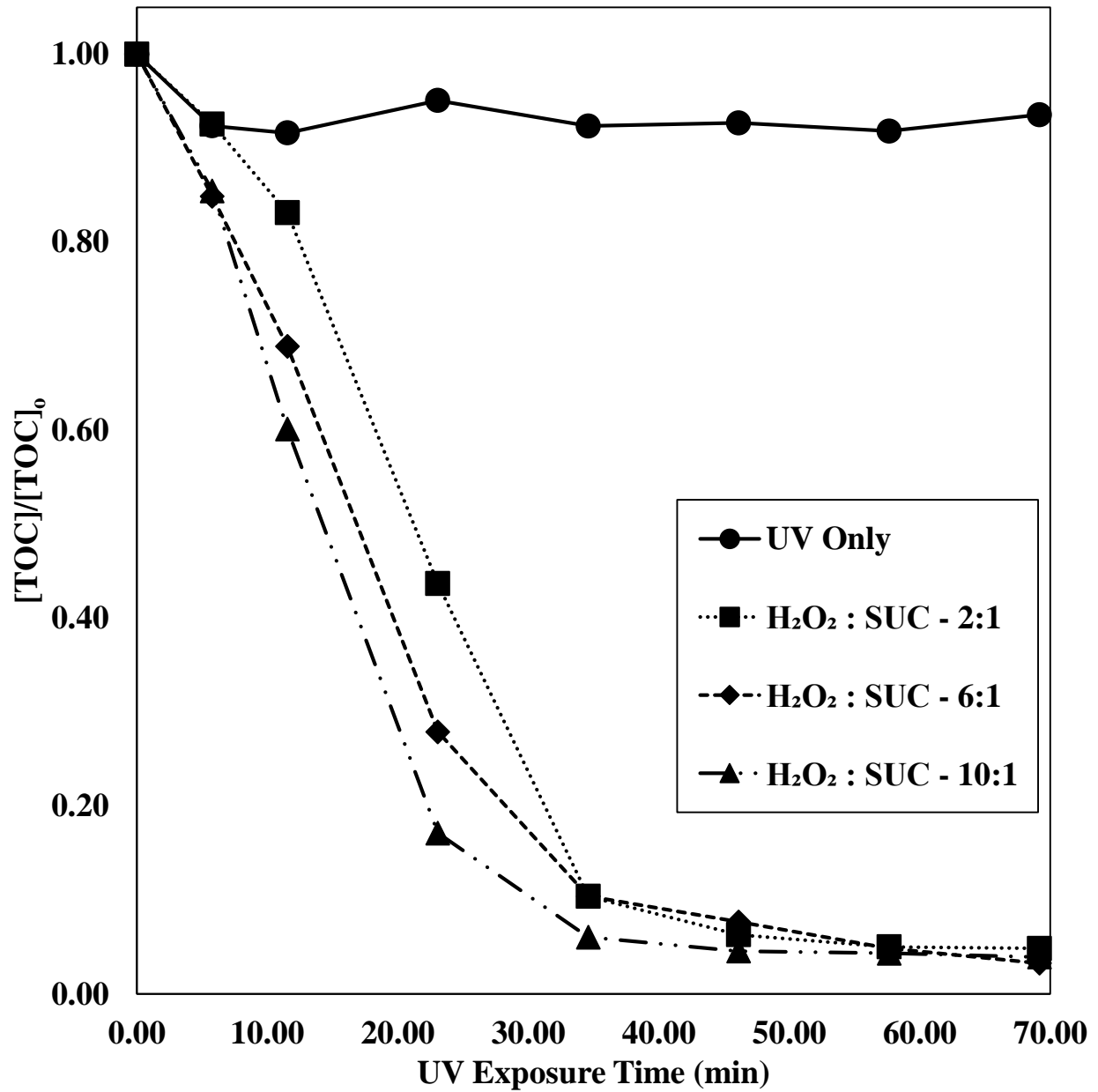


**Figure 4-10:** The degradation of SUC (150 mg/L) under UV irradiation and various  $H_2O_2$  doses by UV/ $H_2O_2$  with two photoreactors in series

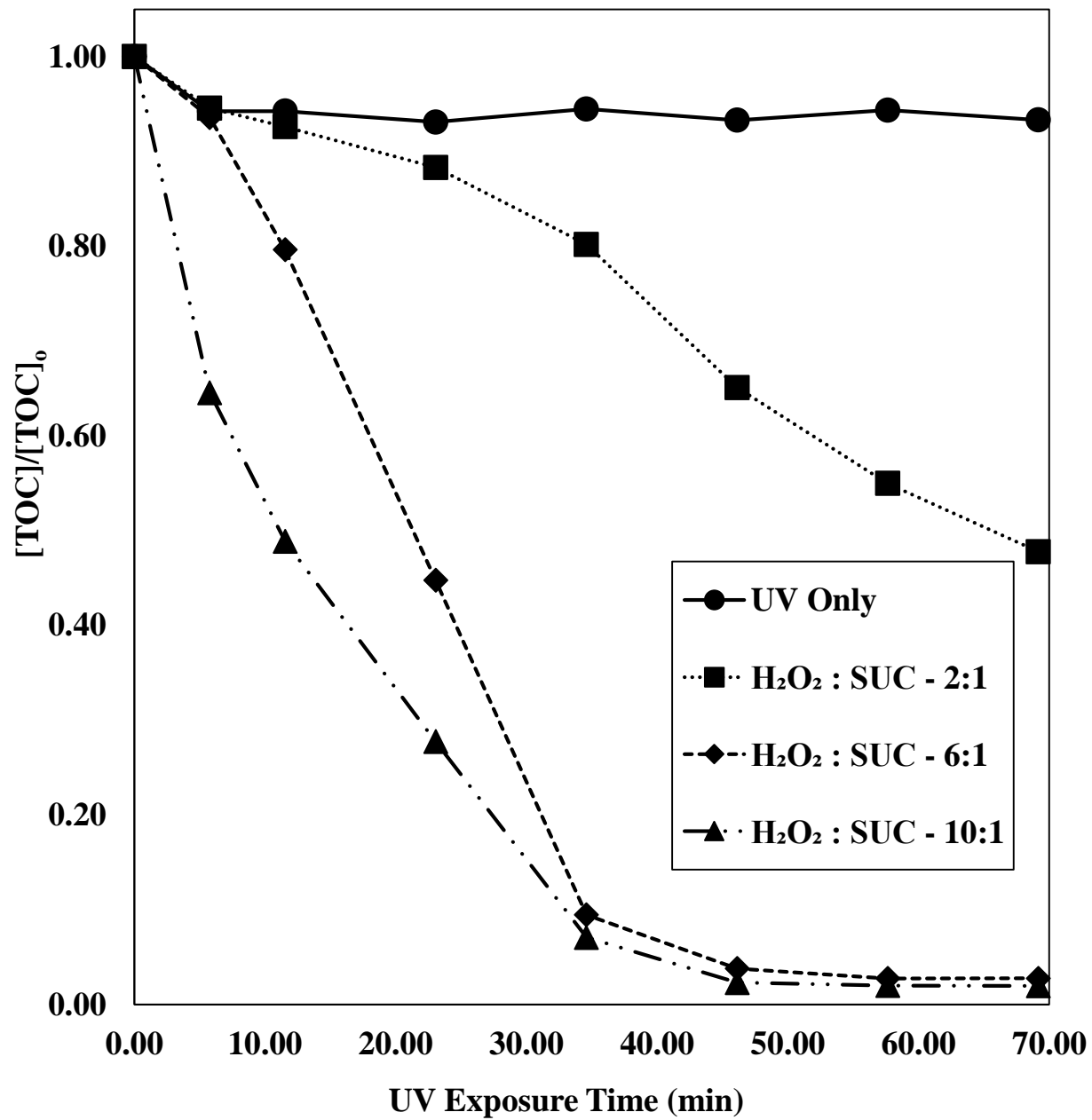


**Figure 4-11:** The degradation of SUC (300 mg/L) under UV irradiation and various H<sub>2</sub>O<sub>2</sub> doses by UV/H<sub>2</sub>O<sub>2</sub> with two photoreactors in series

#### ***4.2.3.1 Effect of UV Irradiation on TOC Removal***

UV irradiation ( $\lambda \cong 254$  nm) alone was found to be ineffective in the reduction of TOC in all tests after 70 min of UV exposure, resulting in a mean  $[\text{TOC}]/[\text{TOC}]_0$  reading of  $0.94 \pm 0.01$ . This was expected as SUC is not known to absorb UV irradiation in this range, with absorption occurring at a wavelength of  $\lambda \cong 190$  nm (Kirk, 2010). Similar results are reported in another study where the no degradation was observed for the treatment of SUC under UV irradiation ( $\lambda \cong 254$  nm) alone (Xu et al., 2016).

#### ***4.2.3.2 Effects of H<sub>2</sub>O<sub>2</sub> Dosing on TOC Removal***

TOC removal was improved significantly when UV irradiation ( $\lambda \cong 254$  nm) was accompanied with H<sub>2</sub>O<sub>2</sub> dosing. A TOC removal of over 90% ( $[\text{TOC}]/[\text{TOC}]_0$  reading of 0.07) was observed with an applied H<sub>2</sub>O<sub>2</sub>:SUC ratio (mass basis) of 2:1 at a SUC concentration of 75 mg/L. Applied H<sub>2</sub>O<sub>2</sub>:SUC ratios (mass basis) of 6:1 and 10:1 resulted in virtually identical TOC removal responses. Very similar results were also observed for a SUC concentration of 150 mg/L. However, the TOC removal was significantly reduced when the concentration of SUC was increased to 300 mg/L with a H<sub>2</sub>O<sub>2</sub>:SUC ratio (mass basis) of 2:1 as seen in **Figure 4-11**, with a  $[\text{TOC}]/[\text{TOC}]_0$  reading of only 0.48. The mean  $[\text{TOC}]/[\text{TOC}]_0$  ratio with an applied H<sub>2</sub>O<sub>2</sub>:SUC ratio of 2:1 was found to be  $0.20 \pm 0.2$ . Applied H<sub>2</sub>O<sub>2</sub>:SUC ratios (mass basis) of 6:1 and 10:1 still performed very well, both resulting in the same  $[\text{TOC}]/[\text{TOC}]_0$  readings of  $0.04 \pm 0.02$ . It was once again observed that an increase from H<sub>2</sub>O<sub>2</sub>:SUC ratio from 6:1 to 10:1 did not improve the overall amounts of TOC removed, likely due to the scavenging effect of large amounts of H<sub>2</sub>O<sub>2</sub> in the system.

The performance of the system was somewhat surprising as other studies only reported the maximum TOC removal to be about 60% for an equivalent H<sub>2</sub>O<sub>2</sub>:SUC ratio of 1.3:1 (mass basis) for SUC concentrations of 50 mg/L (Xu et al., 2016). However, the experiments were performed in a standard laboratory beaker rather than a specially designed photoreactor. This further highlights the importance of utilizing specialized photoreactors as they are designed to maximize the use of photons emitted through internal reflection. Furthermore, the concentrations were significantly lower than the ones investigated in this study. Therefore, deviations in the system behaviour are to be expected due to differences in experimental setup. The degradation of SUC



through UV/PDS (Peroxydisulfate) AOP has also been investigated by other studies, which reportedly performed better than a comparable UV/H<sub>2</sub>O<sub>2</sub>, with maximum TOC removals of up to 93% (Xu et al., 2016). Nevertheless, this level of TOC removal was achieved with a UV/H<sub>2</sub>O<sub>2</sub> process in this study.

#### 4.2.4 Concluding Remarks

In the preliminary experiments, the overall system behaviour was investigated for each of the artificial sweeteners. Based on the experimental results obtained, no significant TOC removal was detected for three selected artificial sweeteners ASP, ACE and SUC with UV irradiation ( $\lambda \cong 254$  nm) alone. Further investigations showed that the three artificial sweeteners can be effectively removed from aqueous matrices by the UV/H<sub>2</sub>O<sub>2</sub> processes. The degradation trends with of various H<sub>2</sub>O<sub>2</sub> doses under UV irradiation were also determined.

The degradation of ASP was studied for the first time under UV irradiation ( $\lambda \cong 254$  nm) alone and in a UV/H<sub>2</sub>O<sub>2</sub> system. It was observed that the exposure of ASP to UV irradiation ( $\lambda \cong 254$  nm) results in the formation of colour in an otherwise clear and colourless solution. Hence, the use of H<sub>2</sub>O<sub>2</sub> should be considered if UV irradiation is to be implemented in for the degradation of ASP.

ACE was found to respond very well to UV/H<sub>2</sub>O<sub>2</sub> treatment, with the TOC removal results approaching 90%. Such results were achievable even with an H<sub>2</sub>O<sub>2</sub>:ACE ratio (mass basis) of 2:1. All the studied H<sub>2</sub>O<sub>2</sub>:ACE ratios (mass basis) were found to yield the same TOC removal trends across every concentration of ACE studied. In comparison to other UV based AOPs in the literature, a UV/H<sub>2</sub>O<sub>2</sub> system when applied in the UV-C region ( $\lambda = 254$  nm) of irradiation outperformed the UV/H<sub>2</sub>O<sub>2</sub>/Fe<sup>2+</sup> and the UV/S<sub>2</sub>O<sub>8</sub><sup>2-</sup>/Fe<sup>2+</sup> in the UV-A region ( $\lambda = 315$ -400 nm).

It can also be concluded that UV/H<sub>2</sub>O<sub>2</sub> was effective in the removal of TOC for aqueous solutions of SUC. An applied H<sub>2</sub>O<sub>2</sub>:SUC ratio (mass basis) of 2:1 did not perform well at SUC concentration of 300 mg/L. Nevertheless, an appropriate ratio can be selected based on the investigations carried out and desired SUC concentrations. Finally, experimental results suggest that increasing the H<sub>2</sub>O<sub>2</sub>:SUC ratio (mass basis) 6:1 to 10:1 did not improve TOC reduction. Hence, larger ratios are not recommended for the concentration ranges investigated in this study.

### 4.3 Statistical Design of Experiments – The Photochemical Degradation of Multicomponent Systems of Artificial Sweeteners by UV/H<sub>2</sub>O<sub>2</sub>

Based on the experimental results obtained from the preliminary studies, efforts were made to study the system behaviour with aqueous solutions containing ASP, ACE and SUC as a multicomponent system. Five factors were selected at two levels. These factors include the initial TOC due to ASP (TOC<sub>ASP,ini</sub>, Factor A), the initial TOC due to ACE (TOC<sub>ACE,ini</sub>, Factor B), the initial TOC due to SUC (TOC<sub>SUC,ini</sub>, Factor C), the applied H<sub>2</sub>O<sub>2</sub>:TOC<sub>total,ini</sub> (Factor D, mass basis), and the operating temperature (Factor E). The factor levels were previously reported in **Table 3-15**. The levels of the experimental factors were selected based on the results obtained from the preliminary experiments. As discussed earlier, large H<sub>2</sub>O<sub>2</sub> doses (e.g. mass ratios of 10:1) did not improve TOC reduction due to the scavenging effect. Hence, the H<sub>2</sub>O<sub>2</sub>:TOC<sub>total,ini</sub> ratios (mass basis) were selected in a manner as to limit the H<sub>2</sub>O<sub>2</sub> amounts to approximately 2:1–6:1 (mass basis) for each sweetener in all runs. Hence, H<sub>2</sub>O<sub>2</sub>:TOC<sub>total,ini</sub> ratios (mass basis) of 5:1 (low-level) and 10:1 (high-level) were applied. These ratios were tested again in the multicomponent system to confirm their applicability in such systems as well. Finally, it was observed that UV exposure of 45 min was sufficient with the experimental setup used in this study. Hence, a constant UV exposure of 45 min was maintained for all runs in the statistical design. All the experiments were carried out to achieve a UV exposure of 45 min corresponding to a total run time of 120 min (see Appendix F – Determination of UV Exposure Time and Conversion Per Pass for calculations). The main effects and interactions of the experimental factors were identified and analyzed. Experimental data were analyzed throughout the entire treatment process for all runs. Six center-point replicates were used to estimate experimental error (see Section 3.5.1). The center-points were also used to test for the presence of curvature in the response surface. The DOE was generated and randomized by the statistical software Design Expert 11 by Stat-Ease, Inc. The experimental conditions were reported in **Table 3-15**, which can be found in Section 3.5. The experimental setup was shown in **Figure 3-7**. Detailed discussions regarding the inferences of the experimental results are presented in this section from a statistical point of view. An overview of the experimental results can be found in **Table 4-2**.

**Table 4-2:** Overview of the experimental results for the treatment of multicomponent aqueous systems of ASP, ACE and SUC with UV/H<sub>2</sub>O<sub>2</sub> at a UV exposure of 45 min

Run	Coded Values					TOC
	[TOC] <sub>ASP</sub>	[TOC] <sub>ACE</sub>	[TOC] <sub>SUC</sub>	H <sub>2</sub> O <sub>2</sub> :TOC <sub>total,ini</sub>	Operating Temp (°C)	Removal
1	-1	1	1	1	-1	85.05%
2	1	-1	-1	1	1	92.37%
3	-1	-1	1	-1	-1	87.18%
4	0	0	0	0	0	85.68%
5	1	1	1	-1	-1	72.08%
6	-1	1	1	-1	1	86.83%
7	0	0	0	0	0	88.41%
8	1	-1	-1	-1	-1	79.88%
9	1	1	-1	-1	1	87.56%
10	1	1	1	1	1	92.55%
11	-1	-1	-1	-1	1	89.47%
12	0	0	0	0	0	86.85%
13	-1	1	-1	1	1	92.17%
14	1	1	-1	1	-1	82.29%
15	0	0	0	0	0	88.44%
16	1	-1	1	-1	1	89.27%
17	-1	1	-1	-1	-1	82.21%
18	0	0	0	0	0	88.71%
19	-1	-1	1	1	1	92.52%
20	-1	-1	-1	1	-1	89.02%
21	1	-1	1	1	-1	86.76%
22	0	0	0	0	0	87.78%

#### 4.3.1 Identification of Significant Effects

A quick look at **Table 4-2** reveals a trend in terms of system performance. Every time the TOC removal was over 92%, the operating temperature and the H<sub>2</sub>O<sub>2</sub>:TOC<sub>total,ini</sub> (mass basis) were also at their respective high levels, highlighted as green entries. The opposite is true for TOC removal

results of 82% and below, highlighted as red entries. In order to confirm and understand the extent of the effects of these factors, statistical tests can be employed. One of the quickest methods for the selection of significant effects is by analyzing a half-normal probability plot of the absolute values of the standardized effects. In theory, this approach is a statistical hypothesis testing method in which the calculated standardized effects corresponding to each independent factor are hypothesized to be zero. Small deviations from the hypothesized value are taken to be due to random experimental error. Hence, factors with no effects will be (approximately) normally distributed around a mean (zero) and will follow straight line on a half-normal probability plot. Factors that do not follow this trend are then considered to be significant (Montgomery, 2005). In this case, factors E (operating temperature) and D ( $\text{H}_2\text{O}_2\text{:TOC}_{\text{total,ini}}$ , mass basis) were found to be significant. **Figure 4-12** shows the half-normal probability plot of the effects for the overall treatment process at a UV exposure of 45 min.

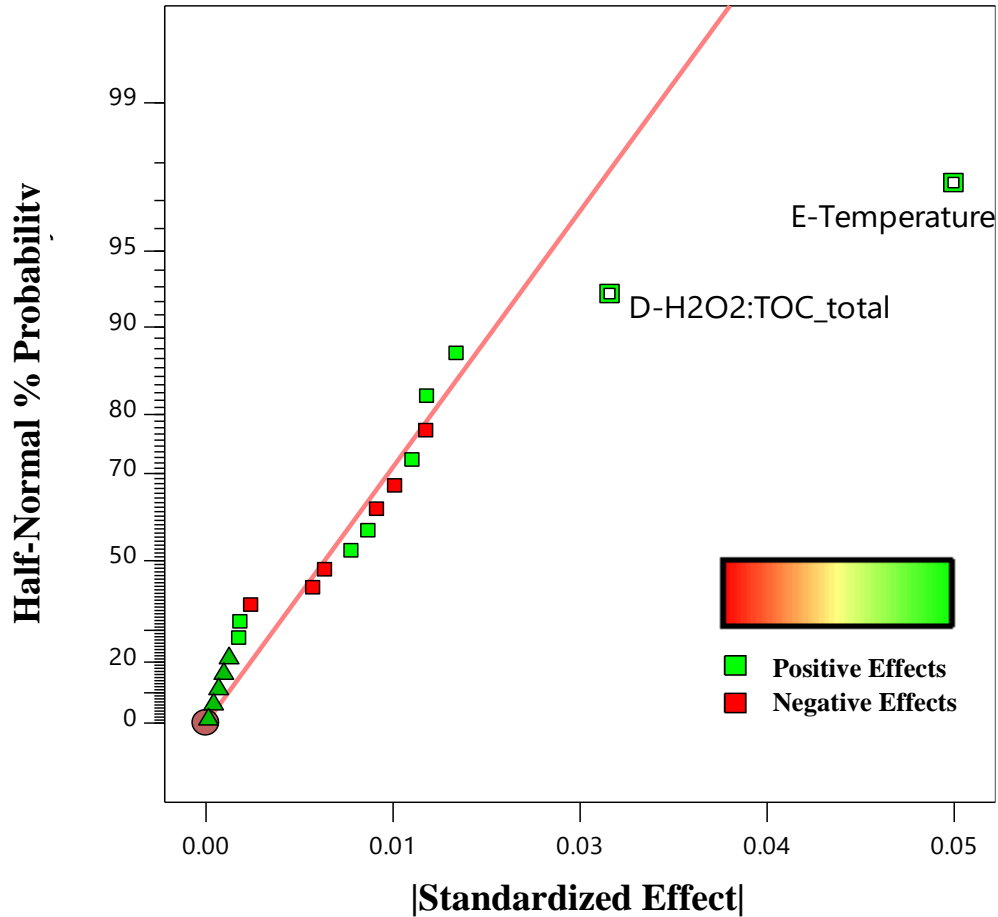


**Figure 4-12:** Half-normal probability (%) plot of standardized effects investigated at a UV exposure of 45 min (experimental endpoint). Factors D ( $\text{H}_2\text{O}_2:\text{TOC}_{\text{total,ini}}$ ) and E (operating temperature) were found to be the most significant effects

To further confirm the results observed in **Figure 4-12**, the two identified significant effects are selected for regression analysis and their significance is analyzed through a Pareto chart against the resulting *t-value* limit. The *t-value* limit is obtained based on the resulting *t-value* of selecting two parameters (factors D and E) for regression analysis at a confidence interval of 95%. By definition, the calculated *t-values* of the effects that are larger than the *t-value* limit are very likely to be significant. In other words, their deviation from the hypothesized mean of zero is very likely due to some physiochemical exertion on the system (in this case, TOC removal). In this case, the *t-value* of the effects of both factors E (operating temperature) and D ( $\text{H}_2\text{O}_2:\text{TOC}_{\text{total,ini}}$ , mass basis) are well beyond the resulting *t-value* limit of the regression analysis. This is shown in **Figure 4-13**.

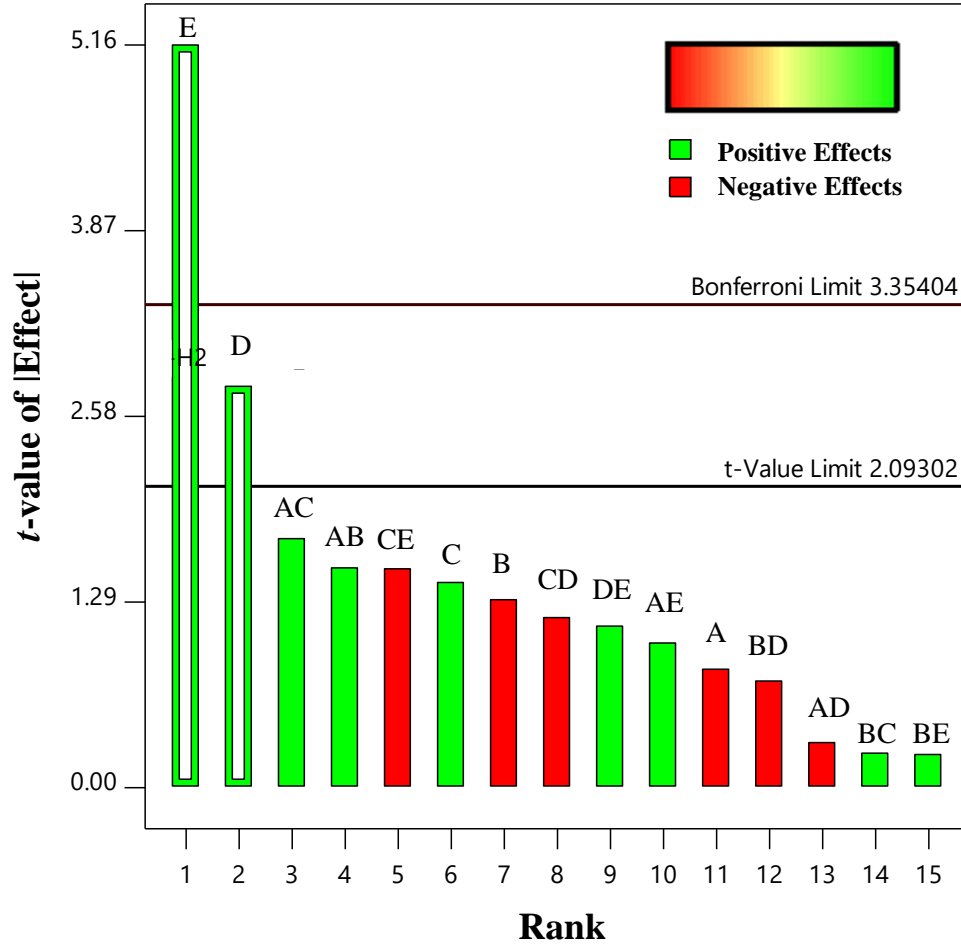


**Figure 4-13:** Pareto chart of standardized effects of decreasing rank order plotted against corresponding  $t$ -values at a UV exposure of 45 min (experimental endpoint). Factors D ( $\text{H}_2\text{O}_2:\text{TOC}_{\text{total,ini}}$ ) and E (operating temperature) were found to be the most significant effects

Based on the results of the statistical tests carried out on these effects, the observations from **Table 4-2** are verified. Hence, factors D ( $\text{H}_2\text{O}_2:\text{TOC}_{\text{total,ini}}$ , mass basis) and E (operating temperature) were found to be the most influential factors on the removal of TOC after 45 min of UV exposure. Other factors and interactions were found to be insignificant in this regard.

Although the primary focus of these experiments was to understand the behaviour of the process as a whole, samples were collected and analyzed through the experimental runs, prior to completion. The half-normal probability plot and the Pareto chart tests were also done for all the samples to screen for interactions and other potentially interesting observations. As a result, an unexpected interaction effect was detected between factors A ( $\text{TOC}_{\text{ASP,ini}}$ ) and C ( $\text{TOC}_{\text{SUC,ini}}$ ) at a

UV exposure of 22.5 min. The results of the half-normal probability plot analysis are shown in **Figure 4-14**.

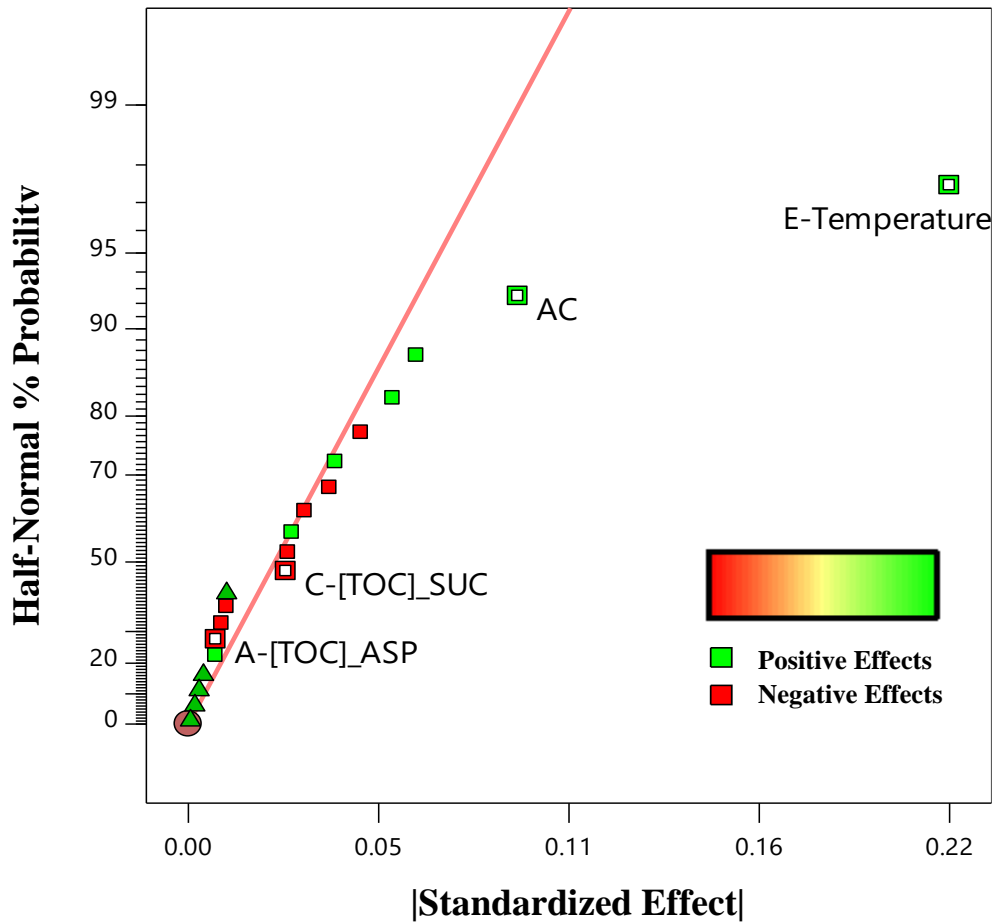


**Figure 4-14:** Half-normal probability (%) plot of standardized effects investigated at a UV exposure of 22.5 min (experimental midpoint). Factor E (operating temperature) was found to be the most significant effect.

Based on the results shown in **Figure 4-14**, the individual effects of factors A ( $\text{TOC}_{\text{ASP},\text{ini}}$ ) and C ( $\text{TOC}_{\text{SUC},\text{ini}}$ ) alone did not have any significant exertion on the removal of TOC. However, the interaction of these factors resulted in a temporary increase in the TOC removal from the system at a UV exposure of 45 min. It can once again be observed that factor E (operating temperature) had a significant effect on the removal of TOC at 22.5 min of UV exposure. The selection of these parameters for regression analysis results in the Pareto chart seen in **Figure 4-15**. The justification along with relevant discussion is presented in Section 4.3.2.3.

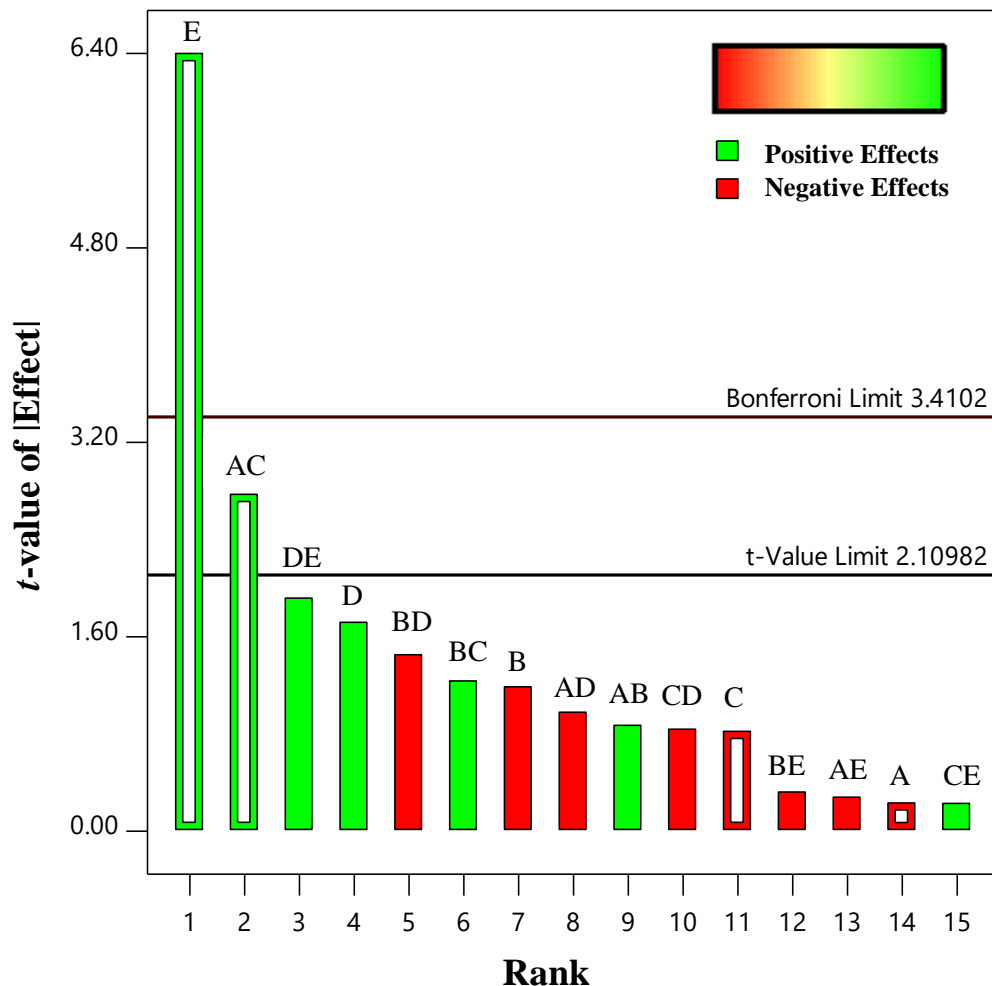


**Figure 4-15:** Pareto chart of standardized effects of decreasing rank order plotted against the corresponding *t-values* at a UV exposure of 22.5 min (experimental midpoint). Factor E (operating temperature) was found to be the most significant effect, followed by the interaction effect of factors A and C

#### 4.3.2 The Effects of Factors and their interactions on TOC Removal

The primary objective of the experimental work in this study was to investigate the degradation of ASP, ACE and SUC in a multicomponent system of artificial sweeteners treated through UV/H<sub>2</sub>O<sub>2</sub>. Thus far, it has been shown that the overall treatment process is strongly influenced by the operating temperature and the H<sub>2</sub>O<sub>2</sub>:TOC<sub>total,ini</sub> (mass basis). It was also shown that SUC and ASP interact to temporarily improve TOC removal at a UV exposure of 22.5 min. The effect of each factor is obtained by calculating and comparing the mean response values for that factor at its high (+1) and low (-) levels respectively. This is calculated for each independent factor according to the following equation:



$$x_j = \frac{\text{Mean Response for } X_j \text{ at } (+1) - \text{Mean Response for } X_j \text{ at } (-1)}{2}$$

$x_j \equiv$  the calculated magnitude of  $X_j$

$X_j \equiv$  independent factor ( $j$ )

These calculations were carried for all independent factors at UV exposures of 22.5 and 45 min respectively. These results are best seen through graphical representation as seen in **Figure 4-16** and **Figure 4-17**. In these plots, the TOC removal results from the centre point replications are shown as red points placed between the high and low levels of each factor.

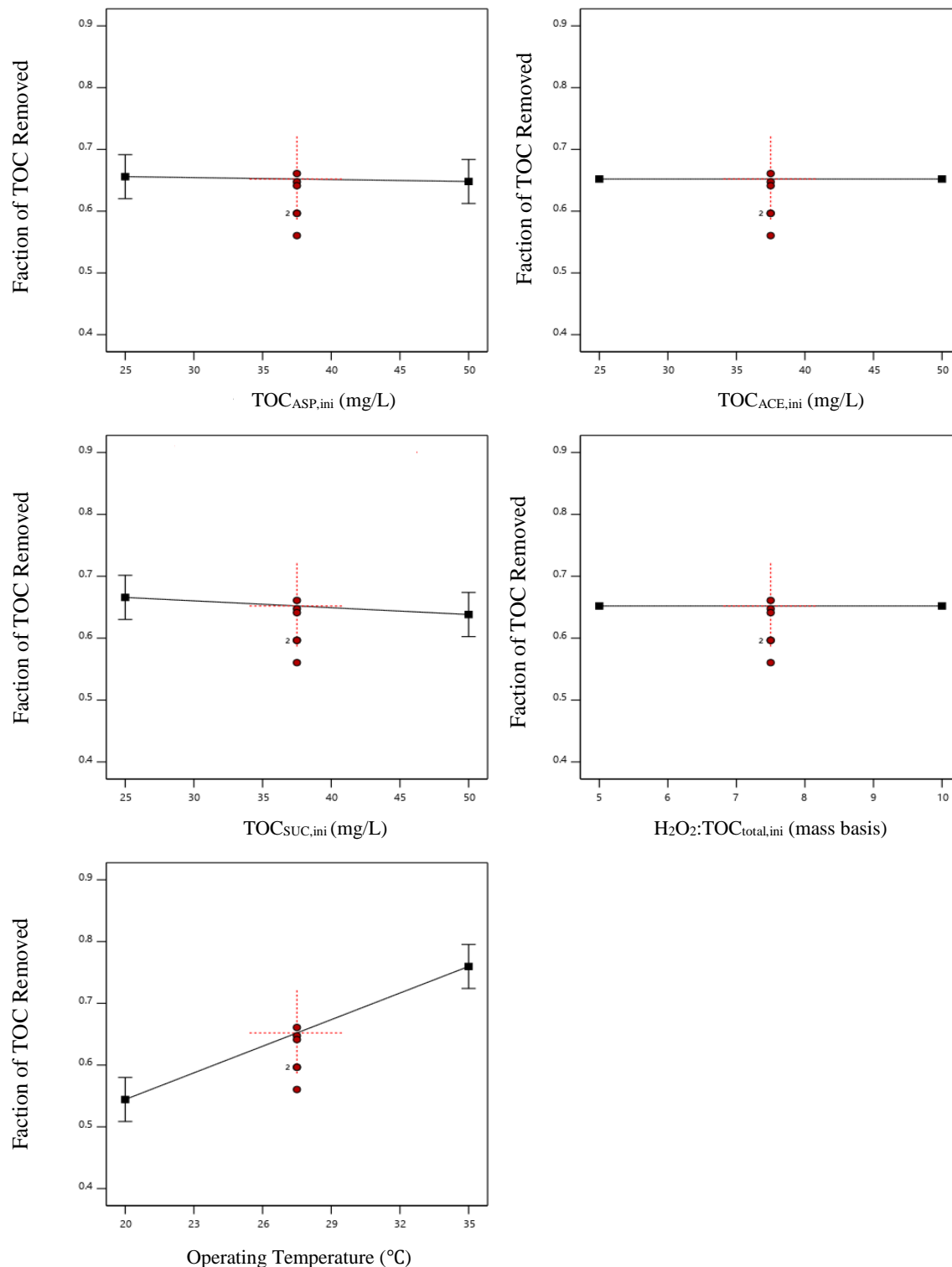


**Figure 4-16:** The influence of the independent factors on the mean TOC removal at their respective 2 levels in a UV/H<sub>2</sub>O<sub>2</sub> process with a UV exposure of 22.5 min. Red dots represent the fraction of TOC removed in each centre point replication.

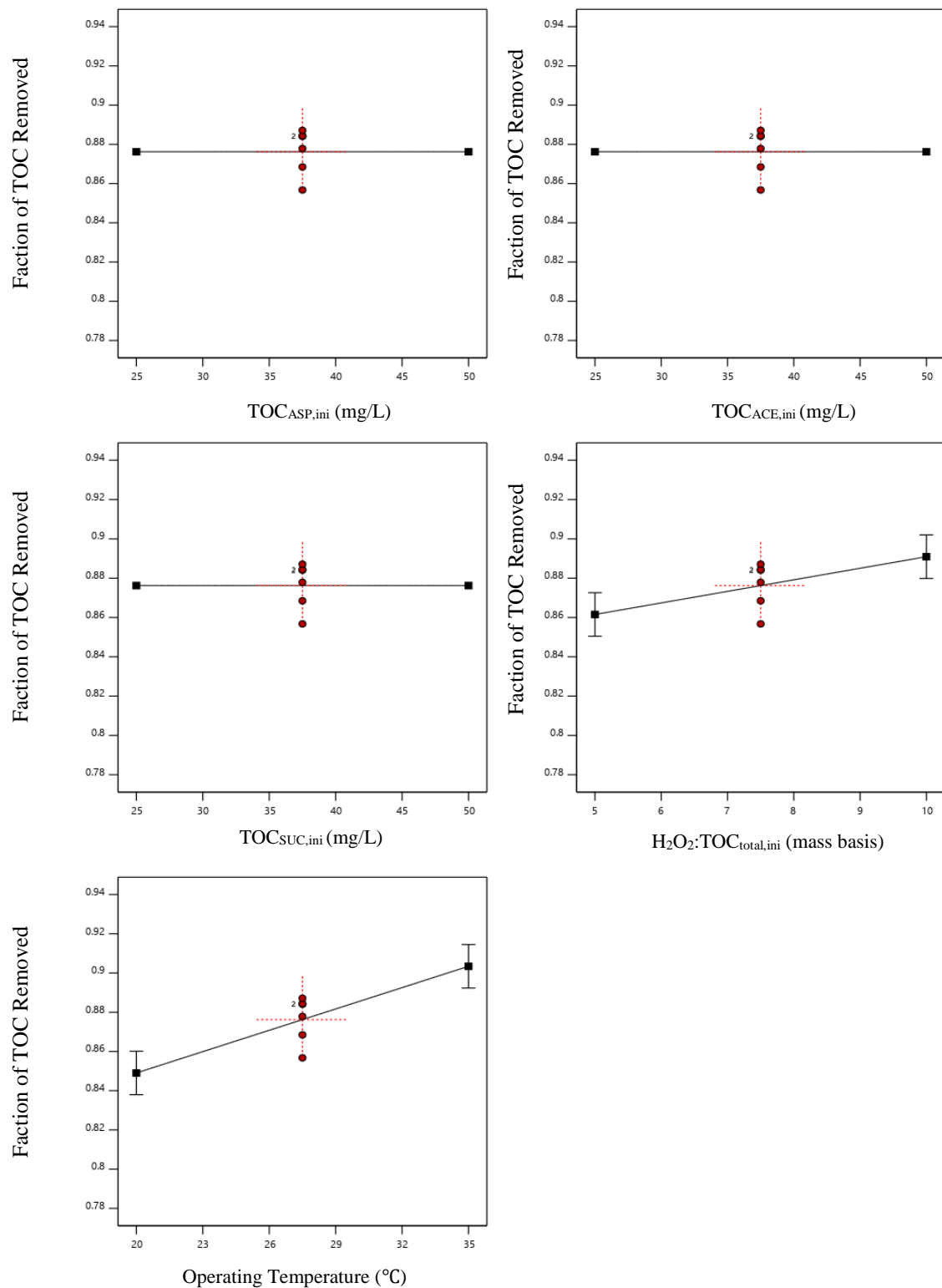


**Figure 4-17:** The influence of independent factors on the mean TOC removal at their respective 2 levels in a UV/H<sub>2</sub>O<sub>2</sub> process with a UV exposure of 45 min. Red dots represent the fraction of TOC removed in each centre point replication.

The plots shown in **Figure 4-16** and **Figure 4-17** show the mean TOC removal values of all the runs when each factor is set to its low and high level. For example, in **Figure 4-17**, the mean TOC removal in 8 runs at low temperature (20°C) is compared with the mean TOC removal at high temperature (35°C). These plots also help in assessing the relative significance of each factor, especially temperature and  $\text{H}_2\text{O}_2:\text{TOC}_{\text{total,ini}}$  (mass basis), on the TOC removal. In this section, extensive discussions are presented to explain the experimental results obtained. It should be noted that a negligible effect does not necessarily denote the independence of the response variable from the factor. For example, the effect of ACE on the TOC removal was found to be negligible in all cases. However, it is clear that TOC due to ACE is still reactive with  $\text{HO}^\bullet$  and is perceived to negatively affect the TOC removal in large enough concentrations.

#### 4.3.2.1 The Effect of Temperature

The operating temperature proved to be the dominating effect throughout every experimental run. Although the operating temperature was expected to be significant, the extent of its significance was somewhat surprising. The effect of the operating temperature on the TOC removal at 22.5 and 45 min of UV exposure are highlighted in **Figure 4-18** and **Figure 4-19** respectively.

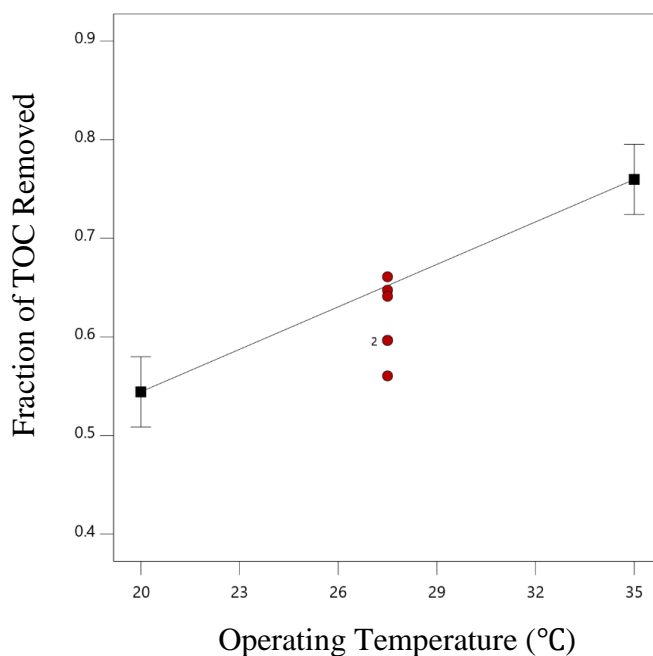


**Figure 4-18:** The effect of temperature on the mean TOC removal response at two levels with a UV exposure of 22.5 min. Red dots represent the fraction of TOC removed in each centre point replication.

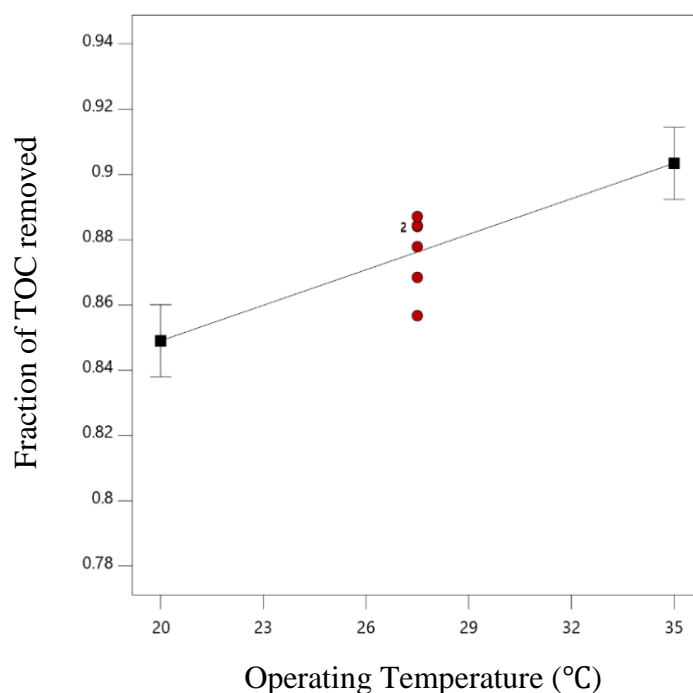


**Figure 4-19:** The effect of temperature on the mean TOC removal response at two levels with a UV exposure of 45 min. Red dots represent the fraction of TOC removed in each centre point replication.

The observations can be attributed to the strong correlation between temperature and the reaction kinetics, more specifically, the reaction of  $HO^\bullet$  with the parent compounds of the three artificial sweeteners and the resulting reaction intermediates. The rate constants ( $k$ ) of the reaction of  $HO^\bullet$  with the artificial sweeteners are summarized in **Table 4-3**, as reported in the literature (Toth et al., 2012).

**Table 4-3:** Experimental rate constant ( $k$ ) values of the reaction of hydroxyl radicals with artificial sweeteners. Adapted from (Toth et al., 2012)

Sweetener	$k$ ( $10^9 M^{-1} s^{-1}$ )
Aspartame	$6.06 \pm 0.05$
Acesulfame K	$3.80 \pm 0.27$
Sucralose	$1.50 \pm 0.01$

Note: rate constants valid for  $T \cong 20 - 22^\circ C$

Considering the large magnitudes of the rate constants, it is evident as to why the operating temperature has such a significant effect on the TOC removal. Although kinetic data does not exist

for all the reaction pathways, the strong effect of temperature is expected to hold for subsequent reactions of  $HO^\bullet$  with transformation products formed in a UV/H<sub>2</sub>O<sub>2</sub> process.

#### 4.3.2.2 Effect of H<sub>2</sub>O<sub>2</sub> Dosage

Considering the importance of H<sub>2</sub>O<sub>2</sub> in UV/H<sub>2</sub>O<sub>2</sub> processes, the effect of H<sub>2</sub>O<sub>2</sub> dosage (in the form of H<sub>2</sub>O<sub>2</sub>:TOC<sub>total,ini</sub>, mass basis) was not as significant as expected. Analysis of the experimental data disclosed that the dose of H<sub>2</sub>O<sub>2</sub> only became significant at a UV exposure of 45 min. Even then, the significance of the temperature effect still surpassed the effect of H<sub>2</sub>O<sub>2</sub> dosage. The effect of H<sub>2</sub>O<sub>2</sub>:TOC<sub>total,ini</sub> (mass basis) on TOC removal at 45 min of UV exposure is highlighted in **Figure 4-20**.

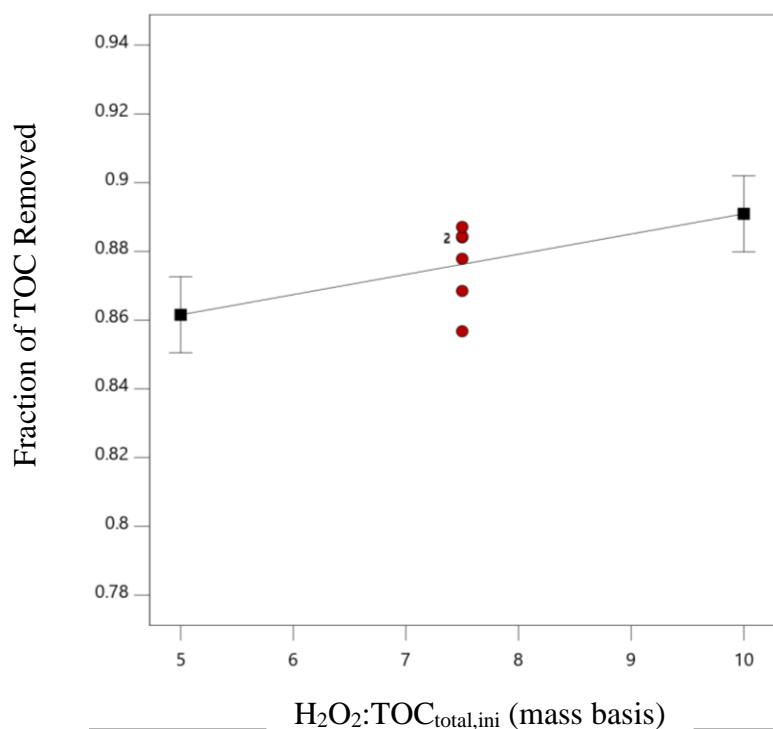


**Figure 4-20:** The effect of H<sub>2</sub>O<sub>2</sub>:TOC<sub>ini</sub> ratio (mass basis) on the mean TOC removal response at two levels with a UV exposure time of 45 min. Red dots represent the fraction of TOC removed in each centre point replication.

Although counterintuitive, this is attributed to the reliance of TOC reduction to track the degradation of the three artificial sweeteners. In other words, the fragmentations of the compounds are not detectable. This results in a failure to detect the likely strong correlation between

$\text{H}_2\text{O}_2\text{:TOC}_{\text{total,ini}}$  (mass basis) and the degradation of the parent compounds during the early stages of the treatment process by regression analysis. As the treatment process advances towards completion, the transformation of TOC to inorganic products is detected in the form of TOC reduction. This results in the detection of the significance of factor D by the regression approach only when TOC is destroyed and not when it is transformed.

As a final note on this observation, it is unlikely for the unexpectedly weak correlation to be caused by the scavenging effect of  $\text{H}_2\text{O}_2$  molecules. This is due to the fact that the applied  $\text{H}_2\text{O}_2\text{:TOC}_{\text{total,ini}}$  ratios (mass basis) were below the applied  $\text{H}_2\text{O}_2$  dosages suspected to cause such an effect in the preliminary investigations. However, it is possible for these compounds to behave differently in multicomponent systems. In fact, at least one interaction was confirmed between ASP and SUC (see Section 4.3.2.3.1). Furthermore, it is also possible for the temperature effect to have masked other significant effects.

#### ***4.3.2.3 The Effect of Initial TOC Concentration***

##### ***4.3.2.3.1 Effect of Initial TOC Concentration on TOC Removal at a UV Exposure of 22.5 min***

One of the most interesting observations in this study occurred in the form of an interaction effect between factors A and C ( $\text{TOC}_{\text{ASP,ini}}$  and  $\text{TOC}_{\text{SUC,ini}}$  concentrations respectively). The Pareto chart shown in **Figure 4-15** suggests that the interaction of factors A ( $\text{TOC}_{\text{ASP,ini}}$ ) and C ( $\text{TOC}_{\text{SUC,ini}}$ ) may be potentially significant. The interaction effects are shown in **Figure 4-21** through **Figure 4-23**.

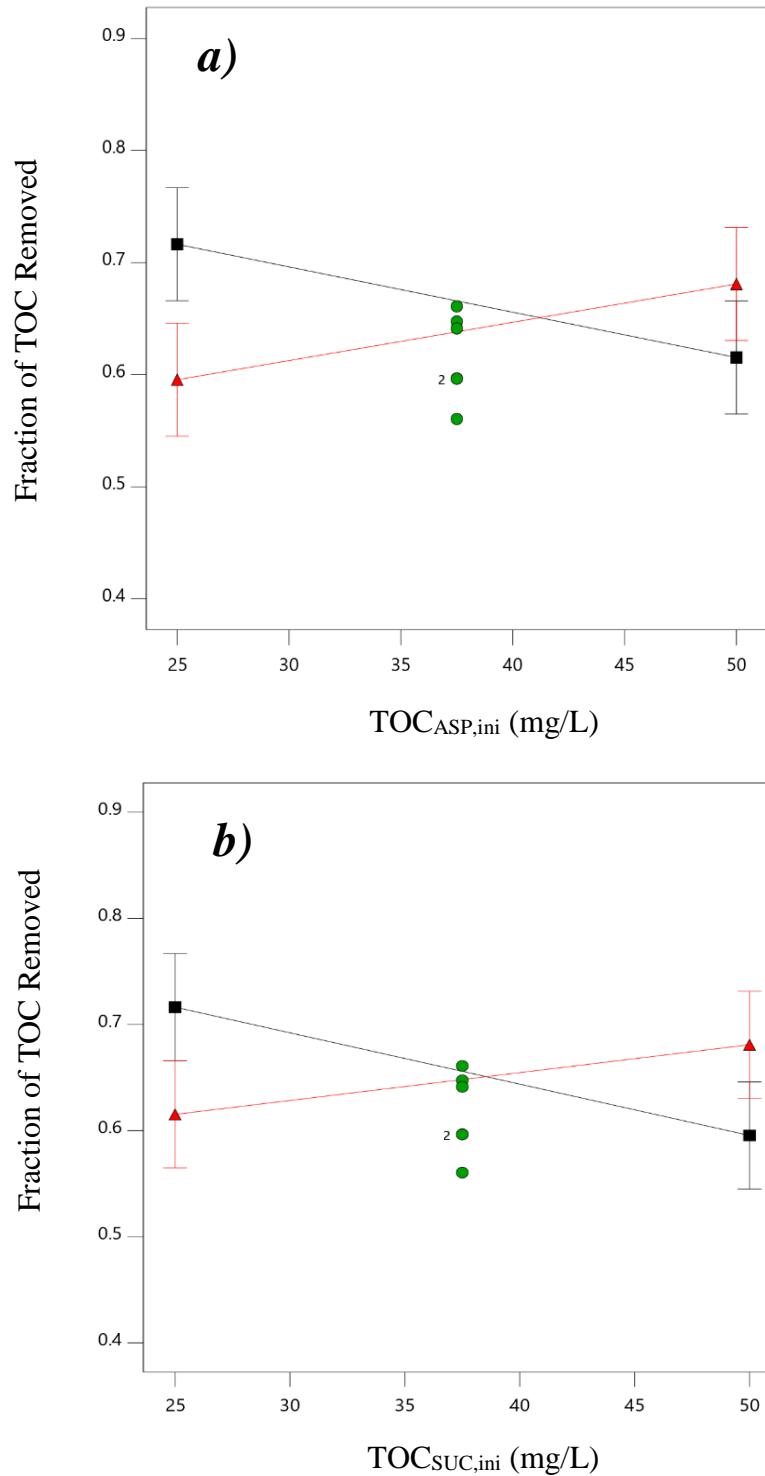


**Figure 4-21:** The interaction of ASP and SUC on TOC removal at a UV exposure of 22.5 min. TOC<sub>SUC,ini</sub> held constant at 25 mg/L (black) and 50 mg/L (red) in (a). TOC<sub>ASP,ini</sub> held constant at 25 mg/L (black) and 50 mg/L (red) in (b). Red dots represent the fraction of TOC removed in each centre point replication.



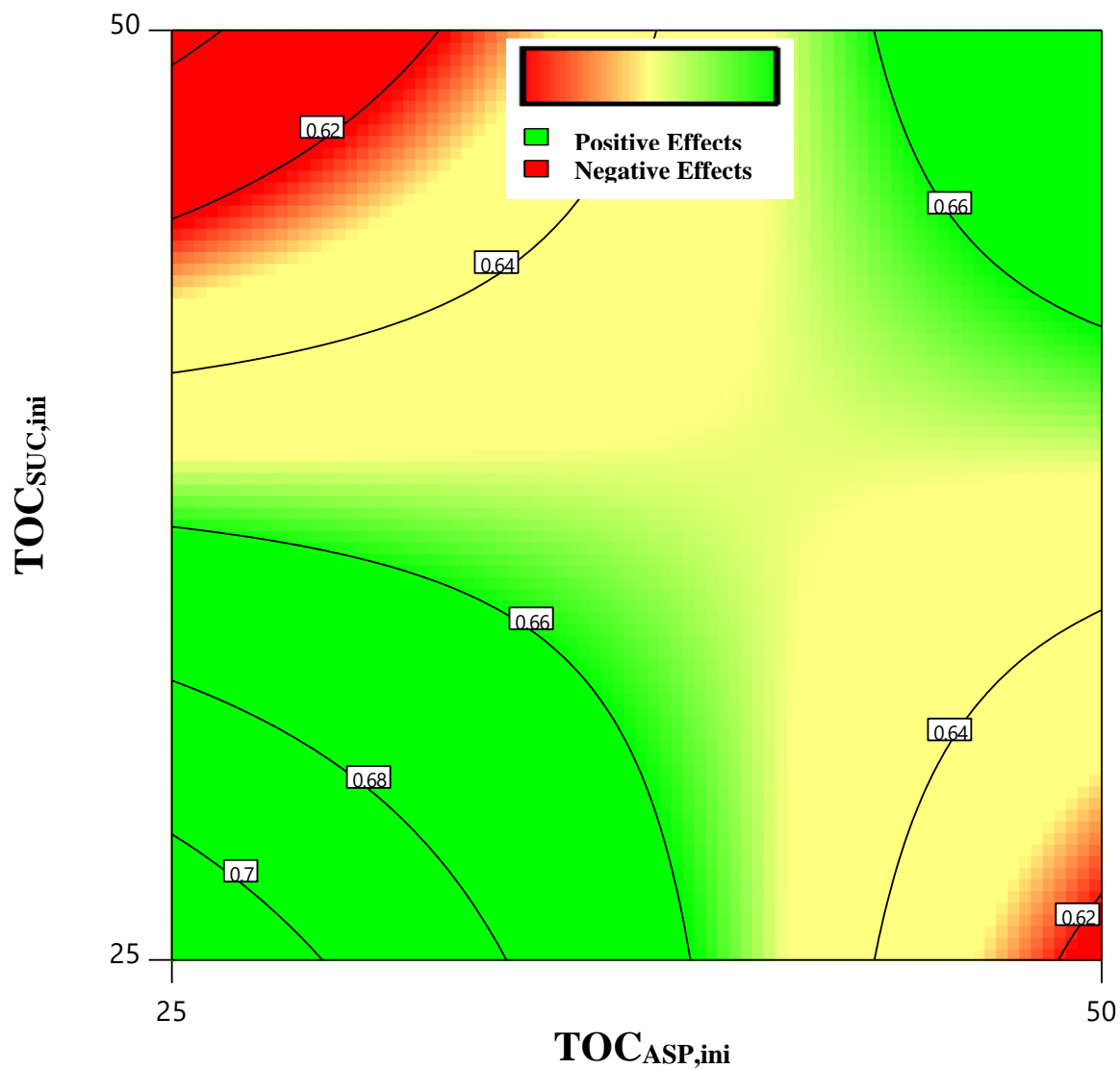


**Figure 4-22:** The contour of TOC removal response as a function of ASP and SUC concentrations. The contour lines represent the magnitudes of fraction of TOC removed at a UV exposure of 22.5 min

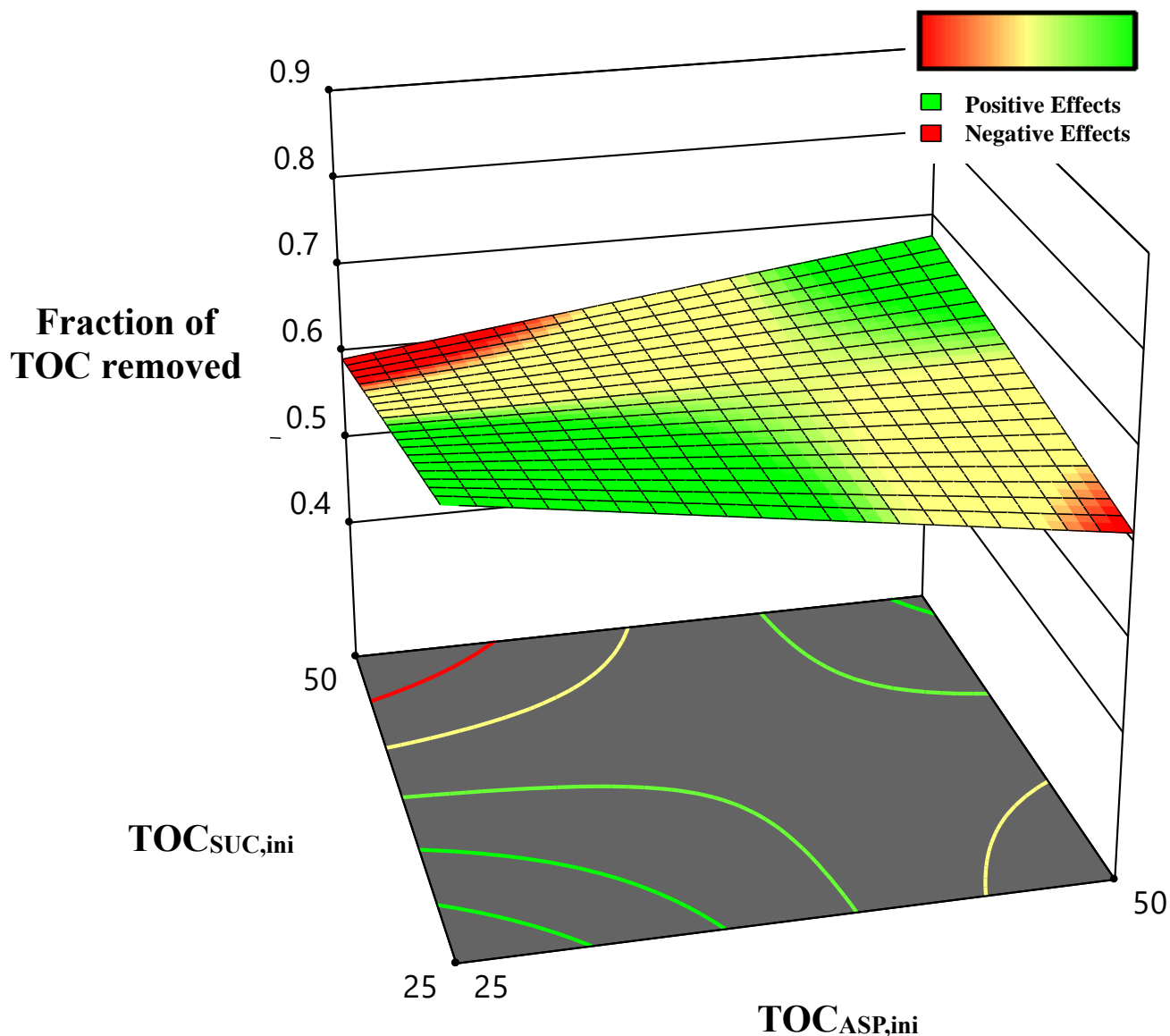


**Figure 4-23:** Response surface plot for the interaction of ASP and SUC concentrations on TOC removal at a UV exposure of 22.5 min

Starting with **Figure 4-21.a**, the *red trend line* shows the response in TOC removal with a changing TOC<sub>ASP,ini</sub> concentration when TOC<sub>SUC,ini</sub> concentration is held constant at 50 mg/L. The *black trend line* shows the response in TOC removal with an increase in TOC<sub>ASP,ini</sub> concentration while TOC<sub>SUC,ini</sub> concentration is held constant at 25 mg/L. In **Figure 4-21.b**, the same interaction is shown with a changing TOC<sub>SUC,ini</sub> concentration while the TOC<sub>ASP,ini</sub> is held constant instead. Both plots essentially show that when the concentrations of both sweeteners increase (in the form of TOC), TOC removal is also improved. To understand the implications of these observations, the

response surface of the contour plot from **Figure 4-22** are shown in **Figure 4-23**. The best system performance in TOC removal (over 70%) occurs when  $\text{TOC}_{\text{ASP,ini}}$  and  $\text{TOC}_{\text{SUC,ini}}$  were present at the lowest concentration levels (25 mg TOC/L). When the concentration of either compound is increased to 50 mg TOC/L while the other is maintained at 25 mg TOC/L, a TOC removal of approximately 60% is observed. Increasing the concentrations of both compounds to their respective high-levels, results in a TOC removal of approximately 68%. Furthermore, all the figures suggest a stronger effect by the SUC concentration than ASP.

Although difficult to explain without further investigations, this is most likely attributed to the presence of chlorine in the molecular structure of SUC. The degradation of the parent compound of SUC is known to release free chlorine into the solution (Lin et al., 2017). This is due the reaction of  $\text{HO}^\cdot$  with SUC which results in the fragmentation of the parent compound into smaller organic compounds and functional groups. Yet, it has also been shown that an increasing concentration of chlorine inhibits the mineralization of SUC in some AOP systems involving ozonation (Xu et al., 2018). As discussed in Section 2.6.1, ozonation is an AOP in which  $\text{HO}^\cdot$  is generated. Hence, the concept is applicable to the AOP used in this study. Considering the strong oxidizing potential of chlorine (see **Table 2-2**) it is possible for the TOC removal to be temporarily improved if free chlorine tends to react with ASP. Hence, the inhibitory effects of chlorine on the mineralization of SUC are negated by the consumption of chlorine through an alternative reaction with ASP. This in turn results in a TOC reduction due to an improved degradation of SUC by  $\text{HO}^\cdot$  along with the degradation of ASP due to both chlorine and  $\text{HO}^\cdot$ . Unfortunately, no data is available in the literature regarding degradation of ASP through chlorination.

A question may arise with respect to the significance of ACE, particularly as to why no interaction is observed with this compound. It should be noted that ACE has shown a tendency to degrade well through chlorination and applied molar ACE:Cl ratio of 1: 25 (Li et al., 2017). Furthermore, the results of the preliminary experiments performed in this study show that mineralization through both UV Irradiation alone and in the presence of  $\text{H}_2\text{O}_2$  were significant enough to likely render the effect of released chlorine as negligible. Hence, even if there are some interactions involving ACE, they are likely masked by others.

#### 4.3.2.3.2 Effect of Initial TOC Concentration on TOC Removal at a UV Exposure of 45 min

Although an interaction was observed at the midpoint of the treatment process, it was determined that neither one of the sweeteners had an impact on the overall TOC removal after 45 min of UV exposure. It seems like the reaction of  $HO^\bullet$  radicals with the parent compounds of the sweeteners and their transformation products are nonselective. In other words, the *overall net reactions* occur independently of each other, with no interactions between the parent compounds themselves and/or their transformation products. This was shown in **Figure 4-17** where only the operating temperature and  $H_2O_2:TOC_{total,ini}$  dosing were found to exert significant effects on the overall TOC removal.

### 4.3.3 Regression Analysis

#### 4.3.3.1 Statistical Models for Point Prediction

The significant effects can be used to model the reduction in TOC within the design space through regression analysis. For demonstration purposes, two statistical TOC removal models were developed, one for a UV exposure of 22.5 and another for a UV exposure of 45 min in terms of coded values. These models are as follows:

$$(TOC\ Removal)_{@ 22.5\ min\ of\ UV\ Exposure} = 0.6520 - 0.0039x_A - 0.0138x_C + 0.1077x_E + 0.0466x_Ax_C$$

$$(TOC\ Removal)_{@ 45\ min\ of\ UV\ Exposure} = 0.8762 + 0.0147x_D + 0.0272x_E$$

Where:

$$x_i \equiv \text{magnitude of } X_j$$

$$X_j \equiv \text{independent factor (j)}$$

Although these models are generated through linear regression, it should be noted that these models are *linear in parameters* only. In other words, the interaction effects of independent factors are certainly expected to result in a curvature in the response surface, as seen in **Figure 4-22** and **Figure 4-23**. Hence, this is not a concern.

The coded coefficients are useful for identifying the relative impacts of the factors. For example, a quick overview of the model developed for a UV exposure of 45 min, reveals that the effect of operating temperature on the removal of TOC is approximately twice as large as the effect of applied  $\text{H}_2\text{O}_2$ : $\text{TOC}_{\text{total,ini}}$  (mass basis).

The same models can be written in terms of actual factor levels. These models can be used to directly predict TOC removal values by inputting the actual factor levels. The statistical models in terms of actual factors are as follows:

$$(\text{TOC Removal})_{@ 22.5 \text{ min of UV Exposure}} = 0.730006 - 0.011504x_A - 0.012298x_C + 0.014359x_E + 0.000298x_Ax_C$$

$$(\text{TOC Removal})_{@ 45 \text{ min of UV Exposure}} = 0.732439 + 0.005877x_D + 0.003626x_E$$

The contour and response surface plots of TOC removal at 45 min of UV exposure are shown in *Figure 4-24* and *Figure 4-25*.

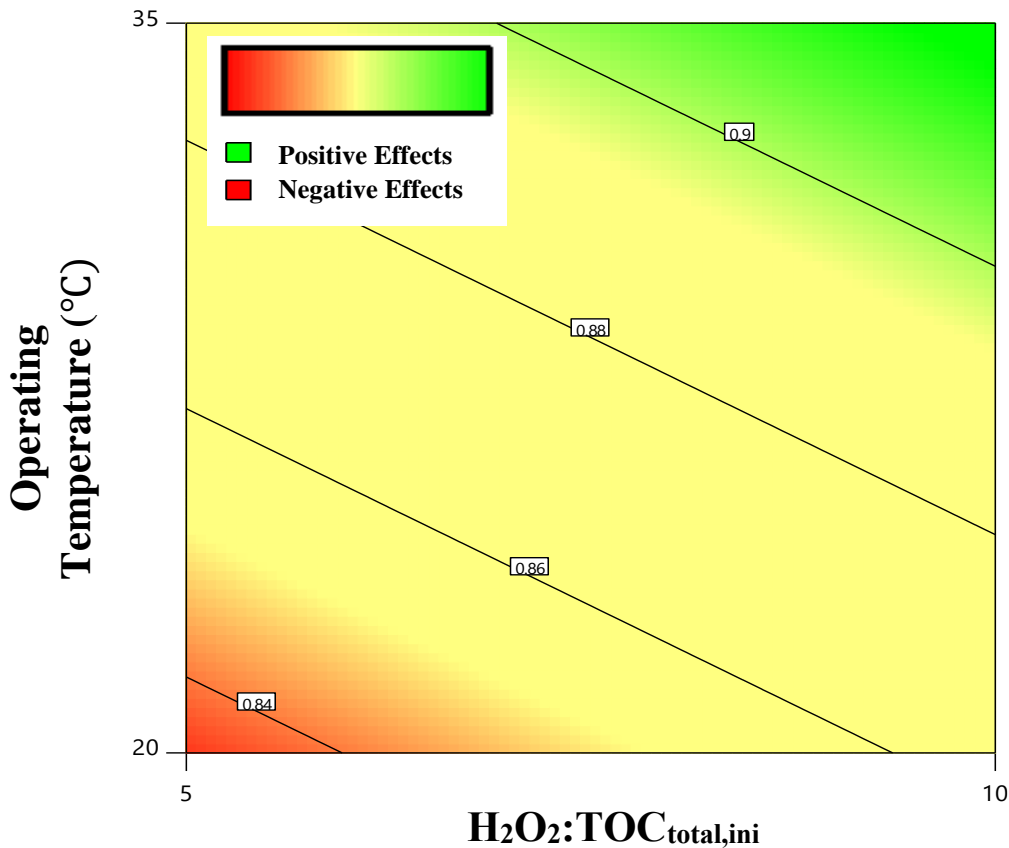


**Figure 4-24:** The contour of TOC removal response as a function of operating temperature and applied  $\text{H}_2\text{O}_2:\text{TOC}_{\text{ini}}$  ratio (mass basis) at a UV exposure of 45 min. The contour lines represent the magnitudes of the fraction of TOC removed after 45 min

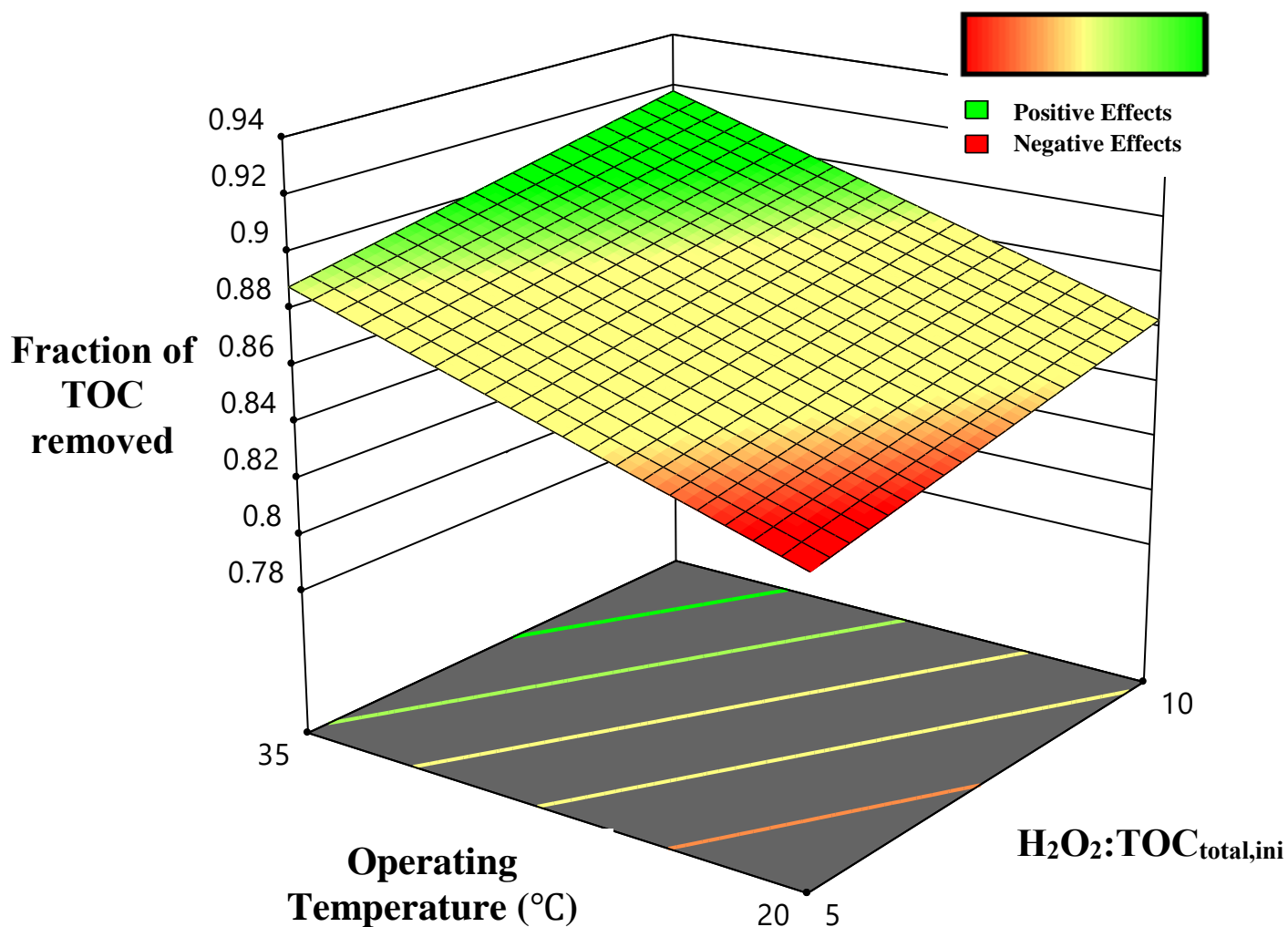


**Figure 4-25:** The corresponding response surface of overall TOC removal as a function of operating temperature and applied  $\text{H}_2\text{O}_2:\text{TOC}_{\text{ini}}$  ratio (mass basis) at a UV exposure of 45 min

#### 4.3.3.2 Analysis of Variance

The construction of an *analysis of variance* (ANOVA) table is very useful in determining the overall adequacy of a regression model. The details of ANOVA are shown in **Table 4-4** for both models.

**Table 4-4:** ANOVA performed on the experimental results and the regression models for TOC removal

<i>TOC Removal at a UV Exposure Time of 22.5 min</i>					
Source	Sum of Squares	Df	Mean Square	F-value	p-value
<b>Model</b>	0.2236	4	0.0559	12.35	<0.0001
<i>A – TOC<sub>ASP,ini</sub></i>	0.0002	1	0.0002	0.0538	0.8196
<i>C – TOC<sub>SUC,ini</sub></i>	0.0031	1	0.0031	0.6753	0.4233
<i>E – Temperature</i>	0.1856	1	0.1856	40.99	<0.0001
<i>AC (Interaction)</i>	0.0348	1	0.0348	7.69	0.0136
<i>Curvature Term</i>	0.0053	1	0.0053	1.17	0.2956
<b>Residual</b>	0.0724	16	0.0045		
<i>Lack of Fit</i>	0.0649	11	0.0059	3.94	0.0708
<i>Pure Error</i>	<b>0.0075</b>	5	0.0015		
<b>Total</b>	0.3014	21			
<i>TOC Removal at a UV Exposure Time of 45 min</i>					
Source	Sum of Squares	Df	Mean Square	F-value	p-value
<b>Model</b>	0.0153	2	0.00765	17.18	<0.0001
<i>D –</i>	0.0035	1	0.0035	7.76	0.0122
<i>H<sub>2</sub>O<sub>2</sub>: TOC<sub>total,ini</sub></i>					
<i>E – Temperature</i>	0.0118	1	0.0118	26.59	<0.0001
<i>Curvature Term</i>	1.846x10 <sup>-7</sup>	1	1.846 x10 <sup>-7</sup>	0.0004	0.9840
<b>Residual</b>	0.0080	18	0.00044		
<i>Lack of Fit</i>	0.0073	13	0.0006	4.09	0.0646
<i>Pure Error</i>	<b>0.0007</b>	5	0.0001		
<b>Total</b>	0.0233	21			

**Note:** fit-statistics are reported in Appendix H – Fit Statistics for Developed Models

The F-value in the ANOVA is the result of an F-test on the variances explained by the regression model and the ones due to noise and/or experimental error. The tests were carried out within a confidence interval of 95%. For a UV exposure of 22.5 min, an F-value of 12.35 was found to be larger than the  $F_{\text{critical}}$  value of  $\sim 2.9$ , suggesting that the model is statistically significant. This means that the variance explained by the model ( $MS_R=0.0559$ ,  $df=4$ ) is significantly larger than

the error term ( $MS_E=0.004525$ ,  $df=16$ ). The same approach yields an F-value of 17.18 for a UV exposure of 45 min, suggesting that the second model is also statistically significant.

Within a confidence interval of 95%,  $p$ -values less than 0.05 indicate significant model terms. Considering this definition, the effect of temperature was confirmed to be significant, with  $p$ -values of  $<0.0001$  in both cases, as seen in **Table 4-4**. The interaction of  $TOC_{ASP,ini}$  and  $TOC_{SUC,ini}$  was found to be significant with a  $p$ -value of 0.0136 for a UV exposure of 22.5 min. This confirmed the results obtained from the half-normal and Pareto charts shown in **Figure 4-12** and **Figure 4-13**. The individual effects for these factors were included in the model to maintain hierarchy. They did not have a significant effect on TOC removal, with  $p$ -values of 0.8196 and 0.4233 respectively. These factors were insignificant at a UV exposure of 45 min, and were not included in the resulting model. The  $H_2O_2:TOC_{total,ini}$  ratio (mass basis) was determined to be significant only at a UV exposure of 45 min, with a  $p$ -value of 0.0278. This factor was not significant at a UV exposure of 22.5 min.

The residuals (Error Sum of Squares or  $SS_E$ ) can be broken down into two components, namely the *pure error* and the *lack-of-fit*. By definition, the pure error is associated with the variation in response that cannot be explained by any models. Lack-of-fit is the variability in response that cannot be explained by the chosen model. In both cases, the calculated F-values are higher than  $F_{critical}$  values (2.85 and 4.82 for UV exposures of 22.5 and 45 min respectively). This simply means that there may be a need for more complex models for better data fitting as mentioned before. The complete analysis of residuals and relevant discussions are carried out in Appendix I – Analysis of Residuals.

#### 4.3.4 Concluding Remarks

Based on the experimental results, it was determined that the operating temperature and  $H_2O_2:TOC_{total,ini}$  (mass basis) were the most influential effects on the removal of TOC at a UV exposure of 45 min. The effect of the operating temperature was found to be approximately twice that of the  $H_2O_2:TOC_{total,ini}$  (mass basis) ratio. A special scenario was identified where the increasing concentrations of both ASP and SUC resulted in an interaction effect to temporarily increase the TOC removal at a UV exposure of 22.5 min. This is attributed to the release of chlorine



into the solution caused by the degradation of SUC and the reaction of the released chlorine with ASP.

Two linear statistical models were fitted to the experimental data to highlight the effects of each significant term. Based on the ANOVA, the significance of each of the model parameters were confirmed. It was determined that the models are able to provide general estimations for TOC removal trends within the design space; however, they are not reliable in offering sound response predictions. Hence, these models should not be considered for accurate TOC removal prediction.

#### **4.4 Determination of the Biodegradation Characteristics of Aspartame, Acesulfame K and Sucralose through Respirometry in both Single and Multicomponent Systems**

Aerobic respirometric tests were performed in batch mode according to standard protocols, (see Section 3.6.2) of dosing a microbial culture with defined amounts of ASP, ACE and SUC. The biochemical reactions were then monitored by measuring *cumulative oxygen uptake*. The control reference was also present in all other reaction vessels. The oxygen uptake curves were then interpreted by comparing the cumulative oxygen uptake amounts measured in presence of the artificial sweeteners to the one obtained for the control reference alone. A larger oxygen uptake curve indicates a biodegradable compound. Equal or overlapping oxygen uptake curves indicate the lack of biodegradability of a compound. A reduced oxygen uptake amount indicates inhibitory effects on the microbial community by a compound. The tests were replicated to ensure repeatability of the results. The plots of the accumulated oxygen uptake for the three artificial sweeteners at a concentration of 150 mg/L is shown in *Figure 4-26* and *Figure 4-27*.

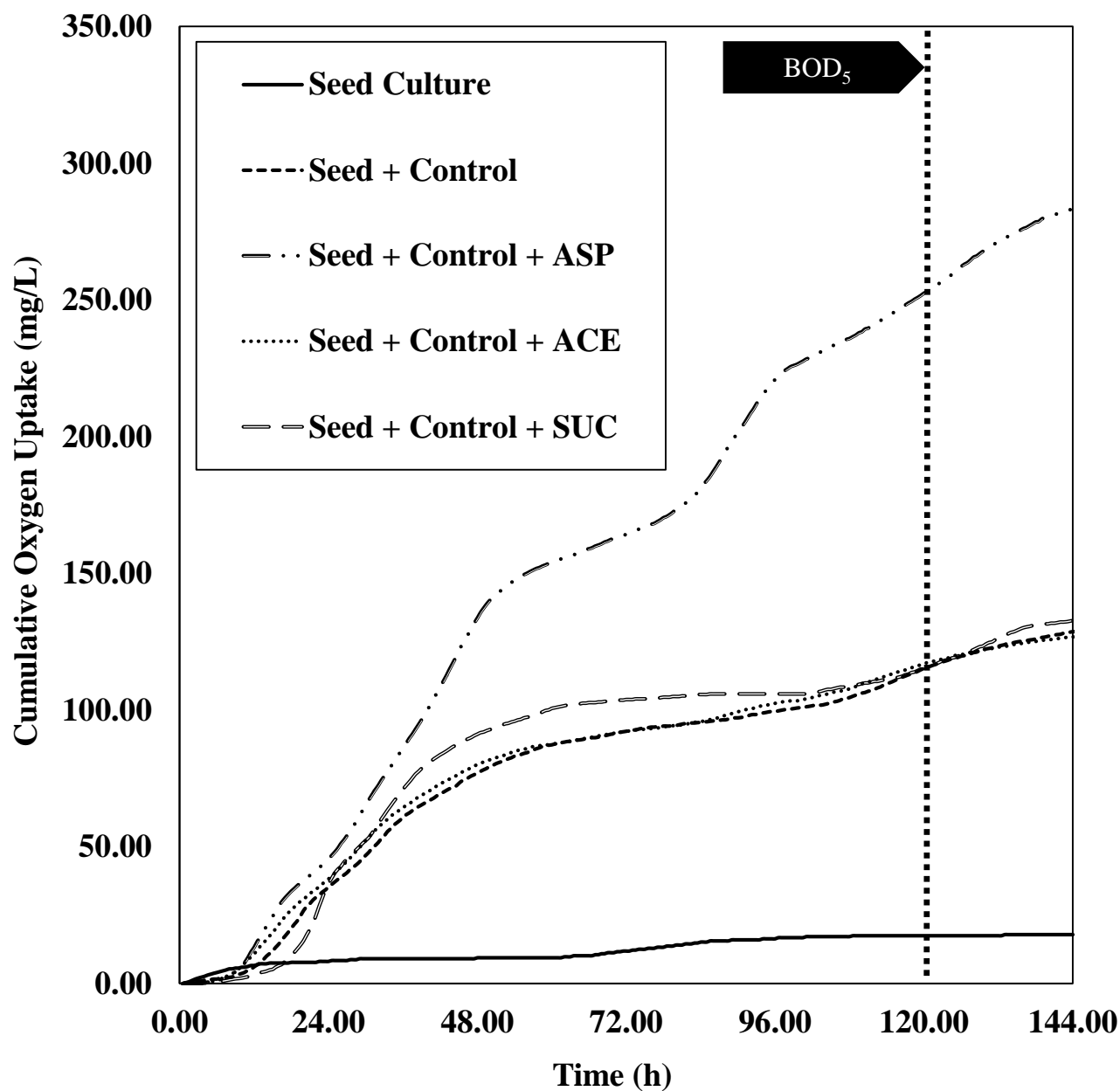


**Figure 4-26:** Respirometric results for single component solutions of ASP, ACE and SUC (150 mg/L) in comparison to a control reference in the presence of activated sludge

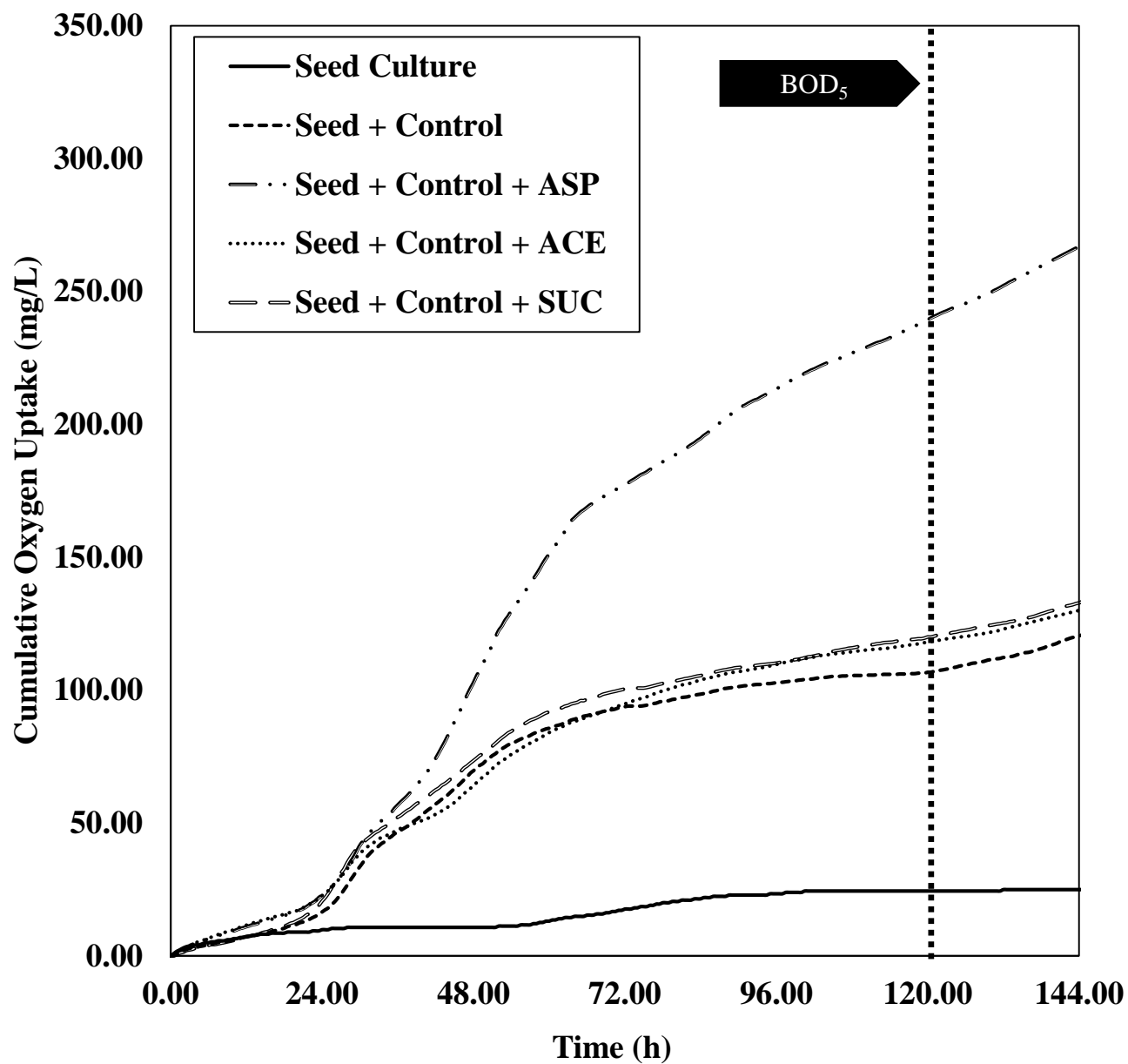


**Figure 4-27:** Replicated respirometric results for single component solutions ASP, ACE and SUC (150 mg/L) in comparison to a control reference in the presence of activated sludge

#### 4.4.1 Acclimation of the Microbial Community

The 6-day BOD ( $BOD_6$ ) readings were used for the determination of biodegradation characteristics of the three compounds. In **Figure 4-26**, the oxygen uptake curve of the seed culture rises immediately whereas a subtle delay is observed for all other tests. This subtle delay is not observed in **Figure 4-27**. The delay in oxygen uptake by the microorganisms observed in **Figure 4-26** is attributed to the acclimation of the microbial community to the sources of carbon present in the reaction vessels. The acclimation takes approximately 7-8 h, after which a sharp increase in oxygen uptake is observed. The lack of such delay in the oxygen uptake by the microorganisms observed in **Figure 4-27** is most likely due to a variation in the Ashbridge's Bay WWTP microbial community and the type of influent received by the plant over time, as the two sets of experiments were performed during different times of the year. This is to be expected, as there may be a significant variation in the composition of the influent to a WWTP as large as Toronto's Ashbridge's Bay ( $818,000 \text{ m}^3/\text{day}$ ) (Toronto Water, 2017). Furthermore, experimental variation may have also contributed to this subtle deviation (see Section 4.4.2). Therefore, this observation is not to be a cause for concern.

#### 4.4.2 Biodegradation Characteristics of Aqueous Solutions of Aspartame

By analyzing the cumulative oxygen curve of ASP, it is clear that the compound exerts a significant oxygen demand on the system in comparison to the control reference. The  $BOD_6/\text{ThOD}$  ratio for ASP was found to be  $0.63 \pm 0.02$  (see calculations in Appendix D – Determination of ThOD and  $BOD/\text{ThOD}$ ). By definition, a  $BOD_{20}/\text{ThOD}$  ( $BOD_{\text{ultimate}}/\text{ThOD}$ ) ratio of 0.6 or higher is interpreted as acceptable biodegradation (Young and Cowan, 2004). In this study, the calculated  $BOD_6/\text{ThOD}$  ratio of  $0.63 \pm 0.02$  highlights the excellent biodegradation potential of this compound in activated sludge processes. Some removal was observed in certain WWTPs in terms of influent and effluent ASP concentration comparisons (Baena-Nogueras et al., 2018; Subedi and Kannan, 2014). However, no other respirometric studies exist for comparison.

An interesting observation occurred at the experimental run period between 50 and 80 h in **Figure 4-26**. A decrease in OUR was observed at the 50-h mark until the 80-h mark. This was followed by a sharp increase in the OUR once again stretching to the 90-h mark. The OUR decreased once again, and remained relatively constant until the end of the experimental run. Usually, such trends

are attributed to *nitrogenous biochemical oxygen demand* (NBOD) when a population of nitrifying bacteria (classified as autotrophic bacteria) are present in the microbial community. In other words, the oxygen demand observed in such cases are not due to the degradation of carbonaceous compounds by heterotrophic bacteria (referred to as *carbonaceous biochemical oxygen demand* or CBOD). This delayed response is due to the slower growth rate of autotrophic species in comparison to heterotrophic bacteria. However, a nitrification inhibitor (Nitrapyrin, 0.53 g/L, see **Table 3-17**) was used in all tests to inhibit this effect. Therefore, this observation cannot be attributed to NBOD. Two other possibilities remain: 1). the temporary formation of slowly biodegradable intermediates during this time period, before being broken down more readily biodegradable compounds; and 2). the formation of intermediates that require the acclimation of the microorganisms before being consumed as a carbon source. Interestingly, the plot shown in **Figure 4-27** does not have such a lag period for oxygen uptake curve of the biodegradation of ASP. Once again, this can be attributed to the variation in the microbial communities in the sludge samples collected (see Section 4.4.1). Hence, the most likely explanation for this deviation is the formation of intermediates that require the acclimation of certain microbial communities that may not have been present in both tests.

Other than the temporarily slower OUR observed in **Figure 4-26**, no other deviations were observed in the cumulative oxygen uptake curves for the biodegradation of ASP (150 mg/L). The overall variation in oxygen uptake was found to be  $\pm 5\%$  variation in cumulative oxygen uptake after 144 h (6 days).

#### **4.4.3 Biodegradation Characteristics of Aqueous Solutions of Acesulfame K**

The cumulative oxygen uptake curves obtained for ACE overlap with the ones obtained for the control reference quite well. As mentioned in Section 4.4, this is an indication of the lack of biodegradability of a compound, corresponding to a BOD<sub>6</sub>/ThOD ratio of zero. This result was expected, as hinted in the literature (Lange et al., 2012; Scheurer et al., 2009; Stolte et al., 2013). It should be noted that the biodegradation of ACE has also been reported in some cases and linked to a potential acclimation of microbial communities over a long period of time (years) (Sandro Castronovo et al., 2017; Nguyen et al., 2018; Yang et al., 2017). In comparison, the experimental runs in this study were carried performed over 6 days. Hence, the concept of long acclimation was

not observed. ACE has been found to be biodegradable in lab scale *sequencing batch reactor* (SBR) processes (Li et al., 2018). These tests were however performed at MLSS concentrations of 3000 mg/L. The significantly different experimental conditions were likely the reason behind these observations. The overall variation in the cumulative oxygen uptake by microorganisms (activated sludge) for the biodegradation of ACE (150 mg/L) was found to be very small ( $\pm\sim 2\%$ ) after 144 h (6 days).

#### **4.4.4 Biodegradation Characteristics of Aqueous Solutions Sucralose**

For the most part, the oxygen uptake curve obtained for SUC overlaps with the one obtained for the control reference. Hence, the resulting BOD<sub>6</sub>/ThOD for SUC solutions was found to be zero. In **Figure 4-26**, an inhibitory effect on the OUR of the microorganisms is observed within the first 24 h. However, the same subtle inhibition effect was not observed in cumulative oxygen uptake curves in **Figure 4-27**. Overall, the lack of biodegradation for SUC has been attributed to the presence of chlorine in the parent compound (Brorstrom-Lunden et al., 2007). However, no other respirometric studies have been carried out in the literature for this compound. This observation is attributed to the presence of alternate microbial communities. The chlorine groups in the parent compounds of SUC may in fact have an effect on the growth of certain microbial species, which requires the acclimation of microorganism populations. However, this cannot be confirmed without detailed studies on this phenomenon. In terms of overall biodegradation, other studies have investigated the removal of SUC in SBR processes (Li et al., 2018). The results simply reiterated the persistence of this compound, even at high MLSS concentrations of 3000 mg/L. The overall variation in the cumulative oxygen uptake by microorganisms (activated sludge) for the biodegradation of SUC (150 mg/L) was found to be negligible ( $\geq 1\%$ ) after 144 h (6 days).

#### **4.4.5 Biodegradation Characteristics of Multicomponent Aqueous Systems of Aspartame, Acesulfame K, and Sucralose**

Following the results obtained from the single-component respirometric studies on ASP, ACE and SUC, more experiments were carried out to investigate the biodegradation characteristics of a multicomponent aqueous system of all three artificial sweeteners (150 mg/L). The cumulative oxygen uptake curves for these systems are presented in **Figure 4-28**.

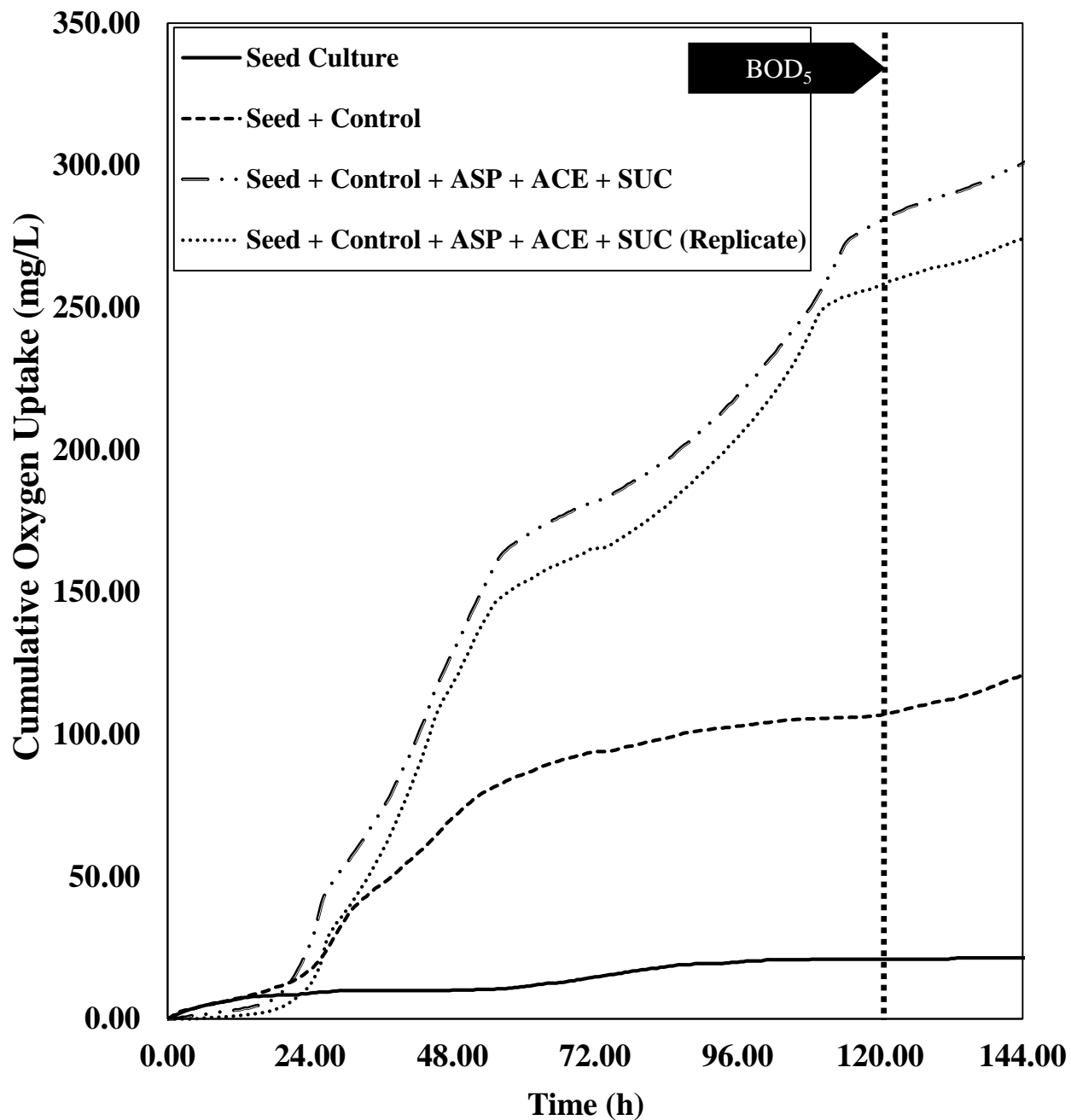


**Figure 4-28:** The respirometric results of multicomponent aqueous systems containing ASP, ACE and SUC (150 mg/L) in comparison to a control reference in the presence of activated sludge

Considering the excellent biodegradation characteristics of ASP and the complete lack of biodegradation for ACE and SUC, the plots of the cumulative oxygen uptake by microbial communities in activated sludge were expected to resemble the ones obtained for ASP alone. The results obtained in all experiments were as expected. The cumulative oxygen uptake curves in

**Figure 4-28** show a short acclimation period followed by a rapid oxygen uptake in both test vessels. In the same figure, it can be observed that the cumulative oxygen uptake curves follow a virtually identical path. Interestingly, the temporary drop in OUR between 50 – 80 h is observed once again, as seen in the biodegradation curve of ASP in **Figure 4-26**. Based on these results, it is evident that microbial communities present in activated sludge are able to metabolize ASP as a carbon source in presence of other artificial sweeteners in multicomponent aqueous matrices. The overall variation in the cumulative oxygen uptake by microorganisms (activated sludge) for the biodegradation of a multicomponent system of three artificial sweeteners (150 mg/L) was found to be quite small (~7%) after 144 h (6 days).

#### 4.4.6 Concluding Remarks

Respirometric studies were carried out for both single and multicomponent systems of ASP, ACE and SUC. The results from this study are summarized in **Table 4-5**.

**Table 4-5:** Summary of respirometric results for ASP, ACE and SUC in single and multicomponent systems

System		Experimental BOD <sub>5</sub> Data (mg O <sub>2</sub> /L)	Experimental BOD <sub>6</sub> Data (mg O <sub>2</sub> /L)	Estimated ThOD (mg O <sub>2</sub> /L)	Estimated BOD <sub>5</sub> /ThOD	Estimated BOD <sub>6</sub> /ThOD
Single Component	ASP	135±3	159±9	237	0.57±0.01	0.63±0.02
	ACE	~0	~0	101	~0	~0
	SUC	~0	~0	227	~0	~0
Multicomponent		163±16	167±19	765	0.21±0.02	0.22±0.02

By analyzing the respirometric data presented in this chapter, it can be concluded ASP possesses excellent biodegradation characteristics. This is highlighted in **Table 4-5** in the form of BOD/ThOD values. Hence, conventional WWTPs should be able to remove this compound from wastewater streams. The cumulative oxygen uptake curve of ACE and SUC showed that no



biodegradation occurred during the 144 h (6-day) duration of the experiments. ACE did not have any inhibitory effects on the OUR of the microorganisms in activated sludge, whereas SUC showed a minor potential in inhibiting the growth of microorganisms. Although, the inhibition effect was very subtle, the primary concern with both ACE and SUC is the complete lack of biodegradation by microbial communities in activated sludge. This was further confirmed with the experimental results obtained from the multicomponent system of artificial sweeteners. The results showed near identical biodegradation characteristics of such systems to systems containing only ASP as an artificial sweetener. Hence, when ACE and SUC present in a wastewater matrix, other processes such as the UV/H<sub>2</sub>O<sub>2</sub> process should be considered for the removal of these compounds from aqueous matrices.

## Chapter 5 – CONCLUSIONS AND RECOMMENDATIONS

The experimental investigations in this study were carried out in three stages. The system behaviour was first determined through individually assessing the degradation of three artificial sweeteners ASP, ACE and SUC. Based on the results, experimental conditions were selected and applied in a 2-level fractional factorial DOE. Finally, the biodegradation characteristics of the three compounds were determined both individually and in multicomponent systems through respirometry. The conclusions drawn from each experimental phase are presented in this chapter, in addition to recommendations for future work.

### 5.1 Conclusions

The degradation of ASP was studied for the first time under UV irradiation. First, under UV irradiation alone ( $\lambda \approx 254$  nm), the appearance of colour in the sample indicated a photo-transformation of the parent compound but resulted in no significant TOC reduction. Then, the use of  $\text{H}_2\text{O}_2$  significantly improved TOC removal and aided in the removal of colour. At this stage, the use of UV irradiation in any aqueous matrix containing ASP is only recommended in the presence of an  $\text{H}_2\text{O}_2$ :ASP ratio of at least 2:1 (mass basis). It was observed that UV irradiation alone ( $\lambda \approx 254$  nm) is capable of reducing TOC concentration up to 30% for aqueous solutions containing ACE (75-300 mg/L). In the case of SUC, no TOC removal was observed. An  $\text{H}_2\text{O}_2$ :ACE ratio of 2:1 (mass basis) resulted in the removal of TOC up to 90% even with higher concentrations of ACE (300 mg/L). With low concentrations of SUC (75 mg/L), an  $\text{H}_2\text{O}_2$ :SUC mass ratio of 2:1 was found to be sufficient. However, a ratio closer for 6:1 is recommended for higher SUC concentrations (300 mg/L).

A two-level fractional factorial design of resolution V was employed to investigate the effects of five independent factors on the TOC removal response in 16 runs. The independent factors were the initial TOC concentration due to ASP ( $X_A$ ), ACE ( $X_B$ ) and SUC ( $X_C$ ),  $\text{H}_2\text{O}_2$ : $\text{TOC}_{\text{total,ini}}$  ratio ( $X_D$ ) and the operating temperature ( $X_E$ ). Overall, it was determined that the performance of the UV/ $\text{H}_2\text{O}_2$  process is excellent for the degradation of ASP, ACE and SUC in multicomponent

aqueous systems. The effect of the operating temperature was found to be the most significant in all cases. At a UV exposure of 45 min, the operating temperature and  $\text{H}_2\text{O}_2:\text{TOC}_{\text{total,ini}}$  were both determined to have a significant effect on TOC removal, with effect of the operating temperature having an impact of approximately twice the magnitude of  $\text{H}_2\text{O}_2:\text{TOC}_{\text{total,ini}}$ . A special scenario was identified where increasing the initial concentrations of both ASP and SUC resulted in an interaction effect to temporarily increase the TOC removal at a UV exposure of 22.5 min.

Two linear statistical models were fitted to the experimental data to highlight the effects of each significant term. Based on the ANOVA, the significance of each of the model parameters were confirmed.

Upon the assessment of the biodegradation characteristics of the three sweeteners, it was concluded that the use of a UV/ $\text{H}_2\text{O}_2$  is justified for the elimination of ACE and SUC from aqueous matrices. Although ASP was found to respond well to treatment in the UV/ $\text{H}_2\text{O}_2$  process, it is concluded that conventional activated sludge processes are preferable when dealing with wastewaters containing ASP only.

## 5.2 Recommendations for Future Work

Based on the conclusions drawn in Section 5.1, it is recommended that a combined system of activated sludge followed by a UV/ $\text{H}_2\text{O}_2$  be investigated for the treatment of a multicomponent aqueous system of artificial sweeteners. In order to achieve this, the parameters selected for the treatment of multicomponent system should be investigated through more advanced DOE techniques (e.g. *response surface methodology* or RSM) to study the TOC reduction response. It is possible that other significant effects and interactions were masked by the effect of temperature on TOC removal. Hence, it is recommended that the other parameters be studied at constant temperature. Furthermore, it is advisable to employ other analytical methods to screen for the degradation of the parent compounds of the artificial sweeteners investigated in this study in addition to TOC analysis. This approach enables the experimenter to assess the true effect of the applied  $\text{H}_2\text{O}_2:\text{TOC}_{\text{total,ini}}$  throughout the treatment process that results in the detection of the fragmentation of the parent compounds, even when the overall TOC mass present in the system is not destroyed. Through *response surface methodology*, it is possible to identify optimal factor levels to be applied to a pretreated multicomponent system of artificial sweeteners by activated

sludge. This sequential approach also enables the extension of the study to aqueous solutions containing natural organic matter, which is a crucial factor in the ultimate treatability of a wastewater matrix. The work can also be extended to real wastewater samples containing artificial sweeteners. Such investigations can ultimately determine if the UV/H<sub>2</sub>O<sub>2</sub> processes are justified and feasible for onsite treatment applications.

As a final note, it is recommended that the investigations be extended to determine the reaction pathways of the transformation of ASP under UV irradiation ( $\lambda \cong 254$  nm) and identify the cause of the formation of colour in such systems. Additionally, the interaction of SUC and ASP should also be investigated further to confirm the reason behind the temporary improvement on TOC removal. More specifically, the determination of the reaction kinetics of ASP with free chlorine can help validate the discussions presented in regarding the positive interaction effect of these two compounds on TOC removal in UV/H<sub>2</sub>O<sub>2</sub> systems.

# Appendices

## Appendix A – Determination of MLSS and MLVSS

A sample of fixed volume (10 mL) was withdrawn filtered under vacuum through a grade 44 ashless filter paper of predetermined mass. The filtrate and the filter paper were then dried in an oven at 105 °C for 2 h. The dried filter paper was then weighed and ignited in a furnace at 500°C for 30 min. The MLSS and MLVSS were determined as follows:

$$MLSS \equiv TSS_{@105^{\circ}C} = W_{filter\ paper+filtrate+aluminum\ dish} - W_{filter\ paper+aluminum\ dish}$$

$$\begin{aligned} MLVSS &\equiv VSS_{@500\pm50^{\circ}C} \\ &= W_{filter\ paper+filtrate+aluminum\ dish} - W_{filter\ paper} - W_{residue} \\ &\quad - W_{aluminum\ dish} \end{aligned}$$

Where:

$$W_i \equiv \text{Weight of component (i)}$$

The MLSS and MLVSS for Phase III experiments (artificial sweetener concentrations of 150 mg/L) were calculated to be:

$$MLSS = 0.0461 \frac{g}{10\ mL} = 0.00461 \frac{g}{mL}$$

$$MLVSS = 0.0268 \frac{mg}{10\ mL} = 0.00268 \frac{g}{mL}$$

For the required MLVSS of  $\leq 30$  mg/L, the volume of mixed liquor required for seeding the reaction vessels can be determined as follows:

$$V_{mixed\ liquor} \leq \frac{30\ \frac{mg}{L}}{2.68\ \frac{mg}{mL}} \leq 11.2\ mL\ mixed\ liquor$$

## Appendix B – The Use of Center Point Replicates for Error Estimation and Curvature Tests

The reasons behind the addition of center points to the  $2^k$  factorial designs are twofold. One of the reasons is to provide protection against curvature from second order effects. A second reason is to allow for an independent analysis for the estimating the experimental error. It should be noted that the use of center points does not affect the validity of the linear models.

In the design used on Phase II of the experimental investigations, six center point replicates were incorporated (in a random order) into the design to account for curvature check and error estimation accordingly. In terms of error estimation, the variance in the center points are summed up to estimate the experimental error.

This is a very useful method in dealing with unreplicated factorial designs. The *mean square* of pure error ( $MS_E$ ) is calculated from the center points as follows:

$$MS_E = \frac{SS_E}{n_c - 1} = \frac{\sum_{center\ points} (y_i - \bar{y})^2}{n_c - 1}$$

Where:

$MS_E \equiv$  mean square error

$SS_E \equiv$  sum of square error

$n_c \equiv$  number of center point replicates

$y_i \equiv$  response of centre point input (i)

$\bar{y} \equiv$  average response of n centre points

The pure error obtained through this approach was reported in **Table 4-4**.

The test for curvature requires a statistical test for the parameter of a potential second order for the following general model:

$$y = \beta_0 + \sum_{j=1}^k \beta_j x_j + \sum_{i < j} \beta_{ij} x_i x_j + \sum_{j=1}^k \beta_{jj} x_j^2 + \epsilon$$

In this second order equation, the  $\beta_{jj}$  term is the parameter of the quadratic term to be tested for curvature. This is done according to the following hypothesis test:

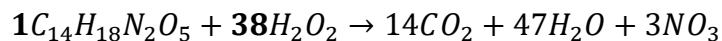
$$H_0: \sum_{j=1}^k \beta_{jj} = 0$$

$$H_1: \sum_{j=1}^k \beta_{jj} \neq 0$$

This approach was carried for both statistical models. The curvature effect was found to be insignificant in both cases. The results were shown in **Table 4-4**. It is possible to drop the curvature terms to simplify the models if desired.

## Appendix C – Determination of Theoretical H<sub>2</sub>O<sub>2</sub> Dosages (Mass Basis)

The theoretical mass ratio of H<sub>2</sub>O<sub>2</sub>:ASP was calculated based on the balanced theoretical chemical reaction of ASP with H<sub>2</sub>O<sub>2</sub> according to the following reaction



The molar ratio of H<sub>2</sub>O<sub>2</sub> and ASP were obtained from the stoichiometric coefficients of the chemical reaction as follows:

$$H_2O_2:ASP \text{ (molar basis)} \equiv 38 \text{ mol}_{H_2O_2} : 1 \text{ mol}_{ASP}$$

The conversion of the molar ratio to mass ratio was calculated based on the molecular weights of the two species as follows:

$$MW_{ASP} = 294.3 \frac{g}{mol}$$

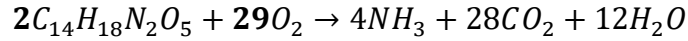
$$MW_{H_2O_2} = 34.015 \frac{g}{mol}$$

$$\begin{aligned} H_2O_2:ASP \text{ (mass basis)} &= 38 \cancel{\text{mol}_{H_2O_2}} \times 34.015 \frac{g_{H_2O_2}}{\cancel{\text{mol}_{H_2O_2}}} : 1 \cancel{\text{mol}_{ASP}} \times 294.3 \frac{g_{ASP}}{\cancel{\text{mol}_{ASP}}} \\ &\equiv 4.39 \text{ g}_{H_2O_2} : 1 \text{ g}_{ASP} \end{aligned}$$



## Appendix D – Determination of ThOD and BOD/ThOD

The calculation of ThOD can be carried out based on the balanced theoretical reaction of an organic compound with O<sub>2</sub> in which organic carbon and nitrogen are converted to CO<sub>2</sub> and NH<sub>3</sub>. In the case of ASP, this theoretical reaction is as follows:



The corresponding ThOD is then calculated as follows:

$$ThOD_{ASP} = \frac{29 \frac{mol_{O_2}}{mol_{O_2}} \times 32 \frac{g_{O_2}}{mol_{O_2}}}{2 \frac{mol_{ASP}}{mol_{ASP}} \times 294.3 \frac{g_{ASP}}{mol_{ASP}}} = 1.58 \frac{g_{O_2}}{g_{ASP}}$$

For an ASP concentration of 150 mg/L, the ThOD is as follows:

$$ThOD_{ASP@150 \text{ mg/L}} = 1.58 \frac{g_{O_2}}{g_{ASP}} \times 150 \frac{g_{ASP}}{L} = 237 \frac{g_{O_2}}{L}$$

The biodegradation characteristics of ASP can be found by reading the BOD<sub>6</sub> values for ASP and control reference from **Figure 4-29** and performing the following calculations:

$$Biodegradability \text{ of ASP} = \frac{\left(282 \frac{mg_{O_2}}{L} - 130 \frac{mg_{O_2}}{L}\right)}{237 \frac{g_{O_2}}{L}} = 0.64$$

Where:

$$282 \frac{mg_{O_2}}{L} = BOD_6 \text{ Values of ASP + Control Reference}$$

$$130 \frac{mg_{O_2}}{L} = BOD_6 \text{ Value of Value of Control Reference}$$

$$237 \frac{mg_{O_2}}{L} = ThOD \text{ Value of ASP } \left(@150 \frac{mg}{L}\right)$$

*Note: The same calculation was carried out with the results obtained in **Figure 4-30** to obtain a mean and standard deviation.*

## Appendix E – Determination of Theoretical Total Organic Carbon (TOC)

The theoretical TOC can be calculated by determining the total number of organic carbons present in the chemical structure of compound. In the case of ASP, the calculation of theoretical TOC can be carried out based its chemical structure (*Table 3-2*) as follows:

$$\text{Chemical Formula} = C_{14}H_{18}N_2O_5$$

$$\text{Organic Carbon Count} = 14 \text{ (all carbons in ASP are organic)}$$

$$\text{Carbon weight per mole of ASP} = 14 \times 12.01 \frac{g}{mol} = 168.14 \frac{g C}{mol_{ASP}}$$

$$\text{organic carbon fraction} \equiv z = \frac{168.14 \frac{g C}{mol_{ASP}}}{294.30 \frac{g ASP}{mol_{ASP}}} = \mathbf{0.571}$$

For an ASP concentration of 150 mg/L, the theoretical TOC can be calculated as follows:

$$ASP TOC_{theoretical@ \frac{150mg}{L}} = 0.571 \times 150 \frac{mg}{L} = 85.65 \frac{mg C}{L}$$

## Appendix F – Determination of UV Exposure Time and Conversion Per Pass

The UV exposure time of the sample was discussed in Section 3.3.1 As an example, the UV Exposure of time for any of the experimental runs carried out in Phase II can be done as follows:

$$t_{\text{exposure}} = \left( \frac{V_{\text{reactor}}}{V_{\text{sample}}} \right) \times t_{\text{reaction}} = \left( \frac{0.92 \text{ L}}{2.5 \text{ L}} \right) \times 120 \text{ min} = \mathbf{44.16 \text{ min}}$$

Where:

$V_{\text{reactor}}$  = *effective reactor volume*

$V_{\text{sample}}$  = *Total Sample Volume in the entire system*

$t_{\text{reaction}}$  = *total reaction run time*

The conversion per pass can be determined experimentally by following the rate of TOC reduction. In the case of ASP (150 mg/L), the highest drop in TOC concentration (corresponding to the highest conversion) was observed between 5 -10 min of UV exposure time (corresponding to an experimental run time interval of 15 min) for all applied dosages of H<sub>2</sub>O<sub>2</sub>. The validation of the assumption of “small conversion per pass” at this point will validate the assumption for the entire experimental run. The conversion per pass for an applied H<sub>2</sub>O<sub>2</sub>:ASP ratio of 10:1 can be estimated by calculating the number of passes at an equivalent run time of 15 min as follows:

$$t_{\text{single pass}} = \frac{V_{\text{sample}}}{Q} = \frac{2.5 \text{ L}}{8.5 \frac{\text{L}}{\text{min}}} = 0.29 \text{ min}$$

$$\# \text{ passes per 15 minutes} = \frac{t_{\text{reaction}}}{t_{\text{pass}}} = \frac{15 \text{ min}}{0.29 \text{ min}} = 51$$

The conversion per pass can then be determined by dividing the TOC reduction obtained between exposure times of 15-30 min (corresponding to a UV exposure time of approximately 5-10 min as seen in **Figure 4-2**) by the number of passes in 15 min as follows:

$$\text{conversion per pass} = \frac{\sim 40\% \text{ TOC Reduction}}{51} = \mathbf{0.78\%} \ll 5\%$$

Therefore, the assumption holds.

## Appendix G – Calibration of the TOC Analyzer

A six-point calibration plot was utilized for TOC analysis by the Apollo 9000 TOC analyzer for the TOC concentration ranges used in this study. The standards were prepared by dissolving 2125 g of KHP in 1 L of distilled water to obtain a stock standard solution of 1000 mg organic C/L. This solution was used to prepare standards of desired concentrations through dilution with distilled water. The calibration plot used for TOC analysis is shown in **Figure G-1**.

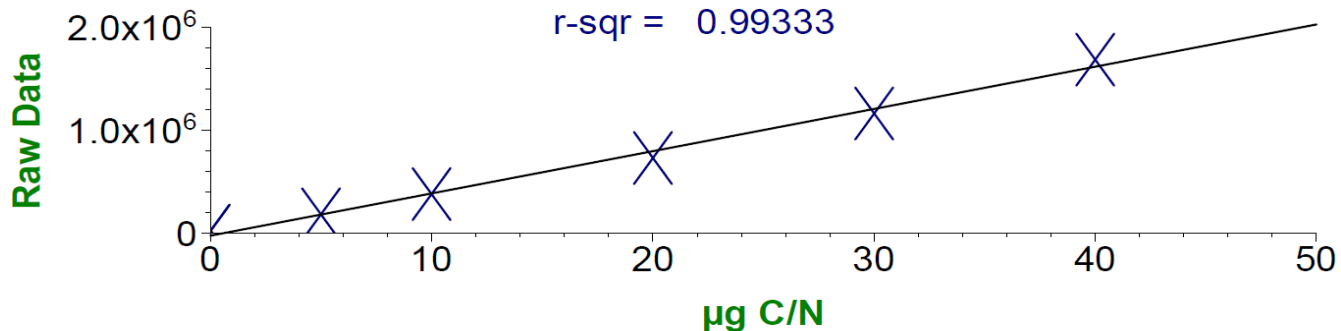


**Figure G-1:** Six-point calibration plot used for TOC analysis

## Appendix H – Fit Statistics for Developed Models

The fit statistics presented in *Table H-1* are of less significance in comparison to the ANOVA and the analysis of residuals. Nevertheless, they are useful in determining the overall validity of the models through a quick overview. The  $R^2$  values of 0.7554 and 0.6562 reported in the *Table H-1* suggest that the models do not fit the experimental data very well. These results agree with the lack-of-fit test results reported in Section 4.3.3.2. The adjusted  $R^2$  values suggest that neither of the models are in risk of being overly fit with terms. This is not a surprise as each model consists of only two significant effects. Finally, the predicted  $R^2$  values are in good agreement with the adjusted  $R^2$  values. However, the magnitudes of the predicted  $R^2$  along with the raw  $R^2$  values suggest that the models' abilities are limited in providing valid response predictions. This is not a concern as the current models will not be used for this purpose.

*Table H-1*: Fit statistics for the statistical TOC reduction models

<i>TOC Removal at a UV Exposure Time of 22.5 min</i>	
<b><math>R^2</math></b>	0.7554
<b>Adjusted <math>R^2</math></b>	0.6942
<b>Predicted <math>R^2</math></b>	0.4995
<b>Signal to Noise Ratio</b>	9.5707
<i>TOC Removal at a UV Exposure Time of 45 min</i>	
<b><math>R^2</math></b>	0.6562
<b>Adjusted <math>R^2</math></b>	0.6180
<b>Predicted <math>R^2</math></b>	0.4814
<b>Signal to Noise Ratio</b>	9.3140

## Appendix I – Analysis of Residuals

The analysis of residuals is the most powerful tool in regression diagnostics. Furthermore, the most important concept regarding residuals is the assumption of normal distribution. This can be analyzed through a normal probability plot of the residuals (Montgomery, 2005). Such plots are shown in **Figure I-1** and **Figure I-2** for UV Exposures of 22.5 and 45 min respectively. Both plots show a series of residuals that for the most part follow a straight line. The presence of some scatter and deviation is not of significant concern as no “definite” patterns (e.g. s-shaped curve) are observed. Hence, the assumption of normality is met.

Another important condition is the assumption of constant variance in experiments. To test for this condition, residuals are plotted against predicted response values in ascending order. These plots are shown for UV Exposures of 22.5 min and 45 min in **Figure I-3** and **Figure I-4** respectively. Furthermore, the residuals can also be plotted against different levels of selected factors as seen in **Figure I-5**, **Figure I-6** and **Figure I-7**. Overall, no systematic trends are observed for the residuals shown in **Figure I-3**. Hence, the condition of constant variance is met in this case. A pattern (descending range of residuals) is observed in the plot shown in **Figure I-4**. Further analysis of **Figure I-6** and **Figure I-7** show that the residuals are within the same ranges for all levels of both factors, except for the high temperature level. This implies that the experimental response variance was lower at a higher temperature level. This is simply due to the fact that in almost all cases, the TOC was reduced to very small amounts, resulting in the variation to be smaller as well. Additionally, F-test on the model is only slightly affected in such cases, if *equal sample sizes* were collected throughout the experimental runs (Montgomery, 2005). Since equal sample sizes were collected in all experiments, this condition holds. Hence, this is not a concern. Finally, the plots of residuals in each experimental run are shown in **Figure I-8** and **Figure I-9** for UV Exposures of 22.5 min and 45 min respectively. These plots simply confirm that variance was constant and independent of experimental run order as no obvious patterns are observed. In other words, daily variability did not affect the experimental results.

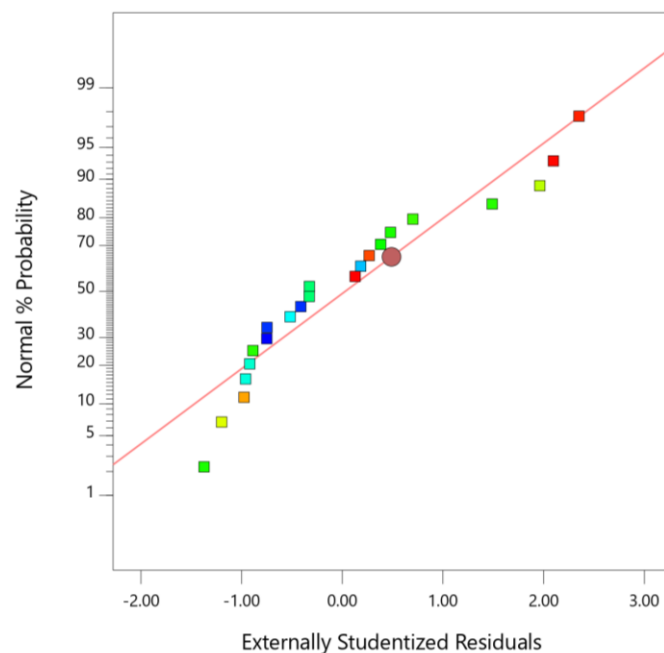


**Figure I-1:** Normal probability plot of residuals for collected samples a UV exposure time of 22.5 min

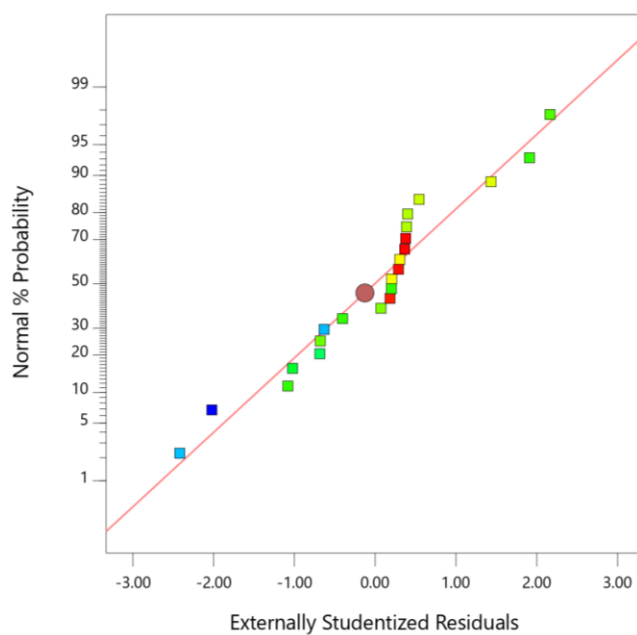


**Figure I-2:** Normal probability plot of residuals for collected samples a UV exposure time of 45 min

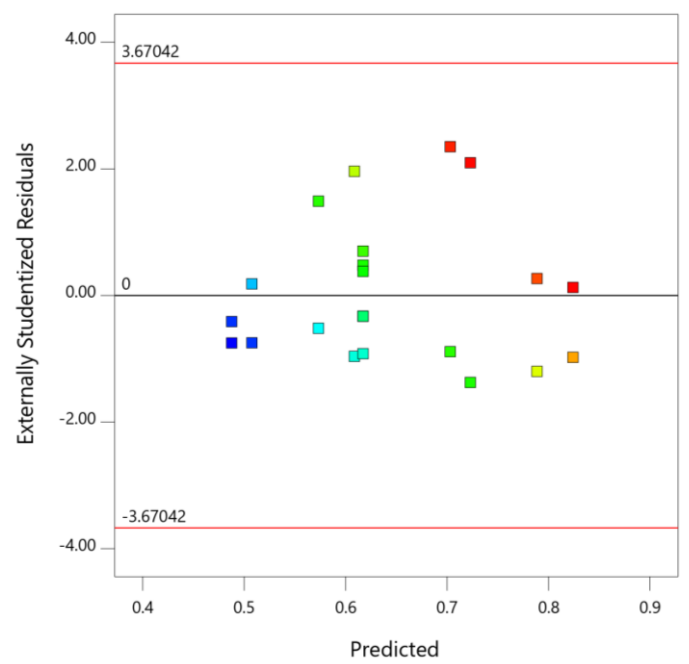


**Figure I-3:** Plot of residuals against ascending predicted response values for samples collected at a UV exposure time of 22.5 min

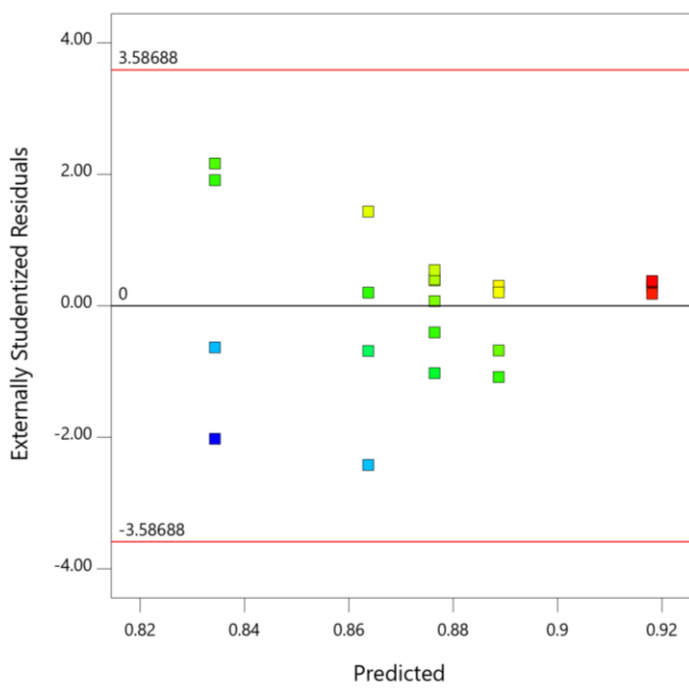


**Figure I-4:** Plot of residuals against ascending predicted response values for samples collected at a UV exposure time of 45 min



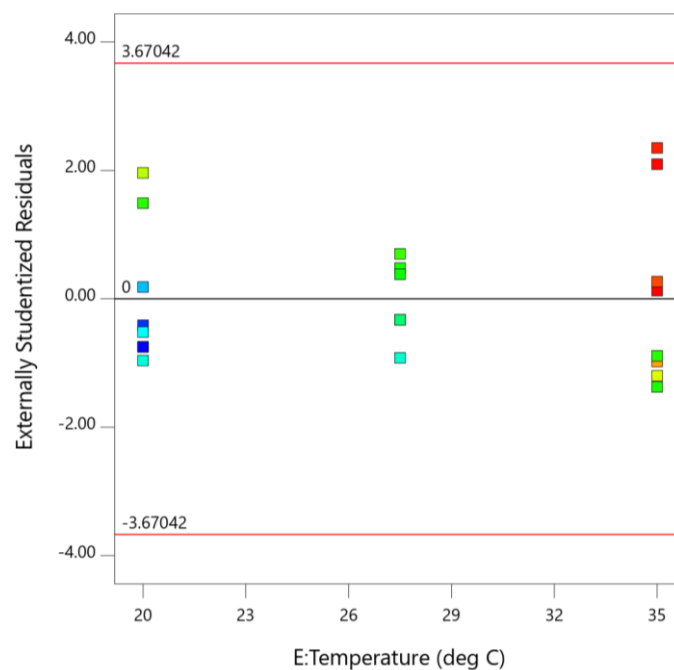


**Figure I-5:** Plot of residuals against high and low levels of temperature for samples collected at a UV exposure time of 22.5 min

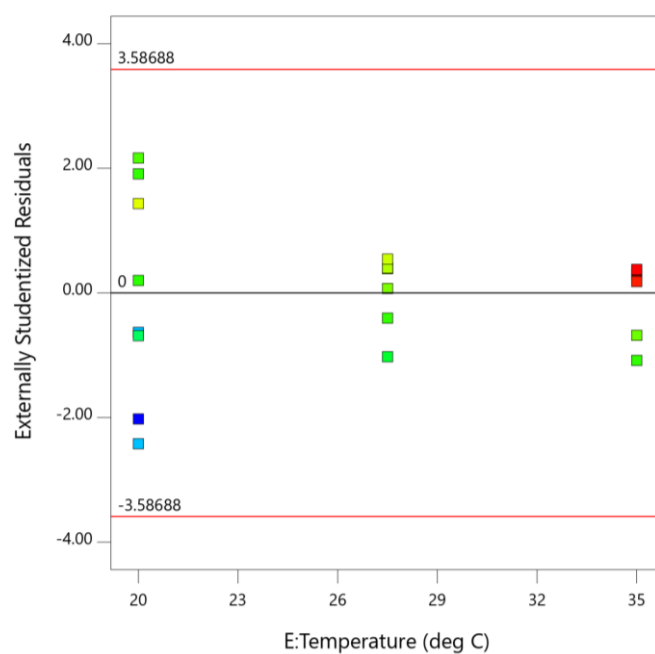


**Figure I-6:** Plot of residuals against high and low levels of temperature for samples collected at a UV exposure time of 45 min

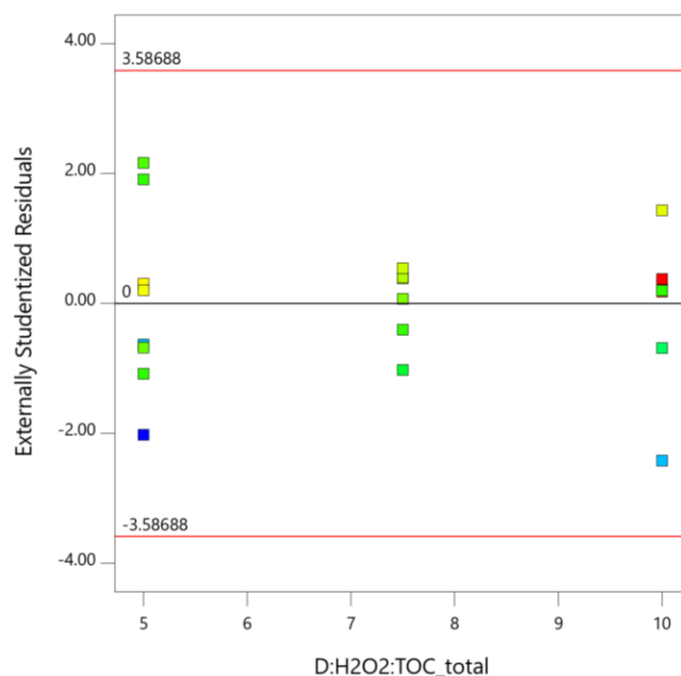


**Figure I-7:** Plot of residuals against high and low levels of H<sub>2</sub>O<sub>2</sub>:TOC<sub>ini</sub> (mass basis) for samples collected at a UV exposure time of 45 min

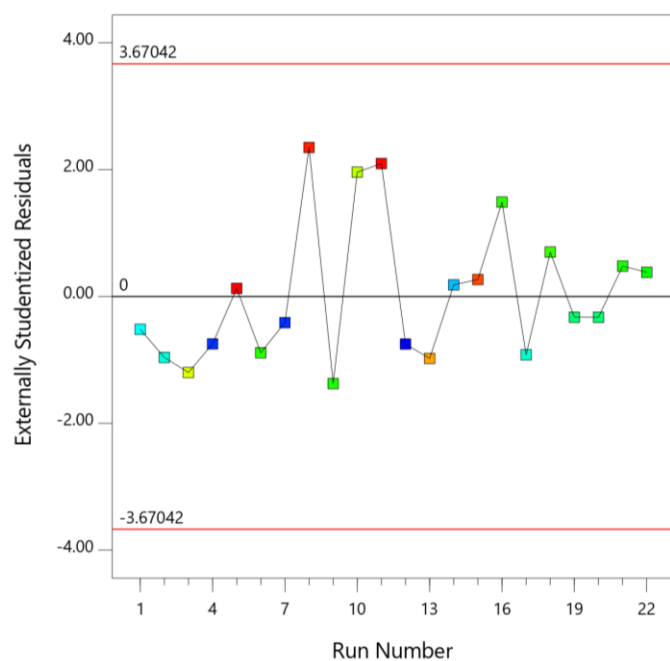


**Figure I-8:** Plot of residuals against experimental run order for samples collected at a UV exposure time of 22.5 min

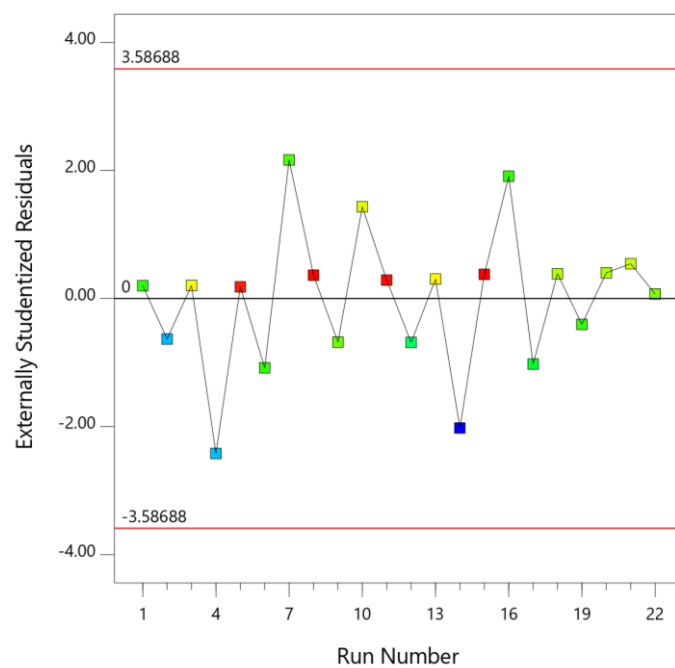


**Figure I-9:** Plot of residuals against experimental run order for samples collected at a UV exposure time of 45 min

## References

- Ali, A., and Devrukhkar, J. (2016). In vitro study on glycation of plasma proteins with artificial sweeteners. *Acta Biologica Szegediensis*, 60(1).
- Amy-Sagers, C., Reinhardt, K., and Larson, D. M. (2017). Ecotoxicological assessments show sucralose and fluoxetine affect the aquatic plant, *Lemna minor*. *Aquatic Toxicology*, 185. <https://doi.org/10.1016/j.aquatox.2017.01.008>
- Baena-Nogueras, R. M., Traverso-Soto, J. M., Biel-Maeso, M., Villar-Navarro, E., and Lara-Martín, P. A. (2018). Sources and trends of artificial sweeteners in coastal waters in the bay of Cadiz (NE Atlantic). *Marine Pollution Bulletin*, 135(July), 607–616. <https://doi.org/10.1016/j.marpolbul.2018.07.069>
- Berset, J., and Ochsenbein, N. (2012). Chemosphere Stability considerations of aspartame in the direct analysis of artificial sweeteners in water samples using high-performance liquid chromatography – tandem mass spectrometry ( HPLC – MS / MS ). *Chemosphere*, 88(5), 563–569. <https://doi.org/10.1016/j.chemosphere.2012.03.030>
- Bian, X., Chi, L., Gao, B., Tu, P., Ru, H., and Lu, K. (2017). Gut microbiome response to sucralose and its potential role in inducing liver inflammation in mice. *Frontiers in Physiology*, 8(JUL). <https://doi.org/10.3389/fphys.2017.00487>
- Biń, A. K., and Sobera-Madej, S. (2012). Comparison of the Advanced Oxidation Processes (UV, UV/H<sub>2</sub>O<sub>2</sub> and O<sub>3</sub>) for the Removal of Antibiotic Substances during Wastewater Treatment. *Ozone: Science and Engineering*, 34(2), 136–139. <https://doi.org/10.1080/01919512.2012.650130>
- Bourgin, M., Beck, B., Boehler, M., Borowska, E., Fleiner, J., Salhi, E., ... McArdell, C. S. (2018). Evaluation of a full-scale wastewater treatment plant upgraded with ozonation and biological post-treatments: Abatement of micropollutants, formation of transformation products and oxidation by-products. *Water Research*. <https://doi.org/10.1016/j.watres.2017.10.036>
- Brorstrom-Lunden, E., Svenson, A., Viktor, T., Woldegiorgis, A., Remberger, M., Kaj, L., ... Schlabach, M. (2007). *Measurement of Sucralose in Swedish Screening Program*. Stockholm.
- Buerge, I. J., Buser, H.-R., Kahle, M., Müller, M. D., and Poiger, T. (2009). Ubiquitous occurrence

- of the artificial sweetener acesulfame in the aquatic environment: An ideal chemical marker of domestic wastewater in groundwater. *Environmental Science and Technology*, 43(12), 4381–4385. <https://doi.org/10.1021/es900126x>
- Buerge, I. J., Keller, M., Buser, H.-R., Müller, M. D., and Poiger, T. (2011). Saccharin and other artificial sweeteners in soils: Estimated inputs from agriculture and households, degradation, and leaching to groundwater. *Environmental Science and Technology*, 45(2), 615–621. <https://doi.org/10.1021/es1031272>
- Bustillo-Lecompte, C. F., Knight, M., and Mehrvar, M. (2015). Assessing the performance of uv/H<sub>2</sub>O<sub>2</sub> as a pretreatment process in TOC removal of an actual petroleum refinery wastewater and its inhibitory effects on activated sludge. *Canadian Journal of Chemical Engineering*, 93(5), 798–807. <https://doi.org/10.1002/cjce.22180>
- Bustillo-Lecompte, C. F., and Mehrvar, M. (2017). Treatment of actual slaughterhouse wastewater by combined anaerobic–aerobic processes for biogas generation and removal of organics and nutrients: An optimization study towards a cleaner production in the meat processing industry. *Journal of Cleaner Production*, 141, 278–289. <https://doi.org/10.1016/j.jclepro.2016.09.060>
- Calza, P., Sakkas, V. A., Medana, C., Vlachou, A. D., Dal Bello, F., and Albanis, T. A. (2013). Chemometric assessment and investigation of mechanism involved in photo-Fenton and TiO<sub>2</sub> photocatalytic degradation of the artificial sweetener sucralose in aqueous media. *Applied Catalysis B: Environmental*, 129. <https://doi.org/10.1016/j.apcatb.2012.08.043>
- Castronovo, S., Wick, A., Scheurer, M., Nödler, K., Schulz, M., and Ternes, T. A. (2017). Biodegradation of the artificial sweetener acesulfame in biological wastewater treatment and sandfilters. *Water Research*, 110, 342–353. <https://doi.org/10.1016/j.watres.2016.11.041>
- Chen, S.-W., Li, W. C., Sun, Z. G., and Xie, H.-Y. (2014). Degradation of artificial sweetener saccharin sodium by advanced oxidation technology. *Applied Mechanics and Materials* (Vol. 448–453). <https://doi.org/10.4028/www.scientific.net/AMM.448-453.7>
- Cooper, S., Grady, L., and Tabak, H. H. (1990). Biodegradation kinetics of substituted phenolics: demonstration of a protocol based on electrolytic respirometry ~ a Ss, 24(7), 853–861.
- CRC Press. (2018). *CRC Handbook of Chemistry and Physics*. (J. Rumble, Ed.) (99th ed.).

- Crittenden, J. C., Trussel, R. R., Hand, D. W., Howe, K. J., and Tchobanoglous, G. (2012). *Water Treatment: Principles and Design* (3rd ed.). John Wiley and Sons. Inc.
- Dantas, R. F., Rossiter, O., Teixeira, A. K. R., Simões, A. S. M., and da Silva, V. L. (2010). Direct UV photolysis of propranolol and metronidazole in aqueous solution. *Chemical Engineering Journal*, 158(2), 143–147. <https://doi.org/10.1016/j.cej.2009.12.017>
- Dattatreya, B. S., Usha, D. V., Susheelamma, N. S., and Bhat, K. K. (2003). Aspartame: Studies on UV spectral characteristics. *International Journal of Food Science and Technology*, 38(7), 767–775. <https://doi.org/10.1046/j.1365-2621.2003.00728.x>
- Edwards, Q. A., Kulikov, S. M., Garner-O’Neale, L. D., Metcalfe, C. D., and Sultana, T. (2017). Contaminants of emerging concern in surface waters in Barbados, West Indies. *Environmental Monitoring and Assessment*, 189(12). <https://doi.org/10.1007/s10661-017-6341-4>
- Ferrer, I., and Thurman, E. M. (2010). Analysis of sucralose and other sweeteners in water and beverage samples by liquid chromatography/time-of-flight mass spectrometry. *Journal of Chromatography A*, 1217(25), 4127–4134. <https://doi.org/10.1016/j.chroma.2010.02.020>
- Gago-Ferrero, P., Gros, M., Ahrens, L., and Wiberg, K. (2017). Impact of on-site, small and large scale wastewater treatment facilities on levels and fate of pharmaceuticals, personal care products, artificial sweeteners, pesticides, and perfluoroalkyl substances in recipient waters. *Science of the Total Environment*, 601–602, 1289–1297. <https://doi.org/10.1016/j.scitotenv.2017.05.258>
- Ghafoori, S., Mowla, A., Jahani, R., Mehrvar, M., and Chan, P. K. (2015). Sonophotolytic degradation of synthetic pharmaceutical wastewater: Statistical experimental design and modeling. *Journal of Environmental Management*, 150. <https://doi.org/10.1016/j.jenvman.2014.11.011>
- Grady, L., Daigger, G., Love, N., and Filipe, C. (2011). *Biological Wastewater Treatment* (3rd ed.). New York: IWA.
- Heider, E. C., Valenti, D., Long, R. L., Garbou, A., Rex, M., and Harper, J. K. (2018). Quantifying Sucralose in a Water-Treatment Wetlands: Service-Learning in the Analytical Chemistry Laboratory. *Journal of Chemical Education*, 95(4), 535–542.

<https://doi.org/10.1021/acs.jchemed.7b00490>

- Hollender, J., Zimmermann, S. G., Koepke, S., Krauss, M., Mcardell, C. S., Ort, C., Siegrist, H. (2009). Elimination of organic micropollutants in a municipal wastewater treatment plant upgraded with a full-scale post-ozonation followed by sand filtration. *Environmental Science and Technology*, 43(20). <https://doi.org/10.1021/es9014629>
- Hoque, M. E., Cloutier, F., Arcieri, C., McInnes, M., Sultana, T., Murray, C., Metcalfe, C. D. (2014). Removal of selected pharmaceuticals, personal care products and artificial sweetener in an aerated sewage lagoon. *Science of the Total Environment*. <https://doi.org/10.1016/j.scitotenv.2013.12.063>
- Hornback, J. (2006). *Organic Chemistry* (2nd ed.). Thompson Brooks/Cole.
- Hu, H., Deng, Y., Fan, Y., Zhang, P., Sun, H., Gan, Z., Yao, Y. (2016). Effects of artificial sweeteners on metal bioconcentration and toxicity on a green algae *Scenedesmus obliquus*. *Chemosphere*, 150, 285–293. <https://doi.org/10.1016/j.chemosphere.2016.02.043>
- Hu, R., Zhang, L., and Hu, J. (2017). Investigation of ozonation kinetics and transformation products of sucralose. *Science of the Total Environment*, 603–604. <https://doi.org/10.1016/j.scitotenv.2017.06.033>
- Jung, J., Kim, Y., Kim, J., Jeong, D. H., and Choi, K. (2008). Environmental levels of ultraviolet light potentiate the toxicity of sulfonamide antibiotics in *Daphnia magna*. *Ecotoxicology*, 17(1), 37–45. <https://doi.org/10.1007/s10646-007-0174-9>
- Kahl, S., Kleinstuber, S., Nivala, J., Van Afferden, M., and Reemtsma, T. (2018). Emerging Biodegradation of the Previously Persistent Artificial Sweetener Acesulfame in Biological Wastewater Treatment. *Environmental Science and Technology*, 52(5), 2717–2725. <https://doi.org/10.1021/acs.est.7b05619>
- Kattel, E., Trapido, M., and Dulova, N. (2017). Oxidative degradation of emerging micropollutant acesulfame in aqueous matrices by UVA-induced  $\text{H}_2\text{O}_2/\text{Fe}^{2+}$  and  $\text{S}_2\text{O}_8^{2-}/\text{Fe}^{2+}$  processes. *Chemosphere*, 171. <https://doi.org/10.1016/j.chemosphere.2016.12.104>
- Kirk, A. (2010). *Photochemical Fate of the Artificial Sweetener Sucralose in the Environment*. University of North Carolina Wilmington.

- Kokotou, M. G., Asimakopoulos, A. G., and Thomaidis, N. S. (2012). Artificial sweeteners as emerging pollutants in the environment: Analytical methodologies and environmental impact. *Analytical Methods*, 4(10). <https://doi.org/10.1039/c2ay05950a>
- Lange, F. T., Scheurer, M., and Brauch, H.-J. (2012). Artificial sweeteners-A recently recognized class of emerging environmental contaminants: A review. *Analytical and Bioanalytical Chemistry*, 403(9). <https://doi.org/10.1007/s00216-012-5892-z>
- Lee, H. J., Kim, K. Y., Hamm, S. Y., Kim, M. S., Kim, H. K., and Oh, J. E. (2019). Occurrence and distribution of pharmaceutical and personal care products, artificial sweeteners, and pesticides in groundwater from an agricultural area in Korea. *Science of the Total Environment*, 659, 168–176. <https://doi.org/10.1016/j.scitotenv.2018.12.258>
- Levenspiel, O. (1972). *Chemical Reaction Engineering* (1st ed.). John Wiley and Sons. Inc.
- Li, A. J., Schmitz, O. J., Stephan, S., Lenzen, C., Yue, P. Y.-K., Li, K., Leung, K. S.-Y. (2016). Photocatalytic transformation of acesulfame: Transformation products identification and embryotoxicity study. *Water Research*, 89. <https://doi.org/10.1016/j.watres.2015.11.035>
- Li, A. J., Wu, P., Law, J. C.-F., Chow, C.-H., Postigo, C., Guo, Y., and Leung, K. S.-Y. (2017). Transformation of acesulfame in chlorination: Kinetics study, identification of byproducts, and toxicity assessment. *Water Research*, 117. <https://doi.org/10.1016/j.watres.2017.03.053>
- Li, S., Geng, J., Wu, G., Gao, X., Fu, Y., and Ren, H. (2018). Removal of artificial sweeteners and their effects on microbial communities in sequencing batch reactors. *Scientific Reports*, 8(1). <https://doi.org/10.1038/s41598-018-21564-x>
- Li, S., Ren, Y., Fu, Y., Gao, X., Jiang, C., Wu, G., ... Geng, J. (2018). Fate of artificial sweeteners through wastewater treatment plants and water treatment processes. *PLoS ONE*, 13(1). <https://doi.org/10.1371/journal.pone.0189867>
- Lin, H., Oturan, N., Wu, J., Oturan, M. A., and Zhang, H. (2018). *The application of electro-Fenton process for the treatment of artificial sweeteners. Handbook of Environmental Chemistry* (Vol. 61). [https://doi.org/10.1007/698\\_2017\\_59](https://doi.org/10.1007/698_2017_59)
- Lin, H., Oturan, N., Wu, J., Sharma, V. K., Zhang, H., and Oturan, M. A. (2017). Removal of artificial sweetener aspartame from aqueous media by electrochemical advanced oxidation processes. *Chemosphere*, 167. <https://doi.org/10.1016/j.chemosphere.2016.09.143>



- Lin, H., Oturan, N., Wu, J., Zhang, H., and Oturan, M. A. (2017). Cold incineration of sucralose in aqueous solution by electro-Fenton process. *Separation and Purification Technology*, 173. <https://doi.org/10.1016/j.seppur.2016.09.028>
- Lin, H., Wu, J., Oturan, N., Zhang, H., and Oturan, M. A. (2016). Degradation of artificial sweetener saccharin in aqueous medium by electrochemically generated hydroxyl radicals. *Environmental Science and Pollution Research*, 23(5). <https://doi.org/10.1007/s11356-015-5633-x>
- Llamas, N., Di Nezio, M., Palomeque, M., and Fernandez Band, B. (2008). Direct Determination of Saccharin and Acesulfame-K in Sweeteners and Fruit Juices Powders. *Food Analytical Methods*, 1(1), 43–48.
- Loos, R., Gawlik, B. M., Boettcher, K., Locoro, G., Contini, S., and Bidoglio, G. (2009). Sucralose screening in European surface waters using a solid-phase extraction-liquid chromatography-triple quadrupole mass spectrometry method. *Journal of Chromatography A*, 1216(7), 1126–1131. <https://doi.org/10.1016/j.chroma.2008.12.048>
- López-Muñoz, M. J., Daniele, A., Zorzi, M., Medana, C., and Calza, P. (2018). Investigation of the photocatalytic transformation of acesulfame K in the presence of different TiO<sub>2</sub>-based materials. *Chemosphere*. <https://doi.org/10.1016/j.chemosphere.2017.11.016>
- Mangala, S. (2019). Ecotoxicology and Environmental Safety Non-nutritive artificial sweeteners as an emerging contaminant in environment: A global review and risks perspectives, 170(December 2018), 699–707. <https://doi.org/10.1016/j.ecoenv.2018.12.048>
- Mawhinney, D. B., Young, R. B., Vanderford, B. J., Borch, T., and Snyder, S. A. (2011). Artificial sweetener sucralose in U.S. drinking water systems. *Environmental Science and Technology*, 45(20), 8716–8722. <https://doi.org/10.1021/es202404c>
- Metcalf and Eddy. (2014). *Wastewater Engineering: Treatment and Resource Recovery* (5th ed.). New York: McGraw Hill. <https://doi.org/10.1007/s13398-014-0173-7.2>
- Mishra, A., Ahmed, K., Froghi, S., and Dasgupta, P. (2015). Systematic review of the relationship between artificial sweetener consumption and cancer in humans: Analysis of 599,741 participants. *International Journal of Clinical Practice*, 69(12). <https://doi.org/10.1111/ijcp.12703>

- Montgomery, D. C. (2005). *Design and Analysis of Experiments* (6th ed.). Hoboken: John Wiley and Sons. Inc.
- Nam, S.-N., Cho, H., Han, J., Her, N., and Yoon, J. (2018). Photocatalytic degradation of acesulfame K: Optimization using the Box–Behnken design (BBD). *Process Safety and Environmental Protection*, 113, 10–21. <https://doi.org/10.1016/j.psep.2017.09.002>
- Nguyen, H. T., Thai, P. K., Kaserzon, S. L., O’Brien, J. W., Eaglesham, G., and Mueller, J. F. (2018). Assessment of drugs and personal care products biomarkers in the influent and effluent of two wastewater treatment plants in Ho Chi Minh City, Vietnam. *Science of the Total Environment*, 631–632, 469–475. <https://doi.org/10.1016/j.scitotenv.2018.02.309>
- Oppenländer, T. (2002). *Photochemical Purification of Water and Air: Advanced Oxidation Processes (AOPs): Principles, Reaction Mechanisms, Reactor Concepts* (1st ed.). Wiley.
- Parsons, S. (Ed.). (2004). *Advanced Oxidation Processes for Water and Wastewater Treatment* (1st ed.). IWA publishing.
- Perkola, N., and Sainio, P. (2014). Quantification of four artificial sweeteners in Finnish surface waters with isotope-dilution mass spectrometry. *Environmental Pollution*, 184. <https://doi.org/10.1016/j.envpol.2013.09.017>
- Rachmilovich-Calis, S., Masarwa, A., Meyerstein, N., and Meyerstein, D. (2005). The Fenton reaction in aerated aqueous solutions revisited. *European Journal of Inorganic Chemistry*, (14), 2875–2880. <https://doi.org/10.1002/ejic.200500097>
- Rao, D. g., Senthilkumar, R., Byrne, J. A., and Feroz, S. (2013). *Wastewater Treatment: Advanced Processes and Technologies* (1st ed.). Boca Raton: IWA publishing.
- Rice, R. G. (1994). *Ozone Reference Guide*. St. Louise, MO.
- Robertson, W. D., Van Stempvoort, D. R., Spoelstra, J., Brown, S. J., and Schiff, S. L. (2016). Degradation of sucralose in groundwater and implications for age dating contaminated groundwater. *Water Research*, 88. <https://doi.org/10.1016/j.watres.2015.10.051>
- Salimi, M., Esrafil, A., Gholami, M., Jonidi Jafari, A., Rezaei Kalantary, R., Farzadkia, M., ... Sobhi, H. R. (2017). Contaminants of emerging concern: a review of new approach in AOP technologies. *Environmental Monitoring and Assessment*, 189(8).

<https://doi.org/10.1007/s10661-017-6097-x>

- Sang, Z., Jiang, Y., Tsoi, Y. K., and Leung, K. S. Y. (2014). Evaluating the environmental impact of artificial sweeteners: A study of their distributions, photodegradation and toxicities. *Water Research*, 52, 260–264. <https://doi.org/10.1016/j.watres.2013.11.002>
- Saucedo-Vence, K., Elizalde-Velázquez, A., Dublán-García, O., Galar-Martínez, M., Islas-Flores, H., SanJuan-Reyes, N., ... Gómez-Oliván, L. M. (2017). Toxicological hazard induced by sucralose to environmentally relevant concentrations in common carp (*Cyprinus carpio*). *Science of the Total Environment*, 575, 347–357. <https://doi.org/10.1016/j.scitotenv.2016.09.230>
- Scheurer, M., Brauch, H.-J., and Lange, F. T. (2009). Analysis and occurrence of seven artificial sweeteners in German waste water and surface water and in soil aquifer treatment (SAT). *Analytical and Bioanalytical Chemistry*, 394(6), 1585–1594. <https://doi.org/10.1007/s00216-009-2881-y>
- Scheurer, M., Schmutz, B., Happel, O., Brauch, H.-J., Wülser, R., and Storck, F. R. (2014). Transformation of the artificial sweetener acesulfame by UV light. *Science of the Total Environment*, 481(1). <https://doi.org/10.1016/j.scitotenv.2014.02.047>
- Scheurer, M., Storck, F. R., Brauch, H.-J., and Lange, F. T. (2010). Performance of conventional multi-barrier drinking water treatment plants for the removal of four artificial sweeteners. *Water Research*, 44(12). <https://doi.org/10.1016/j.watres.2010.04.005>
- Scheurer, M., Storck, F. R., Graf, C., Brauch, H.-J., Ruck, W., Lev, O., and Lange, F. T. (2011). Correlation of six anthropogenic markers in wastewater, surface water, bank filtrate, and soil aquifer treatment. *Journal of Environmental Monitoring*, 13(4), 966–973. <https://doi.org/10.1039/c0em00701c>
- Sharma, V. K., Oturan, M., and Kim, H. (2014). Oxidation of artificial sweetener sucralose by advanced oxidation processes: A review. *Environmental Science and Pollution Research*, 21(14). <https://doi.org/10.1007/s11356-014-2786-y>
- Sladkova, S. V., Kholodkevich, S. V., Olsen, G. H., Geraudie, P., and Camus, L. (2016). Acute and long-term effects of sucralose on the water flea *Daphnia magna* on mobility, survival and reproduction at different temperature regimes, 32(10), 952–960.

- Solarchem Environmental Systems. (1994). *The UV/Oxidation Handbook* (1st ed.). Markham, ON, Canada.
- Spoelstra, J., Schiff, S. L., and Brown, S. J. (2013). Artificial sweeteners in a large Canadian river reflect human consumption in the watershed. *PLoS ONE*, 8(12). <https://doi.org/10.1371/journal.pone.0082706>
- Srivastava, V., Sillanpää, M., Wang, Z., Nguyen Song Thuy Thuy, G., and Ambat, I. (2019). Photocatalytic degradation of an artificial sweetener (Acesulfame-K) from synthetic wastewater under UV-LED controlled illumination. *Process Safety and Environmental Protection*, 123, 206–214. <https://doi.org/10.1016/j.psep.2019.01.018>
- Stolte, S., Steudte, S., Schebb, N. H., Willenberg, I., and Stepnowski, P. (2013). Ecotoxicity of artificial sweeteners and stevioside. *Environment International*, 60, 123–127. <https://doi.org/10.1016/j.envint.2013.08.010>
- Subedi, B., and Kannan, K. (2014). Fate of artificial sweeteners in wastewater treatment plants in New York State, U.S.A. *Environmental Science and Technology*, 48(23), 13668–13674. <https://doi.org/10.1021/es504769c>
- Suty, H., De Traversay, C., and Cost, M. (2004). Applications of advanced oxidation processes: Present and future. *Water Science and Technology*, 49(4), 227–233. <https://doi.org/10.1002/chin.200443274>
- Toronto Water. (2017). *Ashbridge's Bay Wastewater Treatment Plant*. Toronto.
- Toth, J. E., Rickman, K. A., Venter, A. R., Kiddle, J. J., and Mezyk, S. P. (2012). Reaction kinetics and efficiencies for the hydroxyl and sulfate radical based oxidation of artificial sweeteners in water. *Journal of Physical Chemistry A*, 116(40), 9819–9824. <https://doi.org/10.1021/jp3047246>
- Tran, N. H., Hu, J., Li, J., and Ong, S. L. (2014). Suitability of artificial sweeteners as indicators of raw wastewater contamination in surface water and groundwater. *Water Research*, 48(1), 443–456. <https://doi.org/10.1016/j.watres.2013.09.053>
- Tran, N. H., Reinhard, M., and Gin, K. Y. H. (2018). Occurrence and fate of emerging contaminants in municipal wastewater treatment plants from different geographical regions-a review. *Water Research*, 133, 182–207. <https://doi.org/10.1016/j.watres.2017.12.029>

- van Stempvoort, D. R., Robertson, W. D., and Brown, S. J. (2011). Artificial sweeteners in a large septic plume. *Ground Water Monitoring and Remediation*, 31(4), 95–102. <https://doi.org/10.1111/j.1745-6592.2011.01353.x>
- Victor, A. de O., Virleny, M. alves de O., Thayse, W. N. de O., Andressa, N. C. D., Charles, E. de O. S., Stella, R. A. M., ... Joao, M. de C. e S. (2017). Evaluation of cytotoxic and mutagenic effects of two artificial sweeteners by using eukaryotic test systems. *African Journal of Biotechnology*, 16(11), 547–551. <https://doi.org/10.5897/AJB2016.15695>
- Wick, A., Godejohann, M., Scheurer, M., Ternes, T. A., Happel, O., Lange, F. T., ... Ruck, W. K. L. (2011). Structural elucidation of main ozonation products of the artificial sweeteners cyclamate and acesulfame. *Environmental Science and Pollution Research*, 19(4), 1107–1118. <https://doi.org/10.1007/s11356-011-0618-x>
- Wiklund, A. K., Adolfsson-Erici, M., Liewenborg, B., and Gorokhova, E. (2014). Sucralose induces biochemical responses in *Daphnia magna*. *PLoS ONE*, 9(4). <https://doi.org/10.1371/journal.pone.0092771>
- Wiklund, A. K. E., Breitholtz, M., Bengtsson, B. E., and Adolfsson-Erici, M. (2012). Sucralose - An ecotoxicological challenger? *Chemosphere*, 86(1), 50–55. <https://doi.org/10.1016/j.chemosphere.2011.08.049>
- Xu, Y., Lin, Z., and Zhang, H. (2016). Mineralization of sucralose by UV-based advanced oxidation processes: UV/PDS versus UV/H<sub>2</sub>O<sub>2</sub>. *Chemical Engineering Journal*, 285. <https://doi.org/10.1016/j.cej.2015.09.091>
- Xu, Y., Wu, Y., Zhang, W., Fan, X., Wang, Y., and Zhang, H. (2018). Performance of artificial sweetener sucralose mineralization via UV/O<sub>3</sub> process: Kinetics, toxicity and intermediates. *Chemical Engineering Journal*, 353(June), 626–634. <https://doi.org/10.1016/j.cej.2018.07.090>
- Yang, Y.-Y., Liu, W.-R., Liu, Y.-S., Zhao, J.-L., Zhang, Q.-Q., Zhang, M., ... Ying, G.-G. (2017). Suitability of pharmaceuticals and personal care products (PPCPs) and artificial sweeteners (ASs) as wastewater indicators in the Pearl River Delta, South China. *Science of the Total Environment*, 590–591, 611–619. <https://doi.org/10.1016/j.scitotenv.2017.03.001>
- Yang, Y.-Y., Zhao, J.-L., Liu, Y.-S., Liu, W.-R., Zhang, Q.-Q., Yao, L., ... Ying, G.-G. (2018).

- Pharmaceuticals and personal care products (PPCPs) and artificial sweeteners (ASs) in surface and ground waters and their application as indication of wastewater contamination. *Science of the Total Environment*, 616–617, 816–823. <https://doi.org/10.1016/j.scitotenv.2017.10.241>
- Yang, Y. Y., Liu, W. R., Liu, Y. S., Zhao, J. L., Zhang, Q. Q., Zhang, M., ... Ying, G. G. (2017). Suitability of pharmaceuticals and personal care products (PPCPs) and artificial sweeteners (ASs) as wastewater indicators in the Pearl River Delta, South China. *Science of the Total Environment*, 590–591, 611–619. <https://doi.org/10.1016/j.scitotenv.2017.03.001>
- Yin, K., Li, F., Wang, Y., He, Q., Deng, Y., Chen, S., and Liu, C. (2017). Oxidative transformation of artificial sweetener acesulfame by permanganate: Reaction kinetics, transformation products and pathways, and ecotoxicity. *Journal of Hazardous Materials*, 330. <https://doi.org/10.1016/j.jhazmat.2017.02.012>
- Young, J., and Cowan, R. (2004). *Respirometry for Environmental Science and Engineering* (1st ed.). Springdale: SJ Enterprises.